Experimental Investigation and Parametric Optimization of Double Cutting Tool Turning During Dry Condition for AISI 1050 Steel

Kasahun Nuguse Alemu

A Thesis Submitted to

The Department of Mechanical Engineering

School of Mechanical, Chemical, and Material Science Engineering

Presented in Partial Fulfillment of the Requirement for the Degree of Master's in Manufacturing Engineering

Office of Graduate Studies
Adama Science and Technology University

June 2022

Adama, Ethiopia

Experimental Investigation and Parametric Optimization of Double Cutting Tool Turning During Dry Condition for AISI 1050 Steel

Kasahun Nuguse Alemu

Advisor**: Dr. Moera Gutu Jiru**

A Thesis Submitted to

The department of Mechanical Engineering

School of Mechanical, Chemical, and Material Science Engineering

Presented in Partial Fulfillment of the Requirement for the Degree of Master's in Manufacturing Engineering

Office of Graduate Studies

Adama Science and Technology University

June 2022

Adama, Ethiopia

DECLARATION

I hereby declare that this Master Thesis entitled "**Experimental Investigation and Parametric Optimization of Double Cutting Tool Turning during Dry Condition for AISI 1050 Steel**" is my original work. That is, it has not been submitted for the award of any academic degree, diploma, or certificate in any other university. All sources of materials that are used for this thesis have been duly acknowledged through citation.

Kasahun Nuguse Alemu.	__________	___________.
Name of the student	Signature	Date

RECOMMENDATION

I, the advisor of this thesis, hereby certify that I have read the revised version of the thesis entitled "**Experimental Investigation and Parametric Optimization of Double Cutting Tool Turning during Dry Condition for AISI 1050 Steel"** prepared under my guidance by **Kasahun Nuguse Alemu** and submitted in partial fulfillment of the requirements for the degree of Masters of Science in Manufacturing Engineering.

Therefore, I recommend the submission of the revised version of the thesis to the department following the applicable procedures.

Dr. Moera Gutu Jiru	____________	___________
Major Advisor	Signature	Date

APPROVAL PAGE

I, the advisor of the thesis entitled "**Experimental Investigation and Parametric Optimization of Double Cutting Tool Turning during Dry Condition for AISI 1050 Steel**" and developed by **Kasahun Nuguse Alemu;** hereby certify that the recommendation and suggestions made by the board of examiners are appropriately incorporated into the final version of the thesis.

Dr. Moera Gutu Jiru	____________	___________
Major Advisor	Signature	Date

We, the undersigned, members of the Board of Examiners of the thesis by **Kasahun Nuguse Alemu** have read and evaluated the thesis entitled "**Experimental Investigation and Parametric Optimization of Double Cutting Tool Turning during Dry Condition for AISI 1050 Steel**" and examined the candidate during the open defense. This is, therefore, to certify that the thesis is accepted for partial fulfillment of the requirement of the degree of Master of Science in Manufacturing Engineering.

__________________________	____________	___________
Chairperson	Signature	Date
__________________________	____________	___________
Internal Examiner	Signature	Date
__________________________	____________	___________
External Examiner	Signature	Date

Finally, approval and acceptance of the thesis are contingent upon the submission of its final copy to the Office of Postgraduate Studies (OPGS) through the Department of Graduate Council (DGC) and School Graduate Committee (SGC).

__________________________	____________	___________
Department Head	Signature	Date
__________________________	____________	___________
School Dean	Signature	Date
__________________________	____________	___________
Office of Postgraduate Studies, Dean	Signature	Date

ACKNOWLEDGEMENT

Above all, firstly I would like to thank the almighty God for his undying support, encouragement, and endless love throughout the completion of this work.

Secondly, I would like to thank heartily and my best gratitude goes to my advisor **Dr. Moera Gutu Jiru**, Assistant Professor in the Program of Mechanical Design and Manufacturing Engineering, Adama Science and Technology University for his continuous support, guidance, timely comments, and suggestions throughout the thesis work from starting up to the end. His extreme energy, creativity, and excellent skills had been a constant source of motivation for me. I am very glad to have the opportunity to work with an exceptionally experienced scholar like him. He is a great person and one of the best mentors, and I am always very thankful to him.

I would also like to thank my family for their constant inspiration and guidance kept me focused and motivated in my task. Especially, my mother, **W/ro Asnaqu Dibaba Wakjira,** and my father, **Ato Nuguse Alemu Asafa** for their endless love and contribution like financial support, endless comment, and encouragement in my life. They have always equipped me with the courage and patience to face the ups and downs of life and strictly work to complete this thesis successfully. Lastly, I wish to thank my friends for their collaboration in giving me timely support and motivation during my work, and also, I want to thank all other people who have supported me to complete this research work directly or indirectly.

TABLE OF CONTENTS

LIST OF TABLES

LIST OF FIGURES

ACRONYMS AND ABBREVIATIONS

ABMI:	Akaki Basic Metals Industry
AISI:	American Iron and Steel Institute
ANOVA:	Analysis of Variance
ASTM:	American Society for Testing and Materials
D:	Diameter of the Workpiece
d1:	Primary depth of cut
d2:	Secondary depth of cut
DOE:	Design of Experiment
DOF:	Degree of Freedom
f:	Feed Rate
GRA:	Grey Relational Analysis
GRD:	Grey Relational Grade
L:	Chip length
MRR:	Material Removal Rate
N:	Spindle speed
OA:	Orthogonal Array
OES:	Optical Emission Spectroscopy
Ra:	Average Surface Roughness
S/N:	Signal to Noise ratio
t:	Chips thickness
v:	Cutting Speed

ABSTRACT

Optimizing the machining parameters during the machining process is important to achieve a certain desired machined surface quality. Failure of engineering materials starts at the surface. This implies the optimization of cutting parameters to get a high surface finish that reduces mechanical failures caused by wear and corrosion and increases the productivity of mechanical parts could be adapted. In this research, an experimental test was conducted using double tool turning with an auxiliary ceramic inserted cutting tool on AISI 1050 steel material. And also, this paper is intended to study and optimize cutting parameters to achieve a better surface finish, minimum cutting temperature, and optimize material removal rate. Investigation of chip morphology was conducted for each experiment in dry turning operation. Each experiment was repeated two times and each test used a new cutting insert to ensure accurate readings of the surface roughness. Besides, the cutting temperature in both the tooltip was recorded using a contact digital thermometer, and data is observed during each run. Taguchi L16 orthogonal array has been selected for the design of the experiments, signal-to-noise, regression analysis for each response, and grey relational analysis-based optimization were used. Analysis of variance (ANOVA) was used to determine the influences of cutting parameters and a mathematical model was done using regression analysis on each response. The results of variance presented influence of cutting speed, feed rate, first depth of cut, and second depth of cut were 5.83 %, 8.92 %,15.41%, and 64.99% respectively on surface roughness. The minimum surface roughness attained for the optimum cutting parameter was 1.12µm. The minimum tooltip temperatures of 41.5 ^{0}C and 40.2 ^{0}C were measured for both primary and secondary tool turning respectively. The material removal rate is about 112 mm^{3}/sec which is too high due to the double tool turning operation used.

Keywords: AISI 1050 steel, cutting parameters, surface roughness, material removal rate, cutting temperature,

CHAPTER ONE

1 INTRODUCTION

1.1 Background of the Study

The manufacturing process can be divided into cutting and non-cutting processes. The machining processes are the cutting processes in which the material is removed from the metal by cutting action. Almost 90% of engineering components require machining (Syed Irfan et al., 2019). Machining plays an important role in the manufacturing process. It is perhaps most versatile in the manufacturing industry, where desired components/parts are achieved by removing material in the form of chips (Venkata Vishnu et al., 2018). In the metal cutting and fabrication industry, the surface finish and strength of the product are very critical in determining the surface finish that ensures the quality of the product. The influence and optimization of machining parameters on surface roughness in a turning operation are studied using the Taguchi method (Sahithi et al., 2019). Nowadays, the manufacturing industry focuses not only on increasing productivity but also on improving product quality (Shrajal Gupta et al., 2019).

Turning is the removal of metal from the outside diameter of a rotating cylindrical workpiece. Turning is used to reduce the diameter of the workpiece, usually to a specific measure, and create a smooth finish on the metal. Often the workpiece is turned so that adjacent sections have different diameters. In this challenging world, industries around the world are constantly striving for owner-cost solutions with shorter lead times and better surface quality to remain competitive. Turning is the first and most common method of cutting, especially for finishing machined parts. In a turning operation, an important task is to select cutting parameters to achieve high cutting performance. The cutting parameters are reflected in the surface roughness, surface texture, and dimensional variations of the product. The surface finish achieved in manufacturing processes mainly depends on the combination of two aspects: the ideal surface finish provided by marks that the manufacturing process creates on the surface, and the actual surface finish that is created taking into account irregularities and imperfections present in the Surface process, changing initial conditions of manufacture (Kondekar et al 2013). Turning operations on a lathe require two simultaneous basic movements; one motion creates the cutting speed and the other is the feed motion (Patokar et al., 2016).

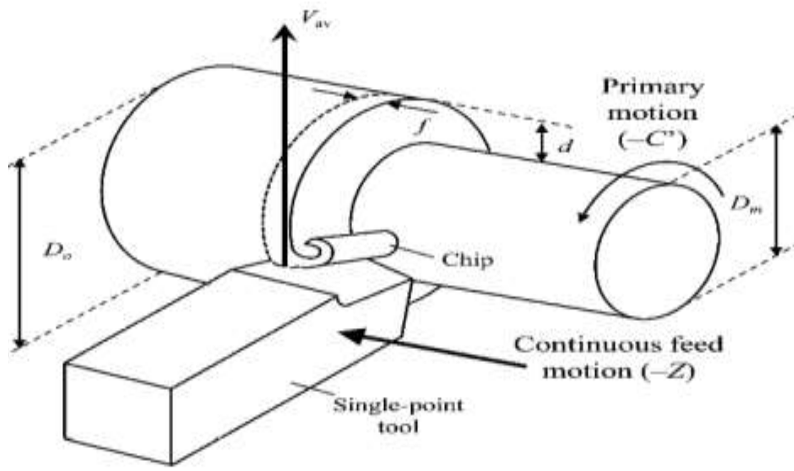

Figure 1.1 Turning operations (Patokar et al., 2016)

1.2 Concept of the Double Cutting Tool Turning Operation

The concept of double cutting tool turning is to use two single-edged cutting tools instead of one to turn the same shaft. The second tool is mounted on the additional tool holder and the additional tool holder is mounted on the same slide and mounted on the same lead screw as the first. Figure 1.2 below shows the schematic of the two individual cutting tools working simultaneously on a single workpiece (Trikal et al., 2016).

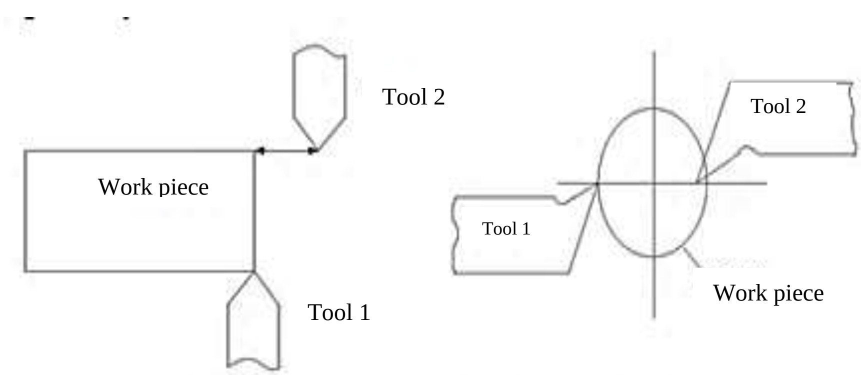

Figure 1.2 Schematic representation of the double cutting tool (Trikal et al., 2016)

A double point cutting tool consists of two cutting tools that can cut or shear simultaneously in a single pass. In contrast, a single-point cutting tool contains only one main cutting edge, and a multi-point cutting tool contains more than one cutting edge for performing the machining operation in a single pass. The primary purpose of the double cutting tool is to simultaneously perform a finish cut turning operation and a shearing operation in a single pass.

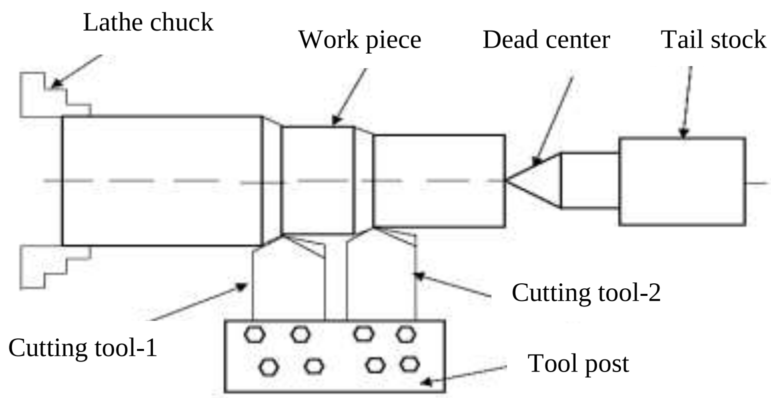

Figure 1.3 Double cutting tools on the same tool post

The dual cutting tool process compares well to conventional single-point cutting because it reduces the number of passes required, improves surface quality and improves productivity, improves the dynamic stability of the rotating workpiece, and provides additional support to the workpiece.

1.3 Concept of the Surface Roughness

The main form of surface roughness created in a lathe is the cylindrical surface. In the turning process, the workpiece is rotated while a cutting tool cuts off the excess material when moved in a direction parallel to the axis of rotation. Surface roughness is the quantitative approach to determining the smoothness of a surface by measuring the height of peaks and the depth of valleys over a fixed length and its important factor that determines the quality of a machined surface. The smoothness of a machined surface is determined by many factors, such as Cutting conditions, vibrations of the machine tool, cutting tools and workpiece holding devices, and cutting parameters (Sarker et al., 2018).

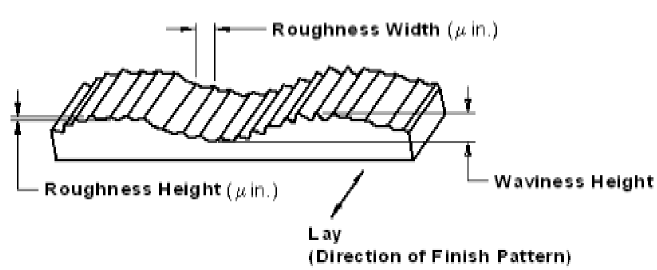

Figure 1.4 Surface Roughness Layouts (Sarker et al., 2018)

The average surface roughness parameter (Ra) is calculated by averaging the surface heights and depths across the surface. This measurement is most commonly displayed as Ra for

Roughness Average, and this value is used to determine the compliance of devices with various industry standards (Sarker et al., 2018).

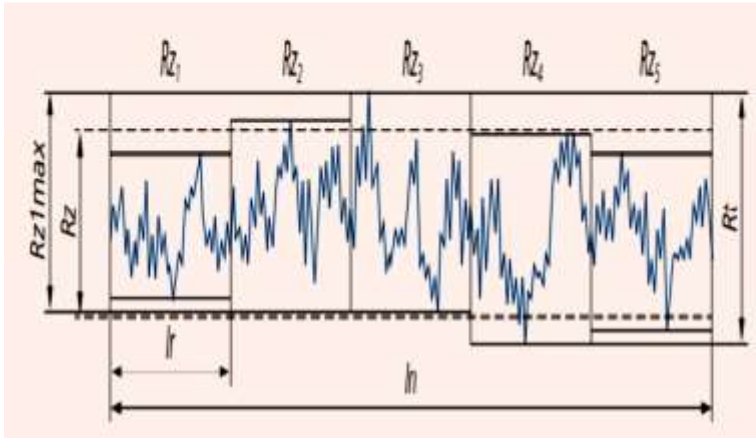

Figure 1.5 Surface roughness terminology (Sarker et al., 2018)

Factors Influencing Surface Quality in Turning

The cause and effect diagram also called as fishbone diagram in figure 1.6 shows different machining parameter that affects surface roughness.

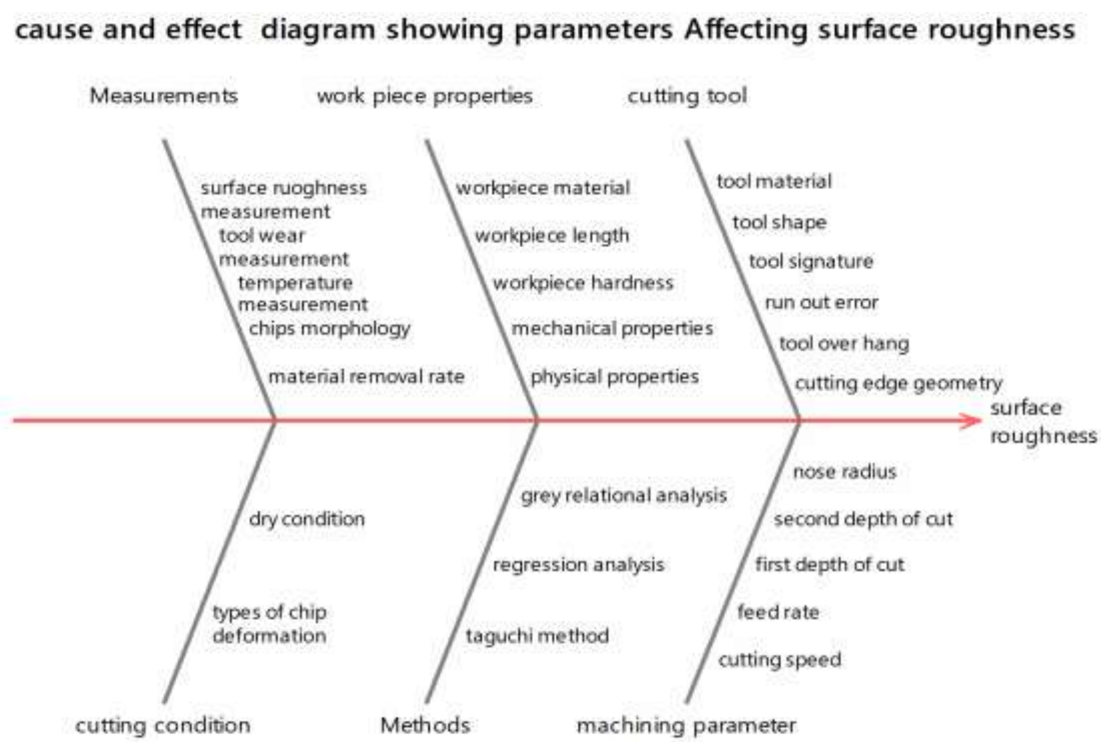

Figure 1.6 Cause and Effect Diagram of Surface Roughness

1.4 Research Motivation

Producing good quality products in a short lead time is the most important thing for customer satisfaction. It was challenged to discuss the high production rate, long product life without defects, and mechanical properties such as (corrosion resistance, and wear resistance) without surface quality. During the machining process, the machined surface quality is one of the most specified customer requirements and plays a crucial role to increase competition among the manufacturers. Much paperwork has been done on this side of the single cutting tool process; no further research on multi-tool turning will be done to reduce machining time and quality during turning operations. Among multi-tool turning processes, double tool turnings require modification to improve product quality and shorten the lead time of the turning process. Therefore, the motivation for this work is mainly due to this reason.

1.5 Statement of the Problem

Machining is one method of producing parts that are applicable in many mechanical components and industries. However, the problem of getting a high surface finish, high material removal rate, and long tool life is a challenge for machining industries. Many papers focus on the study of improving surface finish and productivity using a single cutting tool turning. Because the poor surface finish causes the dimensional inaccuracy, less surface finish precision, rapid wear of parts, crack formation, and propagation which causes final failure of the parts (Karthik et al.2020, shahid et al. 2020). And also, increasing the depth of cut in the single tool turning process can improve productivity, but leads to a problem of short tool life. Controlling cutting parameters are a frequent problem since different work material, and machining methods like double tool turning which is a new research area are very important. However, the single cutting tool turning could not achieve the stated problems as expected as required. To overcome this problem the optimization of cutting parameters using double cutting tools turning is studied, for the seeks of improving machining quality, increasing production rate, and minimizing production costs. Considering cutting factors, AISI 1050 steel was used due to its application area that was affected by tribological properties like surface wear during the operations. Hence, this paper is aimed to conduct an experimental investigation and study the parametric optimization of double cutting tool turning during the dry condition of AISI 1050 steel using a conventional machining process to achieve the optimum machining condition.

1.6 Research Questions

Having all the above-mentioned facts about the machining process in the introductory part and statement of the problem, the following research questions are raised.

1. What are the optimum cutting parameters in the turning of AISI 1050 steel and what are the most significant cutting parameters during dry double cutting tool turning?
2. At what number of experiments the best surface quality is achieved?
3. At what cutting parameters the optimum material removal rate has occurred during the double cutting tool turning of AISI 1050 steel that bridges the gap between productivity and quality is achieved?
4. What is the effect of cutting parameters on cutting temperature at the tooltip during dry machining conditions?
5. What does the chip morphology of AISI 1050 steel look like?

1.7 Objectives

1.7.1 General Objective

The general objective of this research work is to study the parametric optimization of double cutting tool turning during the dry condition of AISI 1050 steel using a conventional machining process to achieve the optimum machining condition.

1.7.2 Specific Objective

To achieve the above general objectives, the following specific objectives are designed.

- To investigate the effect of cutting parameters on surface finish during the dry double tool turning of AISI 1050 steel
- Investigation of material removal rate for a different cutting parameter
- Developing the mathematical model for each response using regressions analysis
- Optimization of surface roughness and material removal rate, and both cutting tooltip temperature using grey relational analysis
- To analyze the effect of cutting parameters on cutting tooltip temperature for dry turning of AISI 1050 steel

- To study chip morphology during turning of AISI 1050 Steel

1.8 Significance of the Study

Double cutting tool turning is using two single cutting tools on the same tool post for the single work piece and it is important to obtain a better surface finish by optimizing the cutting parameters such as cutting speed, feed, and depth of cut for both cutting tool, and also analysis material removal rate, cutting tool tip temperature, and chip morphology. The machining process of different work piece materials largely depends on the performance of a cutting tool and cutting parameters. Therefore, studying the machinability of AISI 1050 steel materials and optimizing cutting parameters that affect the surface quality is very important to manufacture products with high quality. Besides that, it is important to cost reduction, reduce production time, for achieving a good surface finish, increase the service life of the product, enable customer satisfaction, increases the precision of the product, improve the wear and corrosion resistance of parts, and increase market share. Furthermore, the study benefits the manufacturing industry (especially local industries like Akaki Basic Metals Industry and other machine shop industries).

1.9 Scope and Limitation of the Study

The scope is highly focused on experimental analysis of cutting parameters for surface roughness, material removal rate, cutting tooltip temperature, and chip morphology during dry turning of AISI 1050 steel by using a double cutting tool on the conventional lathe machine model of CM260 and also how to improve the surface quality of products in the manufacturing process, to reduce tool wear as well as to increase the customer's satisfaction. Optimize and identify the most significant cutting parameters at which better surface finish is achieved, identify the most significant cutting parameters at which material removal rate is optimal, and cutting tooltip temperature is minimum during double tool turning of AISI 1050 steel without considering cutting tool geometry were studied because considering the simultaneous effect of cutting parameters and tool geometry is very complex. Also, the effect of cutting force and machine vibration on the surface roughness, material removal rate, and cutting temperature was not included because of difficulties to measure cutting forces without a dynamometer and difficulties to measure vibration frequencies.

1.10 Organization of the Research

The thesis contents of five chapters:

CHAPTER ONE: Begins with an introduction and provides the background of the study, the concept of double cutting tool turning, an overview of surface roughness, research motivation, objectives, the problem of the statement, the significance of the study, scopes, and limitation of the study and relevant literature are also enlightened.

CHAPTER TWO: Is concerned with the literature review that is comprised of different researchers' work is revised that is related to machining operations. The review is based on the cutting forces involved in hard machining particularly hard turning, optimization of cutting parameters, tool geometry, cutting tool vibration, the cutting temperature, tool wear, tool life, machining cost, surface integrity, surface roughness, surface finish, material removal rate, and the chip morphology. Finally, the summary of the literature and the research gap is described

CHAPTER THREE: This chapter discusses the experimental details such as the materials used for the experiment, the experimental procedures, the equipment used, and the methodology that achieved the objectives of this study are briefly explained.

CHAPTER FOUR: This chapter deals with the result and discussion, the experimental values. It analysis the effect of process parameters during double cutting tool turning on surface finish, material removal rate, cutting tooltip temperature, and chip morphology during dry machining conditions.

CHAPTER FIVE: A final chapter summarizes and analyzed the experimental investigations during the study, proposed recommendations, and future work for further studies.

CHAPTER TWO

2 LITERATURE REVIEW

2.1 Introduction

This chapter discusses the literature review of the machining process such as the turning process, machining parameters, and the previous study in optimization techniques. The most important process parameters for machining, cutting speed, depth of cutting, and feed rate, influence product quality, and product costs. Optimizing these parameters to minimize surface roughness, tool wear, and product cost, and also to increase the material removal rate within the better surface finish and high machining accuracy, to achieve the desired surface quality of the machined product and to be easily assembled for the desired functionality is important. This cutting parameter also affects surface quality, cutting force, heat build-up, tool life, tool wear, and surface integrity. Many researchers have studied the effect of cutting parameters (cutting speed, depth of cut, feed rate) on surface roughness, chip morphology, cutting force, tool wear, tool life, and production time during the machining process. To overcome these problems, the researchers propose models that attempt to simulate conditions during processing and identify cause-and-effect relationships between various factors and desired product properties. The existence of each method along with its advantages and disadvantages should help both researchers and practitioners by providing compact but adequate ideas for the one that best suits their needs and specific requirements. In the following section, various investigations focus on the turning process and show different results that improve the observed closeness of the results between experimental and predicted values in the turning process.

2.2 Turning Operation

Machining is the most common metalworking process in the mechanical manufacturing industry. The goal of changing the geometry of the raw material to form mechanical parts can be achieved by assembling material. Conventional machining is one of the most important material processes. Machining is a part of the manufacture of almost all metal products. Various machining tools such as lathes, drill presses, horizontal and vertical milling machines, etc. are used to perform cutting operations. Out of this machining process, turning remains the most important operation used to shape metal, because in turning the operating conditions are the most varied. Increasing productivity and reducing manufacturing costs have always been the main goals of a successful company. Again, higher values of cutting parameters offered opportunities to increase productivity, but also came with a greater risk of deteriorating surface quality and tool life. Turning is a very important material removal process in modern industry. Turning is a form of machining, or a material removal process, used to create rotary parts by cutting away unwanted material. The turning process requires a lathe or lathe, a workpiece, a fixture, and a cutting tool. The work piece is a piece of formed material that is attached to the fixture, which in turn is attached to the lathe, and is allowed to rotate at high speed. The cutter is typically a single-point cutting tool that is also fixed in the machine (Kumar Sahu et. al 2017). In turn, process parameters such as cutting speed, depth of cut, feed rate, cutting tool geometry, and material, and the use of cutting fluid affect material removal rates and machining qualities such as surface roughness, the roundness of circular, and dimensional deviations of the products (Brahmbhatt et. al. 2014). When machining, the important task is to select cutting parameters to achieve the highest cutting performance, such as surface roughness, material removal rate, tool wear, and power consumption (Dhabi Samya et.al. 2016).

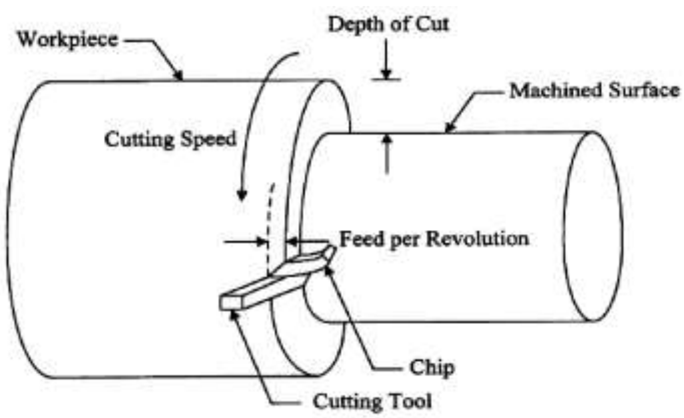

Figure 2. 1 Turning Operations (Dhabi Samya et.al 2016)

2.3 Studies on Optimization of Machining Parameters

Optimizing the machining parameters is valuable in terms of providing high-precision and efficient machining. Attempts are being made to optimize the machining parameters for coated tools by analyzing the surface roughness and tool wear. In the metal cutting process, many factors are related to process planning for machining operations. These factors can be classified as follows: i) types of machining (turning, drilling, milling, drilling, etc.), ii) parameters of the machine tool (rigidity, power, etc.), iii) parameters of a cutting tool (material, tool geometry), iv) parameters the cutting conditions (cutting speed, depth of cut, feed, etc.), v) properties of a workpiece (material, tool geometry, etc.) (R. Nikule. 2017).

Process Parameters

1. Cutting Speed - The cutting speed of a tool is the speed at which the metal is removed from The work material by the tool. On a lathe, it is the peripheral speed of the workpiece in m/min.

V = DN/1000 (m/min) (R. Nikule. 2017).

Where D and N are the diameter of the workpiece (mm) and the cutting speed (rpm) respectively

2. Depth of cut (d): The depth of cut is the vertical distance measured from the machined surface to the unmachined surface of the workpiece in mm (R. Nikule. 2017).

3. Spindle speed - The rotational speed of the spindle and workpiece in revolutions per minute (RPM). The spindle speed is equal to the cutting speed divided by the circumference of the workpiece being cut (R. Nikule. 2017).

4. Feed Rate is the speed of movement of the cutting tool relative to the workpiece when the tool is cutting. Feed rate is measured in inches per minute (IPM) and is the product of cutting feed rate (IPR) and spindle speed (RPM) (R. Nikule. 2017).

2.4 Studies on Surface Roughness, Surface Finish, and Surface Integrity

2.4.1 Surface Roughness

Surface roughness is an important index of the quality of a turning operation. The factors responsible for surface roughness are not limited to just machining parameters (cutting speed, depth of cut, feed rate) and tool geometry (nose radius, rake angle, rake angle), but also include cutting tool vibration, tool wear, tool material, tool error, operator skill, machining environments, and soon, too Surface roughness has a greater impact on the performance of machine parts such as fatigue behavior, corrosion resistance, creep life, etc. and also affect production costs (Pranav R. Kshirsagar et al., 2016). The surface finish formed from hardened steel with a hardness of 45-65 HRC using the special tool is influenced by cutting parameters, tool wear, and the plastic nature of the working materials. The effect of the cutting parameters on the surface roughness under minimum quantity lubrication-assisted hard turning with coated carbide tools was investigated. The study found that cutting speed affects surface roughness

(Mia et al., 2018). To ensure relevant roughness characterization, two main decisions have to be made: relevant measurement techniques and relevant roughness parameters or a set of parameters (Jouini et al., 2009). The analytical model of the surface roughness of PRMMs and the optimal cutting parameter has been developed. The ground profile of the workpiece is created by grooves cut from abrasive grains (Zhang et al., 2019). The distribution of the undeformed chip thickness h or the depth of penetration of abrasive grains can be expressed with Rayleigh probabilities as:

$$f(h) = \{(\frac{h}{\sigma_X^2} - e\frac{h^2}{2\sigma_X^2}\} \qquad \text{For} \quad h \geq o \tag{2.1}$$

$$f(h) = 0 \qquad \text{For} \quad h < 0 \tag{2.2}$$

Where h = unreformed chip thickness

$f(h)$ = Rayleigh probabilities

σ = is a probability density function which is computed as follows:

$$\sigma = \sqrt{\frac{\Delta \cdot v_w}{2 v_s cd.lc} \frac{1}{\tan\theta}} \tag{2.3}$$

Where Δ = is the grinding depth

v_w = is the workpiece speed

v_s = wheel speed

cd = dynamic grit density

Lc = contact length

θ =semi include angle of grain, here it is 45^0.

A high surface roughness value leads to poor surface finish, and the low fatigue life of a machined component (Sharma et al., 2008).

Finally, the developed equation for modeling surface roughness is as follows:

$$R_a = \frac{f^2}{32 r_e} \tag{2.4}$$

Where R_a =surface roughness ($m\mu$)

f =feed rate (mm/rev), and r_e = tool nose radius (mm).

Analysis of variance showed that cutting speed and feed have the greatest impact on surface roughness, the smallest surface roughness being 0.262 for Ni-Hard with 62 HRC using CBN and 0.28 for Ni-Hard with 50 HDC (Chen, 2000). The surface roughness is significantly influenced by workpiece hardness, cutting edge geometry, feed, and cutting speed (OZel et al., 2004). The effects of cutting parameters on the tool and workpiece in terms of flank wear and surface roughness were studied using Taguchi's L9 OA and statistical analysis. The results showed that surface roughness and flank wear are significantly influenced by feed and cutting speed (Ranjan Das et al., 2018).

2.4.2 Surface Finish

The smoothness of a surface is determined by the surface finish and is essential in many situations, e.g. such as precision fittings, mounting holes, fatigue strength, wear resistance, and improving corrosion resistance. The surface finish is improved by reducing the feed rate or increasing the nose radius. It indirectly indicates the height and depth of irregularities in the solid surface. No surface is perfectly smooth; it cannot be determined as each meter has a range of its capability. High surface quality is required in the fields of optics and electronics (lenses, mirrors), medical instruments, microfluidics (nozzle, channel, mixture), and material properties with high durability wear resistance, and toughness. Other factors determine surface finish such as feed, corner radius, cutting speed, depth of cut, feed rate, and workpiece hardness (Kaladhar, 2019, Chen, 2000).

2.4.3 Surface Integrity

Surface integrity is the sum of all elements that describe all conditions occurring on or at the surface of a workpiece. Surface integrity has two aspects. The first is surface topography, which describes the roughness or texture of this outermost layer of the workpiece, i.e. their interface to the base of the matrix material. This term evaluates the effect of manufacturing processes on the properties of the workpiece material.

Surface integrity describes not only the topological (geometric) features of surfaces and their physical and chemical properties, but also their mechanical and metallurgical properties. Surface integrity is an important consideration in manufacturing as it affects properties such as fatigue strength, corrosion resistance, and life (Jitender Sharma Ajay and Kumar Agarwal., 2007).

2.5 Cutting Tool Geometry

In many studies, the cutting tool geometry plays a crucial role in metal cutting. The design of cutting-edge geometry and its influence on cutting performance has long been a research topic in cutting. The cutting edge preparation has a significant impact on tool life. If a tool has the wrong edge, it will quickly fail. Therefore, it is important to consider the tool edge effect to better understand the chip formation mechanism and accurately predict machining performance such as cutting forces, cutting temperatures, tool wear, surface finish, and integrity of the machined surface. The variation in tool geometry is one of the important parameters to consider for desired chip shapes without affecting turning performance. Tool geometry variation is one of the most important parameters to consider in improving turning productivity in terms of tool life, surface finish, and surface integrity (Dogra et al., 2011).

In this study, the influence of tool geometry (cutting edge angle, rake angle, and rake angle) was investigated and tool wear and surface roughness were optimized in hard turning of hardened steel AISI 1055 (52 HRC) using TiN-coated mixed ceramic inserts (Duc et al., 2020).

2.6 Tool Wear

Tool wear is one of the most important aspects affecting tool life and product quality in machining (Sahu & Choudhury, 2015). In the further course of the machining process, the different wear mechanisms lead to increased wear of the cutting tool due to the friction between the workpiece and the tool insert. Three areas can usually be identified in the typical wear growth curve. The first is the break-in period, during which the sharp cutting edge wears out quickly at the beginning of the cutting process and occurs within the first few minutes of cutting. The break-in period is followed by wear that occurs at a fairly steady rate, referred to as the steady-state wear regime. Eventually, wear reaches a level where the wear rate begins to accelerate. This marks the beginning of the failure regime where cutting temperatures are higher and the overall efficiency of the machining process is reduced. If the tool is allowed to continue, it will eventually fail due to a temperature error. The relationship is shown in figure 2.2 for flank wear, a similar relationship is found for crater wear (Groover, 2022).

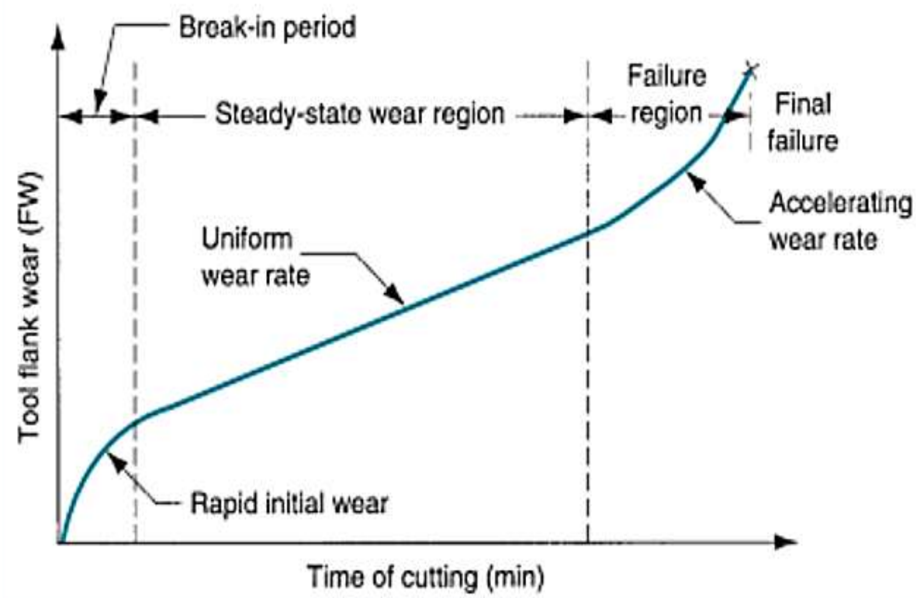

Figure 2. 2 Tool wear as a function of cutting time (Groover, 2022).

Depending on the cutting conditions, work material, and tool material, tool performance is limited by flank wear, crater wear, edge chipping, nose wear, or a combination thereof. Tool wear depends on the tool, workpiece material (physical, mechanical and chemical properties), tool geometry, cutting parameters, cutting fluid, etc. Flank wear was caused by friction between the tool flank and the machined surfaces. Another important wear mechanism for flank wear is adhesion. The interaction between two surfaces can be represented by the metallurgical weld or adhesive bond. Adhesive wear occurs when individual pieces are pulled off the tool surfaces during sliding. Flank wear is attributed to the rubbing of the tool with the workpiece at the interface, resulting in abrasive and/or adhesive wear at high temperatures. Abrasion is the main wear mechanism. Abrasion is the main wear mechanism in flank wear. Crater wear occurs on the rake face of the tool. Wear occurs either gradually through abrasive or adhesive wear, through plastic deformation, through more discrete material losses through discrete fracture mechanisms, or through a combination of these. These effects could be due to high mechanical, thermal, and chemical stresses generated during hard machining. The ability to predict tool wear in hard turning is necessary to determine the optimal cutting variables. It is also useful in avoiding catastrophic tool failures that can damage the workpiece surface and affect machine tool performance (Sahu & Choudhury, 2015).

2.7 Tool Life

Tool life is the machining period during which the cutting tool will perform as desired and satisfactorily. It is the time that a tool cuts satisfactorily and is expressed in minutes between cutting tool changes. Tool life is important in machining because significant time is lost when a tool is changed and reset. Longer service lives lead to higher productivity and lower processing costs. The process of wear and tear of the cutting tool increases the surface roughness and the accuracy of the workpiece deteriorates.

When machining, the tool life mainly depends on the following factors:

- The material of the machined component.
- Cutting material and its shape. Cutting conditions.
- The machining processes.

Taylors Tool Life Equation

Tool wear is always used as a service life criterion because it is easy to determine quantitatively. The flank wear zone is mostly used as a criterion as it affects the roughness and accuracy of the workpiece surface. The Taylor formula for tool life is as follows:

$$VT^n = c \qquad (2.5)$$

Where V is the cutting speed (m/min), T is the tool life (min) required to develop given flank wear, n is an exponent that depends on the cutting parameters, and c is a constant. The values of n and C mainly depend on the tool work materials and the cutting environment.

According to Taylor's original tool life formula, cutting speed is the only parameter that affects cutting tool life. This is because this formula was obtained using high carbon tool material and high-speed steel. With the further development of hard metals and many other cutting materials, it turned out that the cutting feed and the cutting depth are also important. As a result, the Taylor formula for tool life was modified to account for these changes as follows:

$$VT^n f^a t^b = c \qquad (2.6)$$

Where t is the depth of cut (mm) and f is the feed (mm/rev). The exponents n, a, and b are to be determined experimentally for each of the cutting conditions.

2.8 Tooltip Temperature

In this study, examining the cutting temperature during machining is extremely valuable to address metal cutting issues such as dimensional accuracy, surface finish, and tool life (Chinchanikar & Choudhury, 2014). There are three regions in the cutting zone such as primary, secondary, and tertiary shear strain. The heat generated in the primary shear strain zone is due to the plastic deformation of the work material (El-Wardany et al., 1996). The friction between the rake face of the cutting tool chip causes heat generation in the secondary shearing strain zone, while the friction between the tool flank and the machined surface causes heat generation in the tertiary shearing strain zone. The influence of temperature on the machining of steel and the main sources of heat in turning were investigated. According to conducted studies, the following heat was generated when processing materials (Sharma et al., 2008).

- ✓ The heat from the internal friction of the metal during deformation $\left(Q_{def}\right)$.
- ✓ The heat from external friction of the chip on the face of the cutter $\left(Q_{f.fr}\right)$.
- ✓ The heat from external friction of the cutting face and the machined surface $\left(Q_{r.fr}\right)$.
- ✓ The heat is released as a result of chip breakage and scattering $\left(Q_{disp}\right)$.

The total heat generated when cutting hard materials is expressed mathematically as

$$Q = Q_{def} + Q_{f.fr} + Q_{r.fr,} + Q_{disp} \tag{2.7}$$

When the mechanical work is completely converted to heat can be written as

$$Q = (R/E) = p_{zv}(1/E) \tag{2.8}$$

Where p_{zv}R = work of cutting

p_{zv} = component of cutting force along the axis

V= Cutting speed, and

E= mechanical equivalent of heat =427 $\frac{kgfm}{kca}$

In a real situation, not all the cutting work is converted to heat, which means that only part of the work is converted to heat and expressed as

$$Q = P_{zv}\alpha_O / 427 \tag{2.9}$$

Where α_O it takes account of loss

2.9 Cutting Force

Many researchers have studied the force and its effect during the hard machining process. Because knowledge of cutting forces is important to determine power requirements, effectively design machine tools, cutting tools, tool holders, and fixtures, and understand the effects of cutting forces, workpiece machinability, the process of chip formation, and cutting tool wear. A variety of force measuring devices such as dynamometers was able to measure tool forces with high accuracy. One of the most hopeful techniques for identifying cutting conditions is the measurement of cutting forces. Cutting forces are important to achieve dimensional accuracy and stability of the machining system (Thangarasu et al., 2018).

In this study, cutting forces are required for the evaluation of power consumption during machining. In hard machining, the force acting on the cutting material can be decomposed into the thrust force acting in the cutting speed direction, the radial force acting in the radial direction perpendicular to the cutting speed, and the feed force acting in the feed direction. The above three force components act on the tool material during hard turning as shown in Figure 2.3 (Chandra et al., 2018).

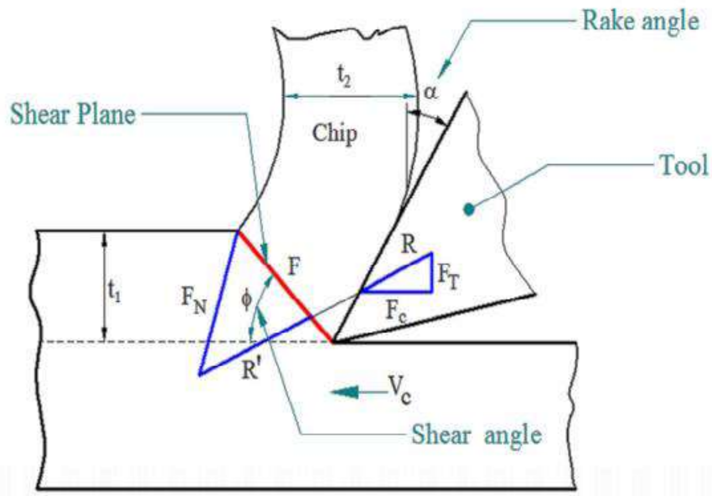

Figure 2. 3 various forces on cutting tool and shear plane (Chandra et al., 2018)

The stability of the machine tool depends on the cutting force that causes the cutting operation and the cutting parameters. In particular, a higher negative rake angle and tool nose radius affect the force increase, especially when using super hard cutting tools, and indicate the need to provide a stable and rigid process (Karkalos et al., 2016, Zhenchao et al., 2018). The equation for the normal and tangential force components per unit width of the grinding process was examined. The grinding force necessary for the grinding state is caused only by the contact between the grinding wheel and the workpiece, which leads to grinding chip formation and friction between grains and the workpiece (Sun et al., 2015). Figure 2.5 shows grinding forces.

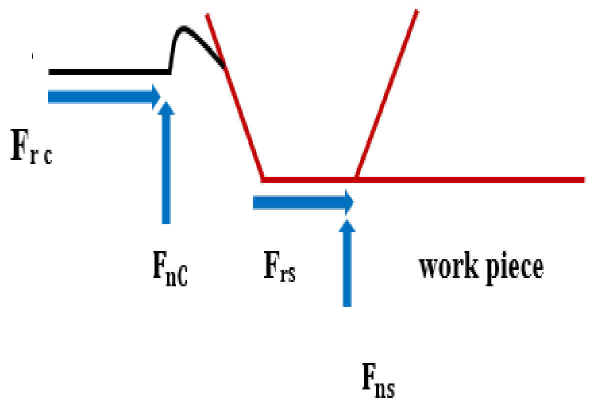

Figure 2. 4 grinding forces (Sun et al., 2015)

Grinding deformation forces and frictional forces are modeled as follows:

$$F_n = F_{nc} + F_{ns} \tag{2.10}$$

$$F_r = F_{rc} + F_{rs} \tag{2.11}$$

Where F_n = Normal grinding power

F_{nc} = Normal grinding force resulting from chip deformation

F_{ns} = Normal grinding force generated by friction

F_r = Tangential grinding force

F_{rc} = Tangential grinding force generated by chip deformation

F_{rs} = Tangential grinding force generated by friction

During high-speed ball milling of Al2O14-T6, the effects of cutting parameters were studied and the cutting force component (tangential force, radial) was measured. The analyzed result shows that the cutting force increases with increasing feed per tooth and axial depth of cut but decreases with increasing cutting speed (Dikshit et al., 2014). Increasing the cutting speed leads to a decrease in cutting force and an improvement in surface finish, and high-speed machining is important to reduce the cutting force in hard machining. In hard milling, milling can be divided into radial force, feed force, and axial force. The axial force has little influence on the cutting process (An et al., 2014).

2.10 Cutting Tool Vibration

In this study, during the machining process, the vibration of the cutting tool is a common problem that affects the machining result and especially the surface finish. Tool life is also affected by cutting tool vibration. As a result of the dynamic movement of the cutting tool and the workpiece, there is often a high level of acoustic noise in the work environment. This means that in all cutting operations such as turning, drilling and milling, vibrations are induced due to the deformation of the workpiece. These indicate several economic and ecological disadvantages (L. Lago et al. 2002). Now the standard way to avoid vibration during machining is to carefully plan the machining parameters. The techniques are usually based on experience and trial and error to obtain appropriate cutting data for each cutting operation involved in machining a product. Machining vibrations occur throughout the cutting process. Although they are influenced by many sources such as machine structure, tool types, and work material, the composition of the machining vibration is complicated. However, at least two types of vibrations have been identified as machining vibrations, namely self-excited vibrations and forced vibrations. Forced vibrations are the result of certain periodic forces present in the machine. the source of these forces can be bad gears, unbalanced machine tool components, misalignment of motors, pumps, etc. self-excited vibrations, also known as chatter. Arise from the interaction of the machining process and the structure of the machine tool, which leads to disturbances in the cutting zone. Chatter always indicates imperfections on the machined surface; Vibrations, especially self-excited vibrations, are associated with the roughness of the machining surface (H. Huang et al., 2001).

2.11 Material Removal Rate

The material removal rate is the size when turning the material/metal that is removed per unit of time in mm3/sec. With each rotation of the job, a circular layer of material is removed.

$$\text{Material Removal Rate (MRR)} = v * f * d \text{ (mm3/sec)} \quad (2.12)$$

Where

v = cutting speed in mm/sec

d = depth of cut in mm

f = feed rate in mm/rev

A process that removes metal faster may not make sense (Manu Garg et.al 2016). With each revolution of the workpiece, a ring-shaped layer of material with the same cross-sectional area is removed. The product of the distance the tool travels in one revolution (feed, f) and the depth of cut (d). The volume of this ring is the product of the cross-sectional area (d) (f) and the average circumference of the ring πD_{avg}.

Where $$D_{avg} = \frac{D_o + D_i}{2} \qquad (2.13)$$

$$d = \frac{D_o - D_i}{2} \qquad (2.14)$$

The RPM of the workpiece is N and the rate of material removal per revolution is πD_{avg} (d) (f) since there are N revolutions per minute and the removal rate is given by

$$MRR = \pi D_{avg} \, df \, N \qquad (2.15)$$

$$MRR = d * f * V_c \qquad (2.16)$$

Where V_c is cutting speed

$$V_c = \pi D_{avg} N \qquad (2.17)$$

(Manu Garg et.al 2016).

2.12 Chip Morphology

In this study, chip morphology is the result of a specific chip formation mechanism that occurs during machining (Davis et al., 2017). Various types of chip morphologies are formed during machining, such as continuous, discontinuous saw teeth that are generated during machining and play a crucial role in optimizing the machining process. Chip formation and effective chip evacuation are important in those machining techniques where the cutting zone is spatially limited, such as drilling, reaming, milling and all turning operations on automatic lathes. It is determined by the combined effects of workpiece materials, cutting parameters, and tool geometry. The chip morphology was studied when hard machining AISI 4340 at high speeds.

The experimental result shows that discontinuous chips are generated due to internal crack initiation and propagation in front of hard materials such as hardened steel, titanium alloy, bearing steel, and die steel due to cutting force oscillation and vibration of a tooling system (X. Zhang et al., 2011). The sawtooth chip formation mechanism of superalloy GH4169 was studied using Finite Element Method (FEM) software and ABAQUS, simulating part deformation during high-speed machining. Various parameters such as cutting force, temperature field, and stress distribution were analyzed to determine the effects of cutting parameters on saw-tooth chip formation and to conclude that tool performance has a major impact on machining parameters and tool life improvement (Kong et al ., 2011).

2.13 Machining Time

The total time, t_{total} to turn a part has three contributors: the time t_{load} it takes to load and unload the part to and from a machine tool; the time t_{active} in the machine tool; and the contribution to the taken to change the turning tool when its edge is worn out. t_{active} is longer than the actual machining time t_{mach} because the tool spends some time moving and being positioned between cuts. t_{active} May be written $\frac{t_{mach}}{f_{mach}}$, where f_{mach} is the fraction of the time spent in removing metal. If machining N parts result in the tool edge being worn out, the tool change time t_{ct} allocated to machining one part is $\frac{t_{ct}}{N}$. Thus

$$t_{total} = t_{load} + \frac{t_{mach}}{f_{mach}} + \frac{t_{ct}}{N} \tag{2.17}$$

(Boothroyd and Knight, 1989).

It is easy to show that as the cutting speed of a process is increased, t_{total} passes through a minimum value. This is because, although the machining decreases as speed increases, tools wear out faster and N also decreases. Suppose the volume of material to be removed by turning is written MRR then

$$t_{mach} = \frac{MRR}{fdv} \tag{2.18}$$

(Boothroyd and Knight, 1989).

The machining time for N parts is N times this. If the time for N parts is equated to the tool lifetime T in the equation above (generalized to $VT^n = c$), N may be written in terms of n and C, f, d, V_{vol} and V, (Boothroyd and Knight, 1989).

$$N = \frac{fdv^{\frac{1}{n}}}{MRRV^{(1-n)/n}} \tag{2.19}$$

(Boothroyd and Knight, 1989).

Substituting equations into the equation

$$t_{total} = t_{load} + \frac{1}{f_{mach} fdv} \frac{MRR}{fdv} + \frac{MRRV^{(1-n)/n}}{fdv^{\frac{1}{n}}} t_{ct} \tag{2.20}$$

(Boothroyd and Knight, 1989)

2.14 Dry Machining

Dry machining is a machining process without the use of cooling lubricants during machining. Dry machining can offer a cost advantage and flexibility on machine tools when large sumps are not required. Dry machining is ecologically desirable and is seen as a necessity for manufacturing companies shortly. The industry will be forced to consider dry machining to enforce environmental health and safety legislation. The advantages of dry machining include non-pollution of the atmosphere (or water); no residues on the chips, which would translate into reduced disposal and cleaning costs; no health hazard; and it is not harmful to the skin and is allergy-free. In addition, it offers a cost reduction in processing (Siva Surya et al., 2017).

2.15 Design of Experiments

2.15.1 Taguchi Optimization Method

The Taguchi Method is one of the most important tools used in industry to shorten product design, save development time and reduce product cost. Taguchi's method also considers the effect of uncontrollable factors on the response. This technique is also very flexible and can assign different factor levels even if the number of factor levels is not the same. In the Taguchi approach, optimization, data analysis, and prediction of the optimal results are provided by the objective function called the signal-to-noise (S/N) ratio. Signal factors represent system control inputs. Noise factors represent variables that are expensive or difficult to control. The commonly used S/N ratios are nominal, the better, the lower the better, and the larger the better. Different parameters affect the reaction to different extents. The relative effect of the various parameters is determined using analysis of variance (ANOVA). S/N ratio and ANOVA provide the determination of the optimal cut parameters for the reaction. Finally, in the Taguchi method, confirm tests are recommended to verify the effectiveness and efficiency of the Taguchi method in optimizing the parameters (Krishnaiah & Shahabudeen, 2012). The Taguchi method involves reducing the variation in a process through the robust design of experiments and developing an experimental design method to study how different parameters affect the mean and variance of a process performance property that defines how well the process is performing is working. The Taguchi-based orthogonal array has the property of reducing the number of experiments without significantly affecting the outcome (Mia et al., 2018).

2.15.2 Hybrid Taguchi and Grey Relational Analysis Optimization

The traditional Taguchi technique can optimize only a single response variable under the effect of multiple parameters. Therefore, this technique is combined with grey relational analysis (GRA) to optimize multi-process parameters for multiple response variables that this research tends to address. GRA is widely used to convert multiple response variables into a single grey relational grade (Fei et al. (2013). In this method, the signal-to-noise (S/N) ratio is used to represent a performance characteristic and the largest value of the S/N ratio is considered. Based on the objective of the experiment, any one of the S/N ratios, namely lower-the-better, the higher-the-better, or the nominal-the-better is selected for further analysis. Grey system theory developed by Prof. Deng in 1982 has proved to be a useful tool in dealing with poor, incomplete, and uncertain information. GRA based on the grey system theory can also be used to solve the complicated interrelationships among the multiple performance characteristics effectively. GRA is used to obtain a grey relational grade to evaluate such multiple performance characteristics. As a result, the optimization of complicated multiple performance characteristics can be converted into the optimization of a single grey relational grade (S Dharmalingaml et al. 2013).

2.16 Summary of Literature Review

Table 2. 1 Summary of literature review

No	Title	Author(s) and years	Material and hardness	Tool/ insert	Work condition			Output response(s)	Method/ techniques	Results
1	Performance analysis of developed micro-textured cutting tool in machining aluminum alloy 7075-T6: assessment of tool wear and surface roughness	Musavi et al. (2022)	aluminum alloy 7075T6	tungsten carbide insert	v	f	d	Tool wear and surface roughness	Taguchi Robust design—An Analysis	Ra= 1.64 µm Tool wear =0.225mm
					100	0.1	0.2			
					125	0.15	0.3			
					150	0.20	0.4			
2	Analysis of tool vibration and surface roughness during turning process of tempered steel samples using the Taguchi method	Kam and Demirtaş(2021)	AISI 4340 46 and 53 HRC	ceramic cutting tool	v	f	d	Surface roughness	Taguchi Method	Ra= 0.255 µm
					180	0.08	-			
					220	0.14	-			
					260	0.20	-			
3	Optimization of Material Removal Rate and Surface Roughness of AISI 316L under Dry Turning Process using Genetic Algorithm	Martowibowo and Kemala Damanik (2021)	AISI 316L (chromium-nickel molybdenum)	cemented carbide tool	v	f	d	material removal rate or the surface roughness	Genetic Algorithm	Ra = 0.458 µm MRR = 0.178mm^3/min
					95	0.053	0.4			
					127	0.11	0.8			
					185	0.21	-			
4	Optimization of turning process parameters in machining heat-treated steel	Shahid (2020)	Heat Treated Steel (EN-9)	Carbide insert	v	F	d	surface roughness	Taguchi's L9 orthogonal array	Ra= 6.13 µm
					300	0.1	0.2			
					450	0.2	0.4			
					600	0.3	0.6			
5	Cutting parameters optimization for surface roughness during dry hard turning of EN 31 bearing steel using CBN insert	Karthik et al. (2020)	EN31 steel	CBN inserts	v	F	d	surface roughness	Taguchi L9 Orthogonal array method and ANOVA	Ra = 0.1492 µm
					100	0.04	0.1			
					200	0.08	0.2			
					300	0.12	0.3			

6	Analysis and modeling of surface roughness based on cutting parameters and tool nose radius in turning of AISI D2 steel using CBN tool	Patel and Gandhi (2019)	AISI D2 steel and 57 HRC	CBN (cubic boron)	v	f	d	Surface Roughness.	ANOVA	Ra = 0.504 µm
					80	0.04	0.2			
					116	0.12	-			
					152	0.2	-			
7	Wear performance and mechanisms of PCBN tool in dry hard turning of AISI D2 hardened steel	Tang et al. (2019)	AISI D2steel at various hardness levels (40–60)	PCBN	250	0.1	0.15	Tool wear mechanism	SEM, S/N	Wear=33 to 39 µm
8	Taguchi S/N-based optimization of machining parameters for surface Roughness, tool wear, and material removal rate in hard turning under MQL cutting conditions.	Mia et al. (2018)	AISI 1060 steel And 47 HRC	Coated cemented carbide tool	v	F	d	Surface roughness, material removal rate, and tool wear parameter	Taguchi orthogonal array, signal-to-noise ratio-based optimization	Ra= MRR=
					45	0.1	1			
					60	0.1	1.5			
					75	-	-			
					90	-	-			
9	Optimization of machining process parameters in conventional turning operation of Al5083/B4C composite under dry condition	Singh et al. (2018)	Al5083 metal matrix composite	HSS cutting tool	v	f	d	Material removal rate	response surface methodology	MRR= $3.64mm^3$/min
					60	0.18	0.087			
					93	0.3	0.187			
					145	0.4	0.218			
					288	0.5	0.250			
					384	0.6	0.312			
10	Multi-Response Optimization On En19 Steel Using Grey Relational Analysis Through Dry & Wet Machining	Siva Surya et al. (2017)	EN19 steel	Carbide cutting tool	v	F	D	material removal rate (MRR) and surface finish	Grey Relational analysis	MRR= $0.895mm^3$/se Ra= 0.866 µm GRG= 0.7565
					500	0.048	0.3			
					770	0.059	0.5			
					1200	0.090	0.7			

11	Effects of coating material and cutting parameters on the surface roughness and cutting forces in dry turning of AISI 52100 steel	Keblouti et al.(2017)	AISI 52100 steel	coated (with TiCN-TiN)	v 150 200 250	f 0.08 0.12 0.16	D 0.15 0.30 0.45	surface roughness and cutting forces	Response Surface Methodology (RSM)	Ra= 0.77 µm F= 78.65N
12	An experimental study of cutting forces and temperature in multi-tool turning of grey cast iron	Kalidasan et al. (2016)	grey cast iron	TiN-coated carbide inserts	v 75 120 185	f 0.08 - -	d 0.25 0.5 0.75	Cutting force and cutting temperature.	Taguchi method	T^0C = 60°C F = 180 N
13	Double tool turning: machining accuracy, cutting tool wear, and chip morphology	Kalidasan, Senthilvelan, et al. (2016)	Cast iron	TiN carbide insert	v 116 - -	f 0.24 - -	d 1 1.5 2	Tool wear and chip morphology	GRA	Ra = 1.86 µm
14	Evaluation and comparison of lubrication methods in finish machining of hardened steel mold inserts	Chan and Xu (2015)	hardened steel	Mold insert	f 0.03 0.06 -	ST 0.05 0.1 -	d 0.1 0.2 -	Surface roughness	Response surface methodology	Ra=0.28 µm
15	Effect of Machining Parameters and Machining Time on Surface Roughness in Dry Turning Process	Qehaja et al. (2015)	cold rolled steel C62D	coated tungsten carbide inserts	f 0.285 0.214 0.178	r 1.2 0.8 0.4	T 3950 2590 1700	Surface roughness	Regression model analysis	Ra=1.012 µm

2.17 Research Gap

The review of the literature reveals that there were limited studies conducted experimentally, to obtain the optimum machining condition of AISI 1050 steel material using a double cutting tool turning operation during the dry condition. As observed from the literature, several researchers have focused on the study of the effect of cutting parameters, workpiece hardness, tool geometry, cutting tool vibration, tool material, cutting fluids on the surface quality of the machined part, and machinability aspects, for different workpieces using single cutting tool turning operation. In addition to this, to achieve the best surface quality the study of the combined effect of cutting parameters during dry machining conditions using the double tool turning method should not be compromised. Identifying the optimal cutting parameters where the surface finish is good, cutting temperature is minimum, and the material removal rate is high to bridge the gap between quality and productivity when turning AISI 1050 steel material by using a double cutting tool turning process under dry machining conditions.

Therefore, to fill this gap an experimental investigation is done to study the parametric optimization of double cutting tool turning during the dry condition of AISI 1050 steel using a conventional machining process to achieve the optimum machining parameters.

CHAPTER THREE

3 MATERIALS AND METHODOLOGY

3.1 Introduction

This work focuses on experimentally studying the machining of AISI 1050 steel material and optimizing the effects of cutting parameters on the Surface finish, Material Removal Rate, Cutting Temperature, and Chip Morphology in inflexible turning with a ceramic cutting tool through experimental work. This chapter aims to present the details of the experimental procedures and the material used for the study. Under dry machining conditions for AISI 1050 steel material double tool turning operations by using a conventional lathe, machine tool model of COMEV CM 260 specification made up of MONTENACHI-Italy. All machines and equipment were presented with supporting photos and schematic diagrams.

3.2 Experimental Procedure

Figure 3.1 shows a general study status of an experimental investigation of the dry machining conditions in double tool turning.

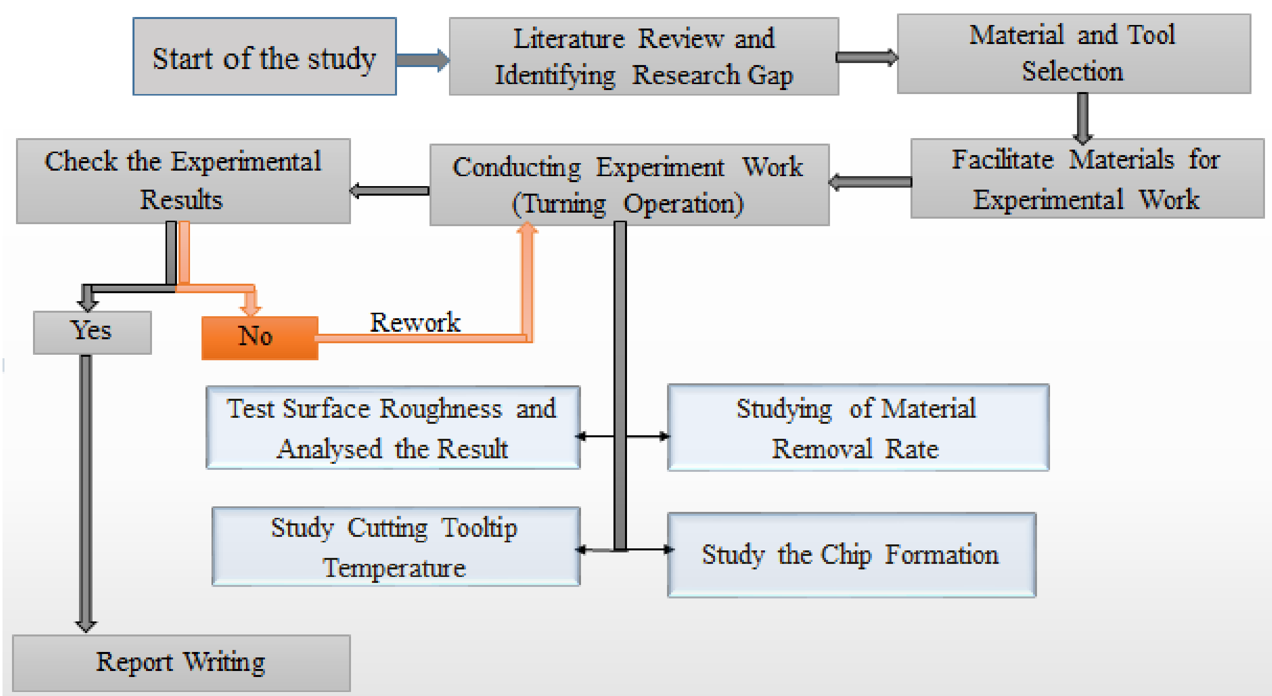

Figure 3. 1 Flow Chart for Experimental Work

3.3 Tool Fixture for Experiment Setup

The tooling fixture used in this experiment was manufactured from high carbon steel by using a vertical milling machine model of MW 50 used to mount the lathe's tool post firmly. The manufacturing process of tool fixtures was performed on lathe machines in Akaki basic metal industry.

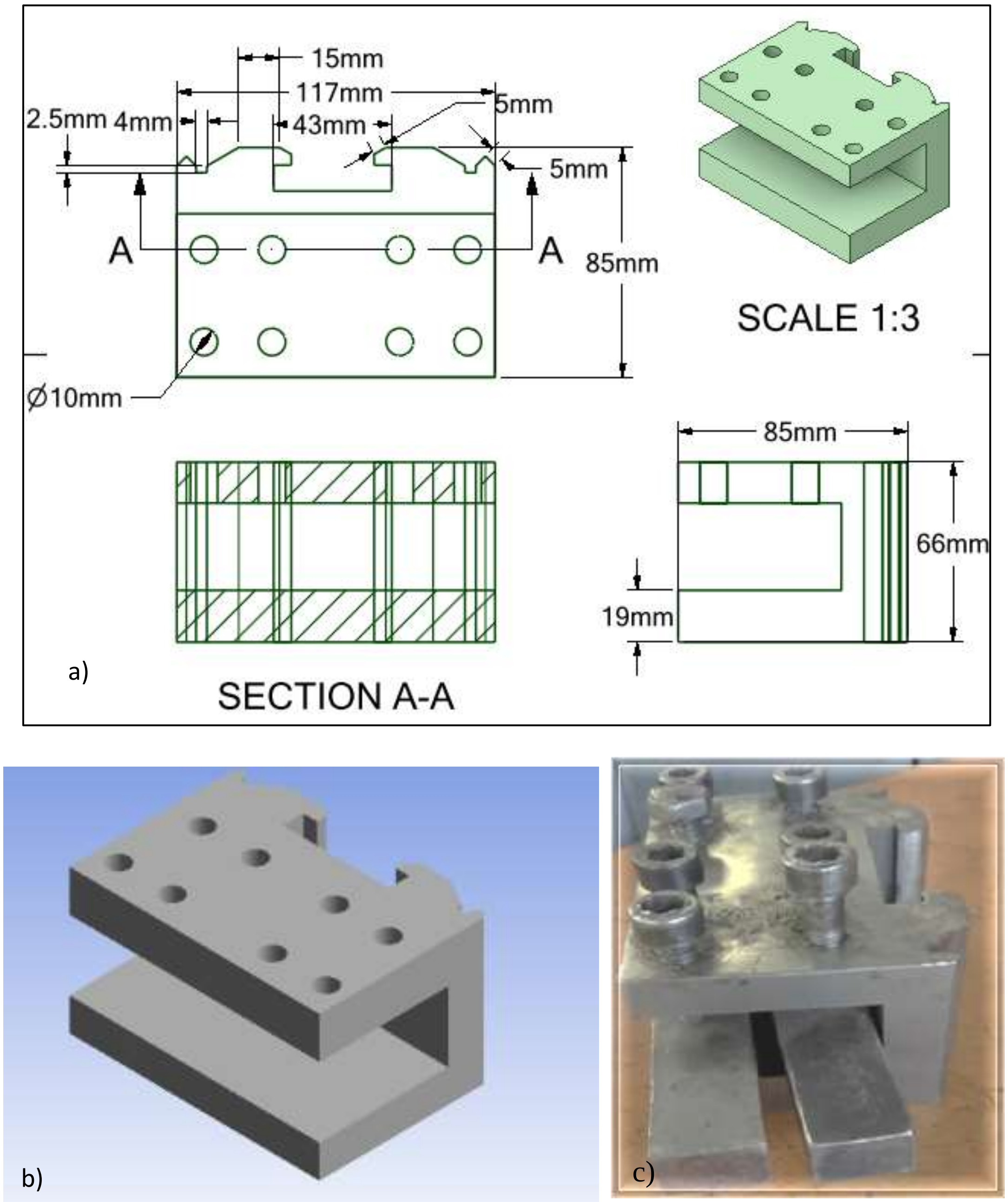

Figure 3. 2 (a, b, c): a) Detail multiview drawing of tool fixtures b) 3D Model of tool fixture, and c) Photos of Tool Fixtures

3.4 Materials and Machine Tools

This subtopic describes the materials and machine tools used for the experimental study of double turning of AISI 1050 steel material on a lathe as follows.

3.4.1 Workpiece Material

The workpiece material used in this study was AISI 1050 steel, which was used for double-cutting tool turning operations on the conventional lathe tool COMEV CM 260. AISI 1050 steel is used as the workpiece material (medium carbon steel) to conduct the experiments to optimize cutting parameters. The AISI 1050 steel material is in the shape of a bar with a diameter of 30mm, a length of 700mm, and a hardness of 58 HRC (Rockwell hardness). AISI 1050 steel material has been used for experimental studies due to its applications in automobiles, crankshafts, spindles, connecting rods, pumps, gears, shafts, bolts, axles, pulleys, drive pinions and many applications in general engineering. AISI 1050 steel material has high tensile strength, good abrasion resistance, and mechanical strength, and has been widely used in industry.

Figure 3.3 AISI 1050 Steel Materials for Experimental Work.

Chemical Composition

As observed from spectrometer testing in weight percentage. The specific chemical composition of the AISI 1050 steel material used for the experimental study is shown in Table 3.1.

Table 3. 1 Chemical Composition of AISI 1050 Steel Material is as follows.

Element	C	Si	Mn	P	S	Cr	Mo	Ni	Al	Co
% of concentration	0.48-0.50	0.16	0.49	0.032	0.021	0.032	0.019	<0.005	<0.003	<0.002

3.4.2 Cutting Tool Materials

In this study, the ceramic insert cutting tool is used for experimental purposes. The ceramic tool is very hard and can withstand high temperatures of more than 1500°C without chemical decomposition. These characteristics recommend the use of ceramic tools in dry machining conditions and for machining metals at high cutting speeds. Therefore, in this study, the ceramic tool is used for investigation because of its excellent properties such as good surface finish, economy, fracture resistance, high hot hardness, high melting point, good chemical inertness, high compressive strength, chemical stability at elevated temperature, thermal shock resistance, high stability against abrasive particles, high resistance to mechanical stress, dimensional stability at elevated cutting temperatures, wear resistance in a wide range of high-speed finishing operations and the high removal rate when machining hard materials (Umbrello et al., 2010, J. R. Davis, 2022, Senthil Kumar et al., 2003).

The ceramic cutting tools are made of fine-grain aluminum oxide (Al2O3), although some manufacturers add other oxides (e.g. zirconium oxide) in small amounts. Other commercially available ceramic cutting tool materials include silicon nitride (SiN), sialon (silicon nitride and alumina, SiNAl2O3), alumina, titanium carbide (Al2O3-TiC), and alumina reinforced with single-crystal whiskers of silicon carbide (Groover, 2022). The ceramics currently used in metal cutting are based on either aluminum oxide (Al2O3) or silicon nitride (Si3N4).

Detail of Cutting Tool

The cutting tool used was a mixed Al2O3-TiC ceramic insert containing 77% Al2O3, 21% Tic, and 2% of another material used according to ISO specification TNGA 160408 with a tool holder of MTJNR2020M10. According to the orthogonal rake angle system of the tool geometry definition, the tool insert used had a tool signature of -6, -6, 6, 6, 30, 0, and 0.8mm. This means that these values apply respectively to the rake angle, orthogonal rake angle, orthogonal major flank clearance, orthogonal margin clearance, minor cutting edge angle, major cutting edge angle, and tip radius of the tool insert. Note that a new tool insert was used for each machining run, so the effect of tool wear remains the same for all trial runs. Each machining run was performed for a length of 30mm (the time for each run varied due to the variation in cutting speed).

Designation of cutting tool inserts / TNGA 160408

T: Triangle 60° (Shape),

N: 0° (Clearance)

G: ± 0.025 mm (Tolerance)

A: Cylindrical (Hole shape)

16: Length of cutting edge,

04: Thickness, and 08: 0.8 mm (Corner radius)

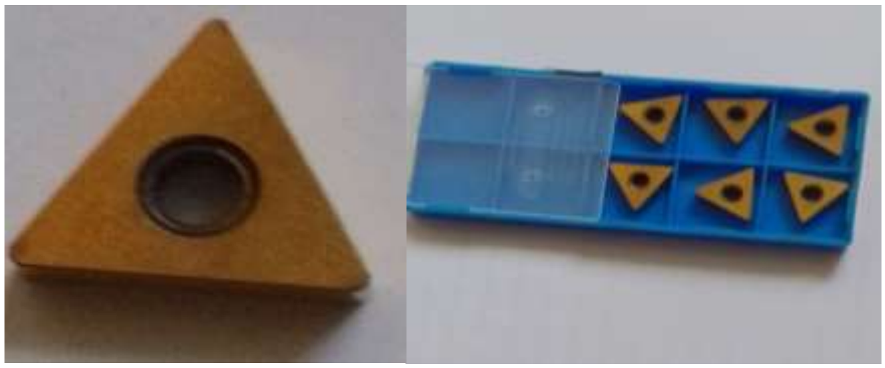

Figure 3. 4 ceramics cutting tool insert

Designation of tool holder/ MTJNR 2020

M10

M: Multi-Lock (Holding Method)

T: Triangle (Insert Geometry)

J: Side cutting edge angle offset (Tool style)

N: Negative (Insert clearance angle)

R: Right hand (Hand of the tool)

20: Square size

20: Rectangle size

M: 20mm (Length of tool holder), and 10:

Cutting edge length (Insert size)

Figure 3. 5 Tool Holder Inserts for Experiment Run.

3.4.3 Lathe Machines

The double tool turning operations were conducted mainly on a conventional lathe machine, a model of COMEX CM260 powered by a 7.5KW motor with a spindle speed range of 36 up to 2500 rpm.

Figure 3. 6 Conventional Lathe Machine used for Experimental Work

3.4.4 Thermocouple

In this study, a contact – types digital thermometer device consisting of sensor metals used in the form of wires contact the end of the cutting tool edges at which the cutting tool and workpiece contact each other, wire contact the edges of the cutting tool. The tool work thermocouple can also be used to measure the temperature at the cutting point of the tool.

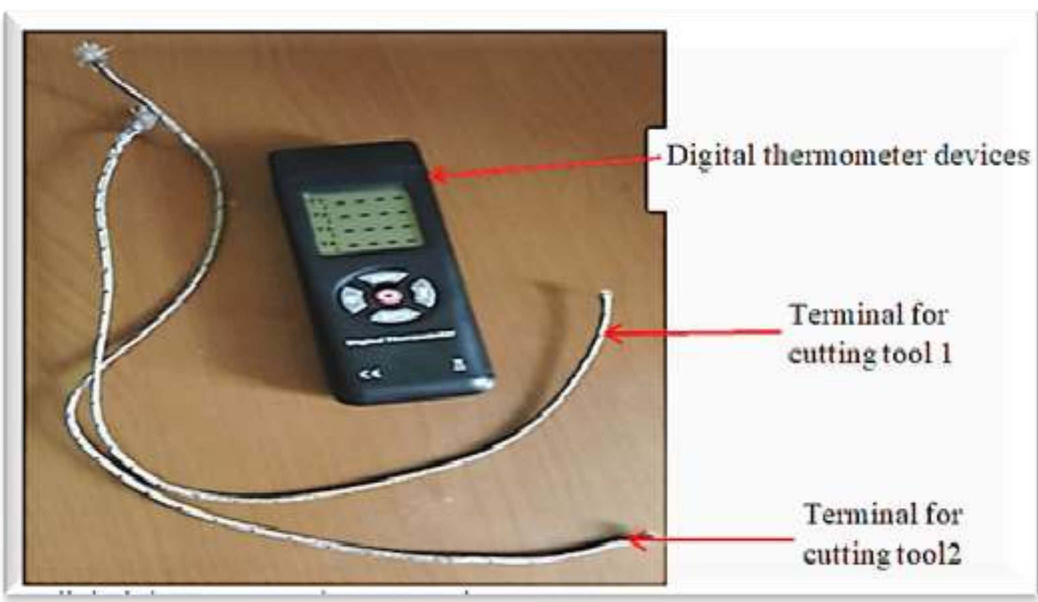

Figure 3. 7 Digital Thermometer Thermocouple Temperature Testers

3.4.5 Profilometer

A Profilometer is a measuring instrument used to measure a surface's profile, to quantify its roughness. The instrument used to measure surface roughness was a contact type, Model:

657111 and SN: A00115021810, reading distance range was 0.6mm and the maximum measuring range was 10μm. Surface Roughness (Ra) data were taken at two different locations, 120 from each other.

Figure 3. 8 Profilometer Measurement of Surface Roughness Device

3.4.6 Spectrometer

Optical Emission Spectroscopy (OES) analysis is a rapid method for determining the elemental composition of a variety of metals and alloys. For testing the chemical composition of AISI 1050 steel material was used SPECTROTEST TXC02 model machine.

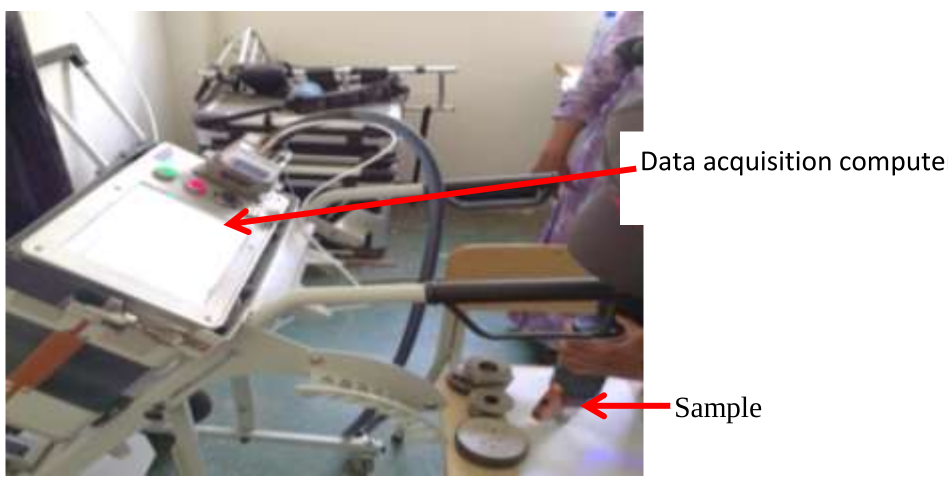

Figure 3. 9 Spectrometer Devices

3.4.7 Experimental Setup

The experiments study had performed in a conventional lathe machine COMEV CM 260 model was used and the cutting tool used was ceramics inserted double tool cutters, both cutting tools were secured in the cutting tool holder that was modified for two cutting tools. According to the process, parameter design conducted experimental work at Akaki Basic Metals Industry (ABMI)

Figure 3.9 shows that the clamped AISI 1050 steel workpiece material diameter of 30mm and 700mm length used for experimental study and double cutting tool holder.

Figure 3. 10 Machine Tool Setup for Experimental Work

3.5 Design of Experiment

3.5.1 Taguchi Optimization Method

Taguchi's, one of the Designs of Experiment (DOE) applications, are used to analyze the effect of numerous parameters and their behavior by running a minimum number of experiments and observing their effect on a specific behavior. It can conjointly determine the optimal conditions for the experiment to achieve a better result. As stated by Taguchi, it has three main phases and consists of planning, execution, and analysis. The optimized parameters are determined by the signal-to-noise ratio (Krishnaiah & Shahabudeen, 2012). Four cutting parameters such as cutting speed, feed, and first and second depth of cut were taken into account. In the Taguchi DOE concept, the preference for an orthogonal array arrangement depends on the total degrees of freedom of the process parameters. The degree of freedom is considered or defined as the number of comparisons between the parameters required to optimize each parameter (factor) with the selected levels. The test planning of the process parameters and the numerical analysis is carried out by the statistical software Minitab 17 with four factors and four test levels.

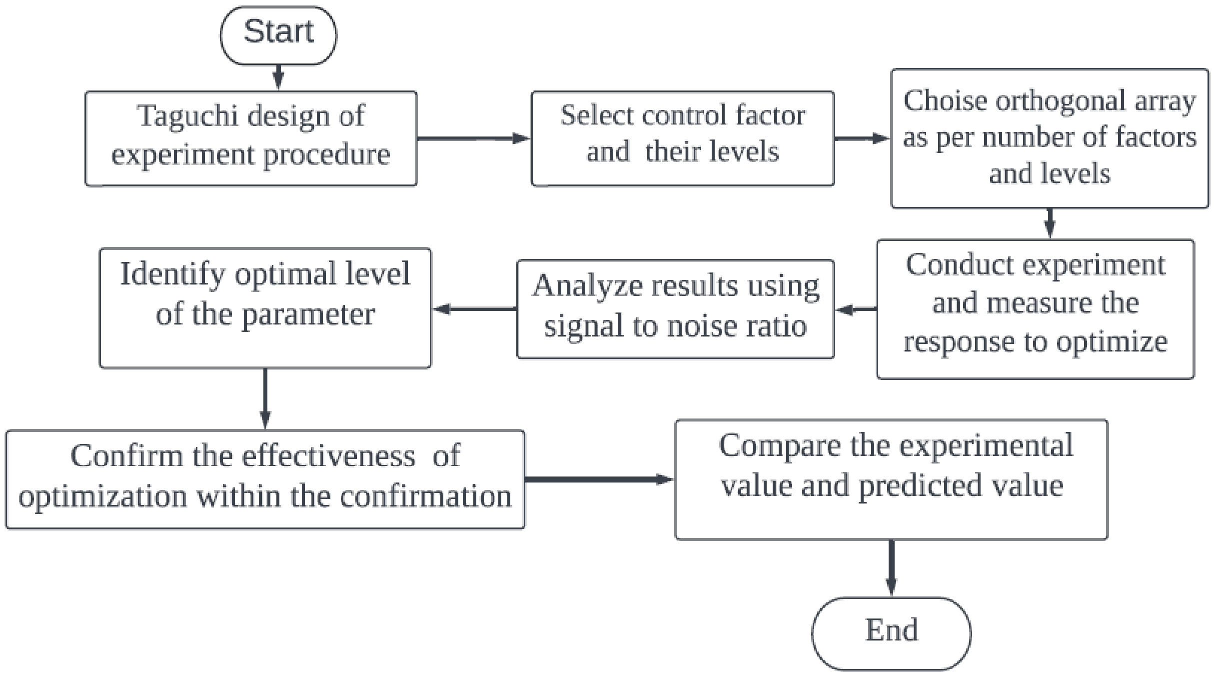

Figure 3. 11 Flow Chart of Experimental Design of Taguchi Method

One of the important tasks is the selection of the cutting parameters for the experimental investigations. In this experimental study, the effect of cutting parameters on surface roughness, cutting tool temperature and material removal rate was evaluated at three study planes in dual tool turning of AISI 1050 steel. Cutting parameters such as cutting speed, feed, and depth of cut for both cutters were selected for test purposes. As mentioned, these cutting parameters were selected depending on the findings found in Preview based on revised literature, following tool manufacturer's recommendations, and current industry practice, specifically in Akaki Basic Metals Industry.

3.5.1.1 Selection of Orthogonal Array

Before choosing the orthogonal array, set the minimum number of experiments to perform based on the total number of degrees of freedom. The minimum number of experiments that need to be performed to study the factors must be larger than the total degrees of freedom available (Krishnaiah & Shahabudeen, 2012). In this study, the selection of a specific orthogonal array was based on the number of levels of various factors. Here, four factors at four levels were selected to carry out the experiments; these parameters are given in table 3.2.

$$DOF = P * (L-1) \quad (3.1)$$

Where, DOF= degree of freedom,

P = number of factors and,

L = number of levels

DOF= 4(4 – 1) = 12≈ L16.

The degree of freedom (DOF) was calculated and then the number of experimental runs was selected from the orthogonal array. The total number of the orthogonal array (OA) experiment should be greater than or equal to the calculated value, so due to this orthogonal array, L16 is chosen for the design of the experiment. Therefore, the Minitab 17 statistical software L16 orthogonal array design has been shown in the following table, and this array specifies sixteen experiments.

Table 3. 2 the Experimental Design of the Cutting Parameters

No	Cutting Parameters			
	Cutting speed(mm/rev)	Feed (mm/rev)	First depth of cut(mm)	Second depth of cut(mm)
1	1	1	1	1
2	1	2	2	2
3	1	3	3	3
4	1	4	4	4
5	2	1	2	3
6	2	2	1	4
7	2	3	4	1
8	2	4	3	2
9	3	1	3	4
10	3	2	4	3
11	3	3	1	2
12	3	4	2	1
13	4	1	4	2
14	4	2	3	1
15	4	3	2	4
16	4	4	1	3

3.5.1.2 Data Analysis and Parameter Optimization

The results obtained from different experiments were analyzed in detail. The parameters were optimized using the statistical software Minitab 17. The surface roughness, material removal rate, and cutting tooltip temperature experimental survey data were converted into the signal-to-noise ratio (S/N). The signal-to-noise ratio is interpreted as the ratio of the mean value of the signal to the standard deviation of the noise value. It is used to determine the rank of input process factors or parameters. There are three types of quality characteristics, namely larger is better, smaller is better, and nominal is best (Krishnaiah & Shahabudeen, 2012). For surface roughness and cutting tooltip temperature, the smaller is the better characteristics shown in the following equations are used

$$\frac{S}{N} = -10\, log(\frac{1}{n}\sum_{j=1}^{3} y_j^2) \quad (3.2)$$

(Krishnaiah & Shahabudeen, 2012)

For material removal rate (MRR) the larger is the better characteristics shown in the following equations are used

$$\frac{S}{N} = -10\log(\frac{1}{n}\sum_{j=1}^{3}\frac{1}{y_j^2}) \quad (3.3)$$

(Krishnaiah & Shahabudeen, 2012)

Where y_j is observation, n is the number of observations. The process parameters and their four levels used for the experimental study of AISI 1050 steel are shown in Table 3.3 Experimental results of response parameters with their corresponding S/N ratio have been listed in a distinctive subtitle.

3.5.1.3 Analysis of Variance

Analysis of variance for the study is calculated by Minitab 17 statistical software and analysis of a response parameter for multiple experimental responses. ANOVA is the statistical technique used to find the influence of all control parameters. Analysis of variance used the percentage contributions of each control factor to measure the corresponding impact on performance characteristics. The significance level of 5% was taken into account, i.e. for a 95% confidence level. From the analysis of variance, the percentage contribution of each influential parameter was calculated using the following formula (Krishnaiah & Shahabudeen, 2012).

$P(\%) = \frac{SSTR}{SST} * 100$ (3.4) (Krishnaiah & Shahabudeen, 2012)

Where P is the percentage contribution of individual factors, SSTR is the sum of squares or treatment sum of squares and SST total sum of squares.

3.5.2 Taguchi and Grey Relational Analysis Optimization Techniques

Several optimization techniques deal with surface roughness and MRR, cutting temperature among all the aforesaid techniques. Grey relational analysis is used for multi-objective optimization problems. Complex problems having minimal information can be solved by grey theory, it is an evaluation technique based on the random uncertainty of small samples. The 'white' system means the system which has complete information, whereas a 'black' system has no known information. Any system lies between these two that is a 'grey' system with limited information.

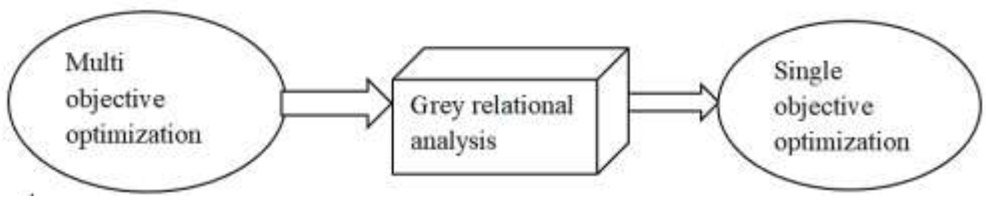

Figure 3. 12 Purpose of Grey Relational Analysis

3.5.2.1 Transform the Original Data from the Taguchi Experiment into S/N Ratios

To transform the original data from the Taguchi experiment into S/N ratios for a response using the appropriate formula depending on the type of quality characteristic now the data has to be transformed into an S/N ratio. Since material removal rate (MRR) has to be maximized, it is larger—the better type of quality characteristic. Hence the S/N ratio for MRR is computed from the following formula:

$$S/N\ ratio(\eta) = -10\log\left(\frac{1}{n}\right)\sum_{i=1}^{n}\frac{1}{y^2_{ij}} \quad (3.5)$$

The second performance measure (response) is smaller—the better type and its S/N ratio are computed from the following formula:

$$S/N\ ratio(\eta) = -10\log\left(\frac{1}{n}\sum_{i=1}^{n} y^2_{ij}\right) \quad (3.6)$$

3.5.2.2 Normalizing Sequence

The Taguchi method optimizes a single response at one time, whereas GRA optimizes multiple responses at a time. In the GRA optimization process, the measured values of k and COF are normalized between 0 and 1. The purpose of this normalization is to remove the variations in the range of responses. To normalize the two quality characteristics, i.e. k and COF, with 'lower-the-better' and 'larger the better' quality characteristics, the following equation 3.7 and 3.8 was used respectively (S. Das et al. 2020).

$$x_i^*(j) = \frac{\max \chi_i(j) - \chi_i(j)}{\max \chi_i(j) - \min \chi_i(j)} \quad (3.7)$$

$$x_i^*(j) = \frac{\chi_i(j) - \min \chi_i(j)}{\max \chi_i(j) - \min \chi_i(j)} \quad (3.8)$$

3.5.2.3 Determination of Deviation Sequence

Where $\Delta_{0i}(j)$ deviation is sequence data and $\chi_0^*(j)$ is the experimental result for the 0^{th} experiment using jth response. $\chi_i^*(j)$ is the experimental result for the i^{th} experiment using j^{th} response (S. Das et al. 2020).

$$\Delta_i(j) = \left| \chi_0^*(j) - \chi_i^*(j) \right| \quad (3.9)$$

3.5.2.4 Determination of Grey Relational Coefficient

Where $\Delta_i(j)$ is the absolute value of the difference between $\chi_0^*(j)$ and $\chi_i^*(j)$, $\Delta\max$ and $\Delta\min$ are global maximum and global minimum values in different data series, generally, the distinguishing coefficient (n) = 0.5 is taken. After the responses are normalized, the grey relational coefficient (GRC) was calculated using equation 3.9 (S. Das et al. 2020).

$$\varepsilon_i(j) = \frac{\Delta\min - \varepsilon\Delta\max}{\Delta_i(j) - \varepsilon\Delta\max} \quad (3.10)$$

ε is usually considered as 0.5

3.5.2.5 Determination of Grey Relation Grade

The mean of the GRC of each quality characteristic was used to estimate grey relational grade (GRG) as depicted in Equation 3.9 (S. Das et al. 2020).

$$y_i = \frac{1}{n}\sum_{j=1}^{n} \varepsilon_i(j) \quad (3.11)$$

3.5.2.6 Determination of Optimal Parameters

In this experiment, the optimization of a parameter is done by the Taguchi optimization method on Minitab 17 statistical software and the grey relational analysis method is used to change the responses into one an S/N ratio, and the GRG value is used to optimize the parameters. This method enables us to optimize several parameters at a time. Grey Relational Grade was calculated for each experiment data and considered as a response for the next analysis. At this stage, the best quality characteristic 'smaller the best' and 'larger the best' has been used for further analysis, as they give the best performance of material removal rate and smaller is better is used for surface roughness and cutting temperature. The GRG obtained is analyzed by Analysis of Variance (ANOVA) and it provides the statistical significance of input process parameter over output and their results were shown in.

3.5.2.7 Prediction of GRG under Optimal Parameters

The next step is to determine and confirm the development of quality traits through the optimal parametric combination using Minitab 17 software. The predicted optimal state can be calculated by software to obtain optimized parameters.

3.5.3 Confirmation Test of the Experiment

A confirmation experiment is conducted using the optimal levels of the significant factors. Once the optimal combination of process parameters and their levels was obtained, the final step is to verify the predicted result against experimental results. If the optimal combination of parameters and their levels coincidently match with one of the experiments in the orthogonal array and then no confirmation test is required.

3.6 Measurement of Surface Roughness

Surface roughness is the most decisive parameter in the machining process, as it is considered the basis of the product quality. It measures the refined inadequacy of the surfaces. The quality of the surface made using conventional and non-conventional machining is important because a smooth surface (better-finished components) reduces the chances of surface damage caused by wear, and corrosion improves fatigue strength, and creep failure, increasing productivity & economics of the industry. Likewise, the quality of a part made by turning operation can affect the performance of the surface for wear and corrosion prevention. The surface profiles of all samples were quantitively analyzed to determine the statistical standard parameter of average roughness, Ra by using a tally surface. The roughness of a surface cannot be easily defined by a single parameter. It’s a basic property of the surface and every test condition was repeated at least two times at different new locations on a specimen surface to ensure the repeatability and reproducibility of the result. In this research, the surface roughness parameters were measured by using the model: 657111 and SN: A00115021810 surface contact profilometer roughness testers. During the surface roughness data collection, the two readings were taken at two different locations after each machining run, and afterward, the mean value was accepted for further analysis.

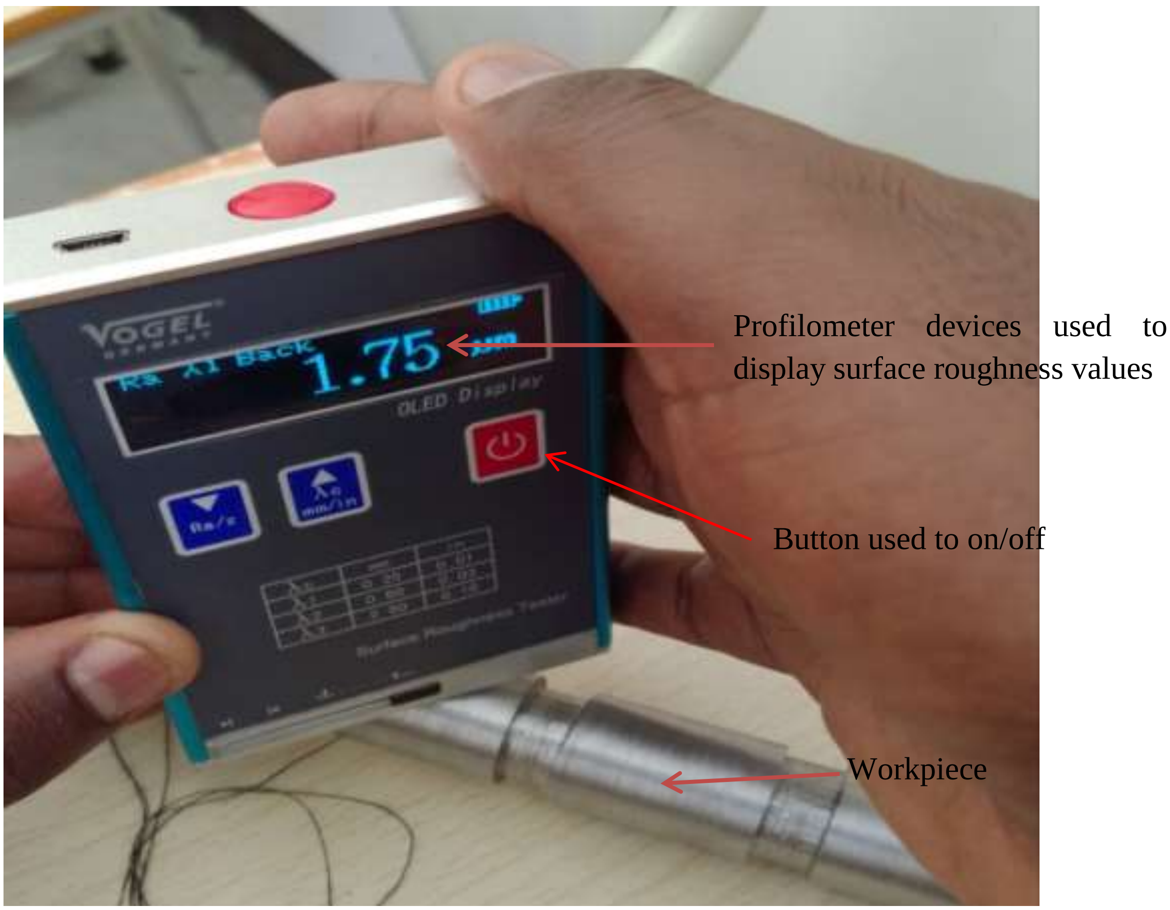

Figure 3. 13 Surface Roughness Testers

3.7 Measurement of Material Removal Rate (MRR)

The material removal rate is the amount of material removed per unit time and ultimately determines machining productivity in roughing operations and production of large batches, the material removal rate needs to be maximized (El-Hofy, 2013). In the present investigation, the following formula has been used to compute the material removal rate

$$MRR = Vc \ x \ f \ x \ ap \tag{3.12}$$

Where, MRR = Material Removal Rate,

f = Feed (mm/rev),

Vc = cutting speed (m/min), and

ap = total depth of cut (mm).

ap = d2+d1

3.8 Measurement of Tooltip Temperature

During machining, the heat generation in the cutting zone has a strong influence on the tool wear, and workpiece surface quality; produces hot chips that cause safety hazards to the machine operator, and can cause inaccuracies in work part dimensions due to thermal expansion of the work material. There are three main zones in the cutting region. They are primary, secondary, and tertiary shear deformation zones. The heat generated in the primary shear deformation zone is due to the plastic deformation of the work material. The friction between the rake face of the tool and chip causes heat generation in the secondary shear deformation zone whereas the friction between the tool flank and the machined surface causes heat generation in the tertiary shear deformation zone. Higher cutting temperature adversely affects the tool life and decreases the wear resistance and hardness of the cutting tool, which causes poor surface finish and dimensional inaccuracy of the machined surface. Therefore, it is important to maintain a lower cutting temperature during the machining process. The cutting tooltip temperatures are measured by a digital thermometer thermocouple device.

Tool-work thermocouple measures the average temperature of the contact area between the cutting tool and work material. On the other hand, the embedded thermocouple measures the temperature of a particular point in the cutting zone. The digital thermometer thermocouple devices technique uses contact to measure the cutting zone temperature. The advantages of a thermocouple thermometer device are faster response time and physical contact with the heat source. In this study, the contact digital thermometer measures the average temperature at the tooltip. A digital thermometer device is used to evaluate the tooltip temperature rising in the cutting zone during the turning of AISI 1050 steel material. It is a contact, digital thermometer used to measure the temperature of a tooltip surface.

During the experimental work, the temperature generated at the tooltip temperature is measured for each of sixteen experiments using a contact-type temperature tester shown in figure 3.14.

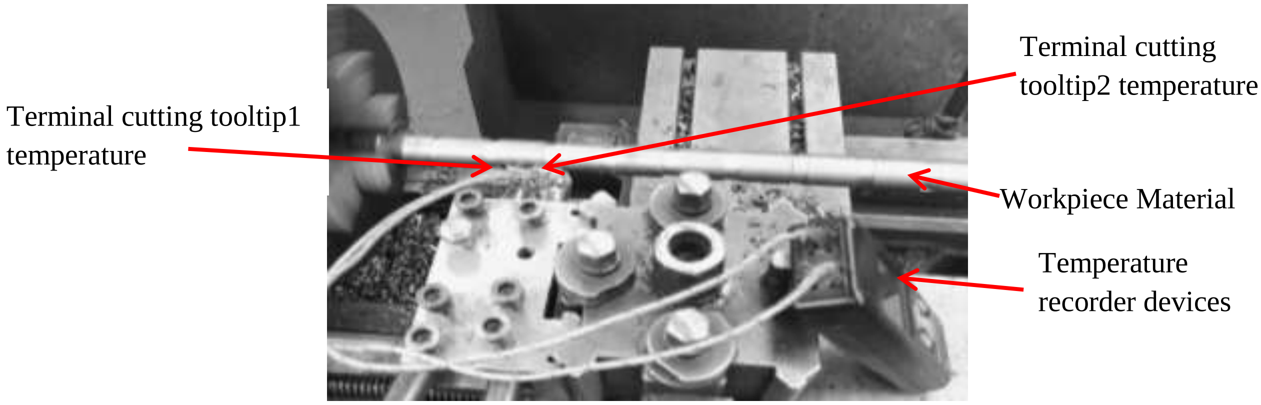

Figure 3.14 Cutting Tooltip Temperature Measurement Setup

3.9 Observation of Chip Morphology

The study of chip morphology is a major concern of turning processes. Both the chip tool interaction and favorable machining state can be easily determined with the help of chip morphology. In this present experimental investigation for each experimental run, chips were collected at the end of each experiment for the successive examinations. The type of chips was studied. Furthermore, the highest chip thickness, the lowest chip thickness, and the average maximum and minimum length of the chips were identified using Vernier caliper 0.02 accuracy for each experimental run by taking two samples for each experiment results.

CHAPTER FOUR

4 RESULTS AND DISCUSSION

4.1 Introduction

In this chapter, the result of the experiment and their discussion were given in detail. The results of the individual experiments were discussed in detail in this chapter. The conducted experimental work was performed to evaluate the effect of the main machining cutting parameters on the Surface Finish, Material Removal Rate, Cutting Tooltip Temperature, and Chip Morphology of AISI 1050 steel material during the double cutting tool turning process. After completion of the turning process, the Response Parameters were measured and the results were recorded. The response results from experimental investigations performed with Orthogonal Array are analyzed using Taguchi Methods, Regression Analysis, and multi-response objective using Grey Relational Analysis Techniques to identify the optimal cutting parameters and the most influential cutting parameters on the surface finish. Generally, the researcher has done sixteen consecutive experiments to relate each result.

All sixteen experiments were performed with different cutting parameters, but with a constant cutting length of 30mm and a diameter of the workpiece prepared for the experimental study of 25mm. This experimental study of the turning process of AISI 1050 steel double cutting tools during dry machining was carried out at different spindle speeds (60m/min, 80m/min, 100m/min, 120m/min) and the feed rate of (0.04mm/rev, 0.08mm/rev, 0.12mm/rev, 0.16mm/rev) and the first and second depths of cut were set as (0.10mm, 0.15mm, 0.20mm, 0.25mm) and (0.05mm, 0.10mm, 0.15mm 0.20mm) were taken. The optimization of the cutting parameters in the double cutting tool turning process was carried out separately on the conventional lathe machine, model: COMEV CM260 for the surface finish. Figure 4.1 shows samples after the double cutting tool turning of AISI 1050 steel material.

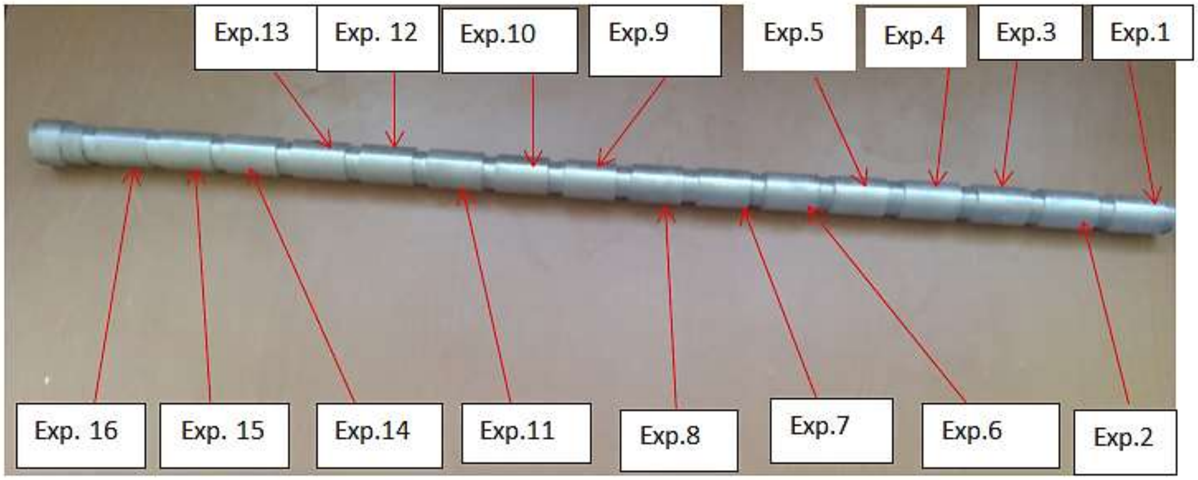

Figure 4.1 Workpiece Sample of AISI 1050 Steel after Turning Process

4.2 Optimization of Cutting Parameters

The main focus of the work was on the experimental investigation and parametric optimization of cutting conditions for turning AISI 1050 steel material using the Taguchi L16 orthogonal array, regression analysis, and Grey Relational Analysis Method. Taguchi's orthogonal array L16 (4^4) was used to provide a systematic and efficient method to study the design space and provide suggestions for improving the design. Table 4.1 shows machining parameters and their levels for the experiment work.

Table 4. 1 Machining Parameters and their Levels

Cutting parameters	Unit	levels			
		1	2	3	4
Cutting speed	(m/min)	60	80	100	120
Feed rate	(mm/rev)	0.04	0.08	0.12	0.16
First depth of cut	(mm)	0.10	0.15	0.20	0.25
Second depth of cut	(mm)	0.05	0.10	0.15	0.20

Notation: v= cutting speed, f = feed rate, d1 = first depth of cut, d2 = second depth of cut

4.3 Analysis of Surface Roughness

Measurements of Surface Roughness data (Ra) were taken at two different locations 120° apart on the machined surface using a surface roughness tester (profilometer) and the mean values were recorded. The measured test results of the surface roughness mean values for each test were shown in Table 4.2. The optimization of the cutting parameters for the dry condition was carried out. For the surface roughness analysis, the smaller is the-better performance characteristics were used. Therefore, in this case, the average surfaces roughness (Ra) and the signal-to-noise ratio (S/N) were defined as follows:

$$\text{Avg. } R_a = \frac{R_1 + R_2}{2} \tag{4.1}$$

Where R_a-Average surface roughness, R_1, and R_2, are the first and second trial tests of surface roughness value

$$\eta = -10 \log\left(\frac{1}{n}\sum_{j=1}^{2} R_j^2\right) \tag{4.2}$$

Where η is the S/N ratio, n is the number of trial tests in each experiment, R_j is the observed data and j is the number of the trial test.

By using equations (4.1 and 4.2,) to calculate the average surface roughness value (Ra) and S/N ratio for surface roughness value. In ANOVA, the 95% confidence level was chosen to determine the effect of cutting parameters on the surface roughness of machined parts.

As shown in Figure 4.2 and Table 4.2 below the variation of the experimental value of surface roughness for different samples, clearly indicate that at different cutting parameter values were obtained different surfaces roughness values from this value the optimum values were obtained at experiment number fifteen. The maximum and minimum values of average surface roughness during the experimental investigation of double cutting tool turning operations.

Table 4. 2 Experimental Results of Surface Roughness

Exp. No.	Cutting parameters				Surface Roughness(µm)			S/N ratio
	V	F	d1	d2	Trail 1	Trail 2	Avg. Ra.	
1	1	1	1	1	1.20	1.24	1.22	-1.72720
2	1	2	2	2	1.60	1.68	1.64	-4.29688
3	1	3	3	3	1.81	1.75	1.78	-5.00840
4	1	4	4	4	1.62	1.58	1.60	-4.08240
5	2	1	2	3	1.42	1.70	1.56	-3.86249
6	2	2	1	4	1.26	1.90	1.58	-3.97314
7	2	3	4	1	1.43	1.41	1.42	-3.04577
8	2	4	3	2	1.50	1.54	1.52	-3.63687
9	3	1	3	4	1.74	1.62	1.68	-4.50619
10	3	2	4	3	2.03	2.01	2.02	-6.10703
11	3	3	1	2	1.58	1.62	1.60	-4.08240
12	3	4	2	1	1.32	1.24	1.28	-2.14420
13	4	1	4	2	1.74	1.64	1.69	-4.55773
14	4	2	3	4	1.52	1.56	1.54	-3.75041
15	4	3	2	1	1.10	1.14	1.12	-0.98436
16	4	4	1	3	1.60	1.50	1.55	-3.80663

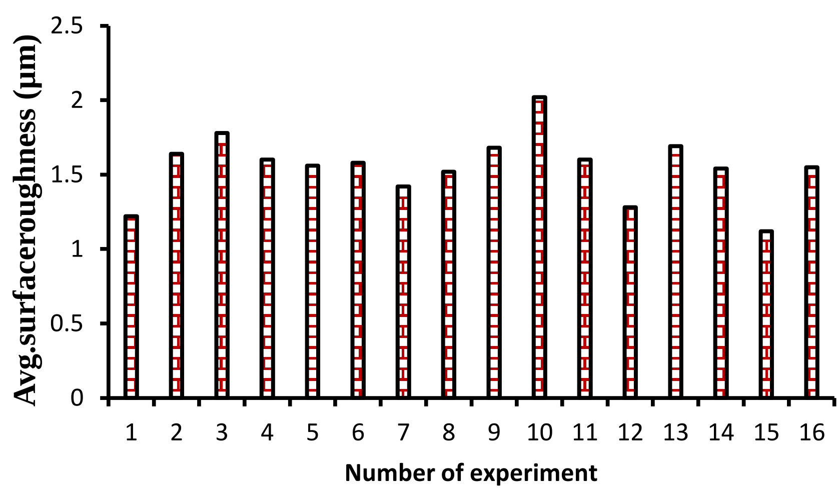

Figure 4.2 Variation of Experimental Value of Surface Roughness for different samples

4.3.1 Analysis of Mean Value of Surface Roughness

The mean value of surface roughness for each factor i.e. cutting speed (v), feed rate (f), first depth of cut (d1), and second depth of cut (d2) at each level were obtained and the result was listed in response to Table 4.3.

An example calculation is shown for factor v (Cutting Speed):

$$\text{Mean value at level } 1(v_1) = \frac{(1.22+1.64+1.78+1.60)}{4} = 1.56$$

$$\text{Mean value at level } 2(v_2) = \frac{(1.56+1.58+1.42+1.52)}{4} = 1.52$$

$$\text{Mean value at level } 3(v_3) = \frac{(1.68+2.02+1.60+1.28)}{4} = 1.645$$

$$\text{Mean value at level } 4(v_4) = \frac{(1.69+1.54+1.12+1.55)}{4} = 1.475$$

In a similar manner calculated the mean for factors f, d1, and d2 in each level. After calculating the average mean value of surface roughness for each factor, the delta value was calculated. Delta value was calculated by subtracting the minimum value from the maximum value for each parameter.

Delta = maximum value – minimum value = 1.645-1.475 = 0.17

Table 4. 3 Response Table for Mean Effect for Small is the Better

Levels	Cutting speed	Feed rate	First depth of cut	Second depth of cut
	v	f	d1	d2
1	1.56	1.538	1.488	**1.365**
2	1.52	1.695	**1.400**	1.612
3	1.645	**1.480**	1.630	1.727
4	**1.475**	1.488	1.683	1.495
Delta	0.17	0.215	0.282	0.362
Rank	4	3	2	1

The factor with the greatest effect on the mean from Table 4.3 is the second depth of cut (Delta = 0.362, Rank = 1). The factor with the least effect on the mean is a cutting speed (Delta = 0.17, Rank = 4). Since the main effect plots for means helps adjust the mean to a better value.

Those parameter levels with better surface finish value of specimens that means **v4f3d12d21** will be taken as a possible parameter combination for better values.

4.3.2 Main Effect of Cutting Parameter on Surface Roughness

As observed from Figure 4.3 shows that within the scope of this investigation the minimum point in the graph for each turning parameter are the optimum conditions. The minimum point for cutting speed was at level four, for feed rate the minimum point on this graph was at level three, for first depth of cut and second depth of cut were at level two and one respectively. This is due to the identified optimum turning parameter being at a low second depth of cut, medium first depth of cut, high feed rate, and high cutting speed which was **v4f3d12d21**.

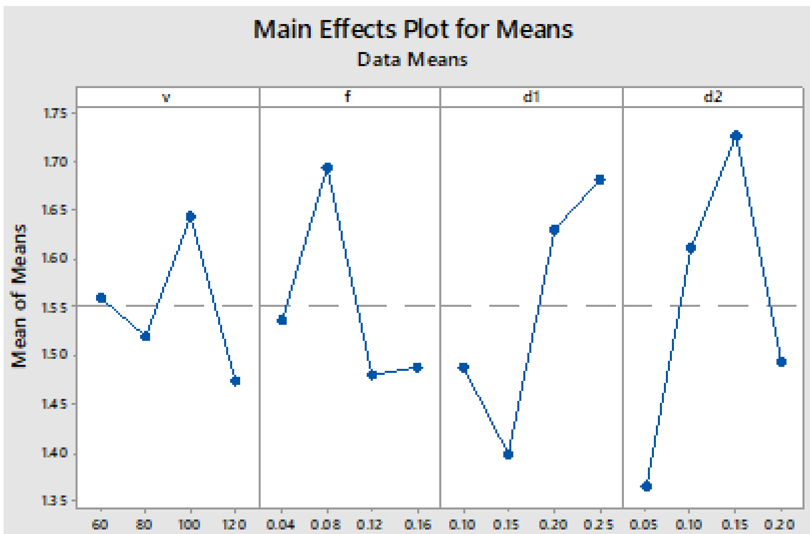

Figure 4. 3 Main Effect Plots for Means

4.3.3 Effect of Cutting Parameter on Surface Roughness

Effect of feed rate on surface roughness

The effects of feed rate on surface roughness (Ra) was shown in Figure 4.4, 4.5, 4.6, and 4.7 shows at v= 60 m/min, 80 m/min, 100 m/min, and 120 m/min respectively. In the equation, the average surface roughness (y) and the feed rate (x) are represented by the polynomial curve fitted equation. R is called the confidence interval. When R-value is more than 0.95 the experiment and mathematical curve fitting values are well agreed. As can be seen from Figures 4.4, 4.5, 4.6, and 4.7 results are very good since as R-value is exactly 0.9995, 0.9995, 0.9984, and 0.999 respectively.

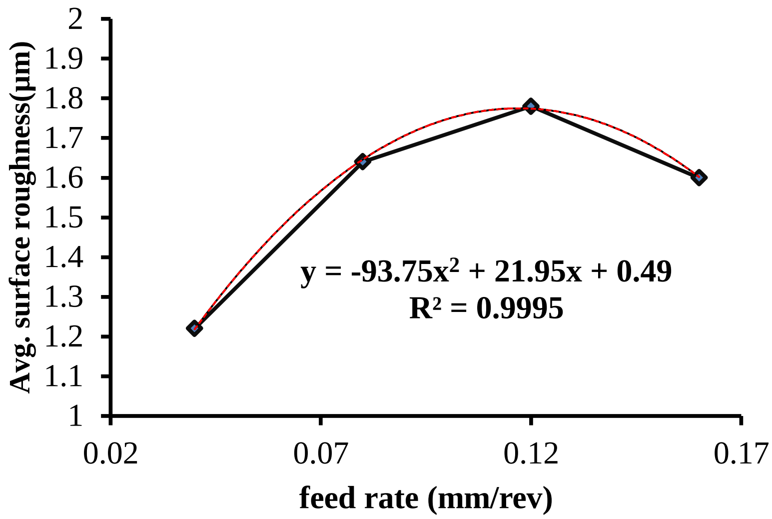

Figure 4.4 Effect of Feed Rate on Surface Roughness at v = 60 m/min

Figure 4.4 shows the effects of feed rate on surface roughness (Ra) at v= 60 m/min. as increasing feed rate from 0.04 mm/rev to 0.12 mm/rev, the surface roughness increased from 1.22 µm to 1.78 µm, then decreased to 1.6 µm as the feed rate increased to 0.16 mm/rev. from this, the decrease in feed rate results in the decrease of surface roughness at minimum feed rate and improves surface quality. Higher feed rates mean more material in contact with the cutting tool hence higher cutting force evolution which causes the appearance of the vibration, which leads to high surface roughness. Higher feed rates also cause in increasing the cutting temperature, which leads to the appearance of the tool wear hence undesired surface roughness.

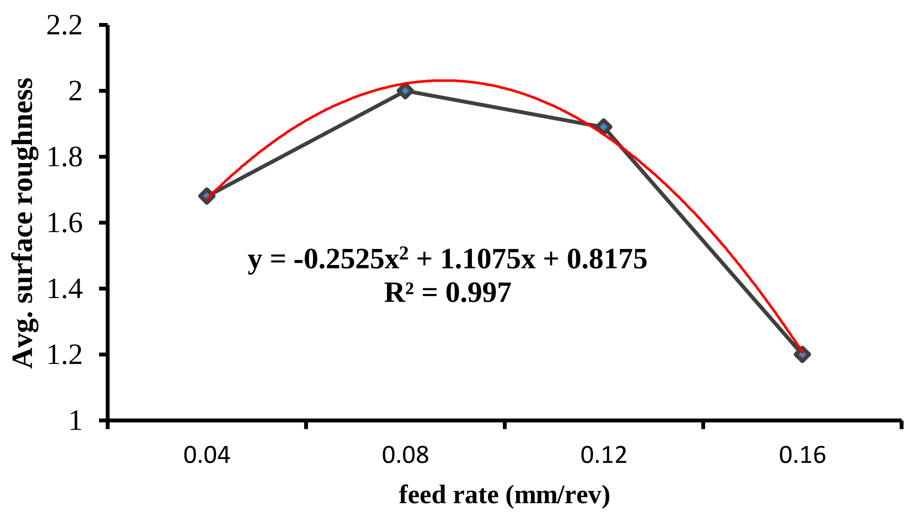

Figure 4.5 Effect of Feed Rate on Surface Roughness at v = 80 m/min

It was observed Figure 4.5 shows the effects of feed rate on surface roughness (Ra) at v= 80 m/min. as increasing feed rate from 0.04 mm/rev to 0.08 mm/rev, the surface roughness increased from1.42 µm to 1.58 µm. then decreased as feed increased to 0.16mm/rev.

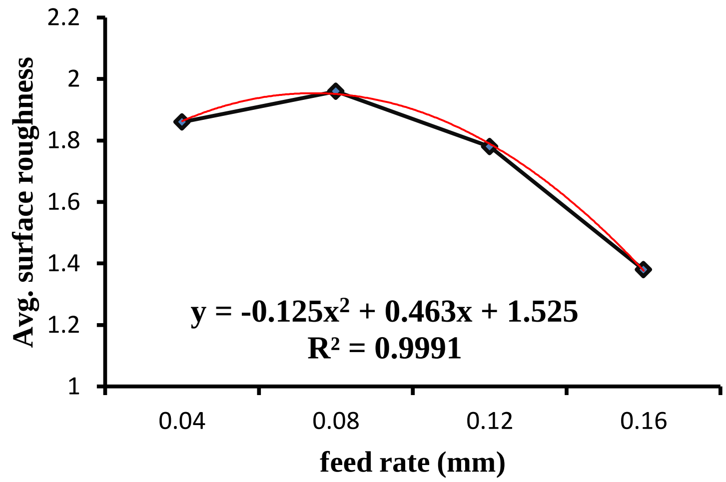

Figure 4.6 Effect of Feed Rate on Surface Roughness at v = 100 m/min

As shown in Figure 4.6, shows that the effects of feed rate on surface roughness (Ra) at v= 100 m/min. as increasing feed rate from 0.04 mm/rev to 0.08 mm/rev, the surface roughness increased from 1.82 µm to 1.98 µm. then as increased, as the feed rate increased from 0.08mm/rev to 0.16mm/rev the surface roughness decreased. As observed from the figure above as the feed rate increases, the surface roughness was decreased, because there is another additional effect there like the first depth of cut for this reason surface roughness decrease.

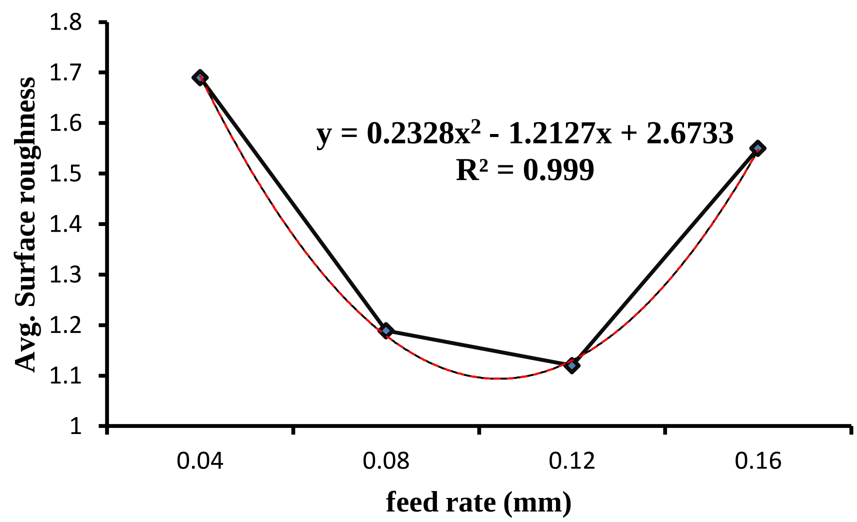

Figure 4.7 Effect of Feed Rate on Surface Roughness at v = 120m/min

As shown in Figure 4.7 as the feed rate increase from 0.04 mm/rev to 0.12mm/rev at constant cutting speed the surface roughness becomes decreased turned specimen. Then the surface roughness was increased with an increase in feed rate from 0.12mm/rev to 0.16mm/rev.

A higher feed rate means more material in contact with the cutting tool hence higher cutting force evolution in the appearance of the vibration, which leads to surface roughness.

Effect of cutting speed on surface roughness

The effect of cutting speed on surface roughness (Ra) was shown in Figure 4.8,4.9, 4.10, and 4.11 shows at f = 0.04 mm/rev, 0.08 mm/rev, 0.12 mm/rev, and 0.16 mm/rev respectively. In the equation, the average surface roughness (y) and the feed rate (x) are represented by the polynomial curve fitted equation. R is called the confidence interval. When R-value is more than 0.95 the experiment and mathematical curve fitting values are well agreed. As can be seen from Figure 4.8, 4.9, 4.10, and 4.11 results are very good since as R-value is exactly 0.9989, 0.9979, 1, and 0.999 respectively.

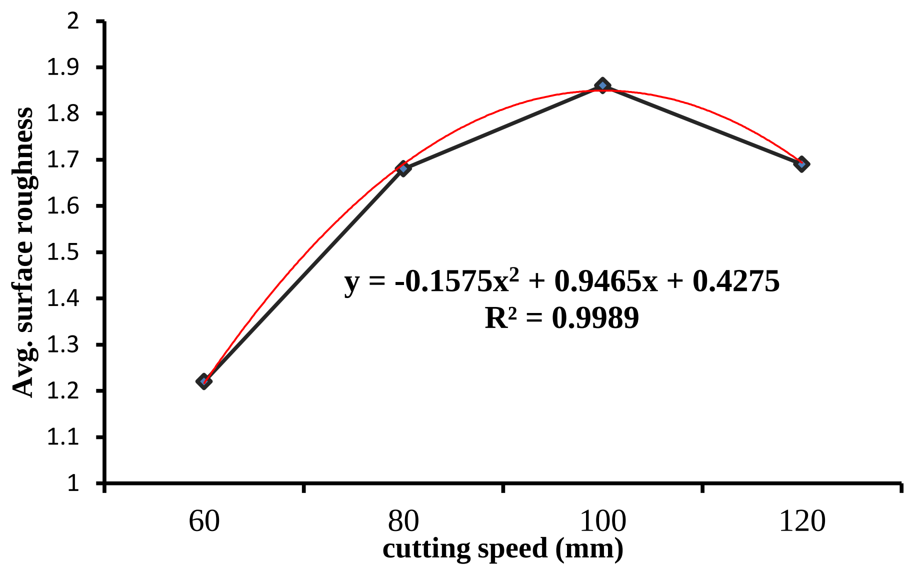

Figure 4. 8 Effect of Cutting Speed on Surface Roughness at f = 0.04 mm/rev

Figure 4.8 indicates the effect of cutting speed on surface roughness at a feed rate of 0.04mm/rev. as increasing cutting speed from 60m/min to 100m/min, the surface roughness was an increase. Then decreased surface roughness increases the cutting speed to 120m/min. as increased cutting speed, the surface roughness decreased.

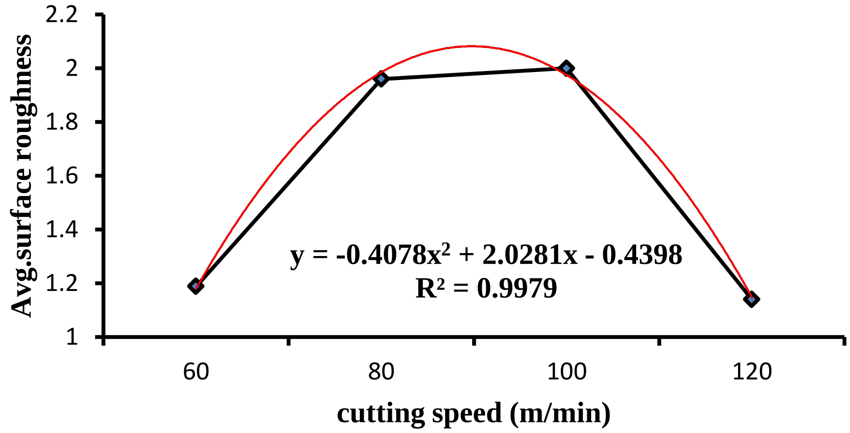

Figure 4. 9 Effect of cutting speed on surface roughness at f = 0.08 mm/rev

As observed in Figure 4.9 shows that the effect of cutting speed on surface roughness at the feed rate of 0.08mm/rev. as increasing cutting speed from 60m/min to 100m/min, then surface roughness was increased. Then surface roughness was decreased as increase cutting speed to 120m/min. as cutting speed increases, the surface roughness was decreased.

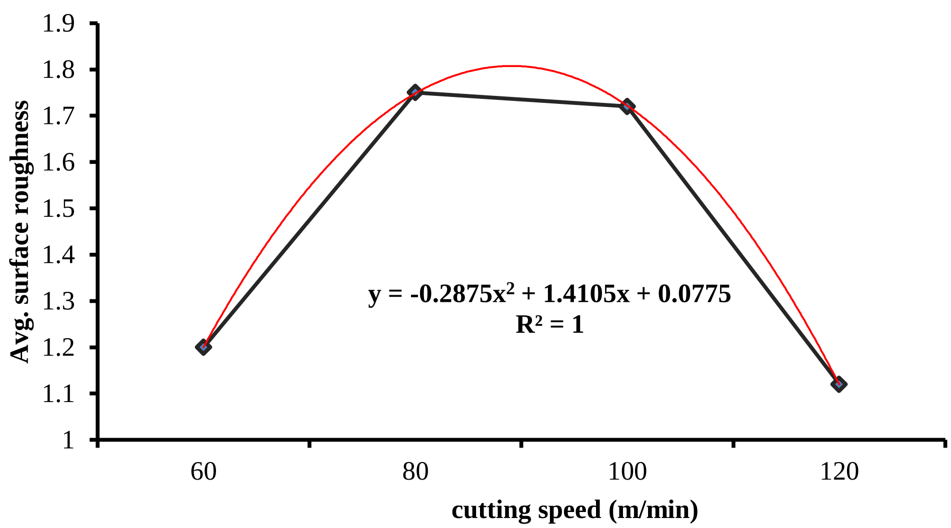

Figure 4. 10 Effect of cutting speed on surface roughness at f = 0.12 mm/rev

Figure 4.9 shows the effect of cutting speed on surface roughness at a feed rate of 0.12mm/rev. as increased cutting speed from 60m/min to 80m/min, and then surface roughness was increased. Then surface roughness was decreased as the increased cutting speed was from 100m/min to 120m/min. as cutting speed increases, the surface roughness was decreased.

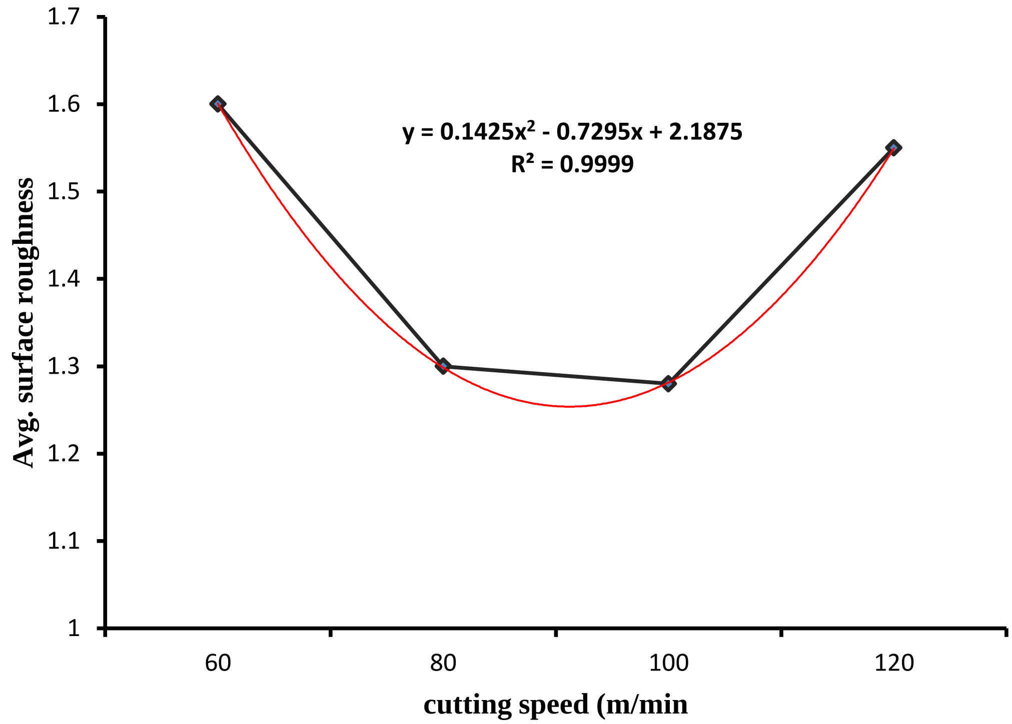

Figure 4. 11 Effect of cutting speed on surface roughness at f = 0.16 mm/rev

Figure 4.9 shows the effect of cutting speed on surface roughness at a feed rate of 0.16mm/rev. as increased cutting speed from 60m/min to 100m/min, and then surface roughness was decreased. Then the surface roughness was increased as increase cutting speed to 120m/min. as cutting speed increases, the surface roughness was decreased.

Effect of first depth of cut on surface roughness

Figure 4.12 shows the effect of the first depth of cut on surface roughness at a different cutting speed of 60m/min, 80m/min, 100 m/min, and 120 m/min. the average surface roughness (y) and the feed rate (x) are represented by the polynomial curve fitted equation. R is called the confidence interval. When R-value is more than 0.95 the experiment and mathematical curve fitting values are well agreed. As the increasing first depth of cut from 0.1mm to 0.15mm, the surface roughness was increased. Then as the first depth of cut increases, the surface roughness also increases.

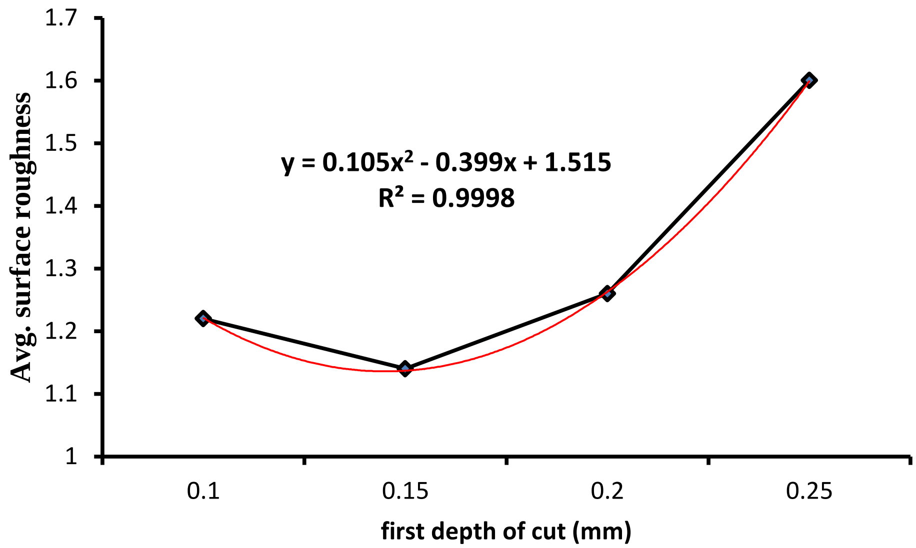

Figure 4.12 Effect of First Depth of Cut on Surface Roughness at V = 60 m/min

Figure 4.12 shows the effects of the first depth of cut on surface roughness at a cutting speed of 60m/min. as increased, the first depth of cut from 0.1mm to 0.15mm, then the surface roughness was decreased. Then the surface roughness was increased as the first depth of cut increased from 0.15mm to 0.25mm. from this, it was concluded that at an increase first depth of cut then the surface roughness decreased.

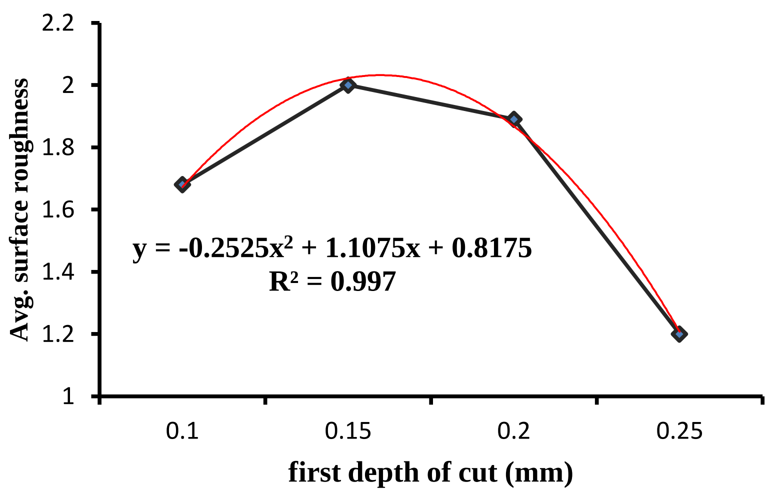

Figure 4.13 Effect of First Depth of Cut on Surface Roughness at v = 80 m/min

Figure 4.13 shows the effect of the first depth of cut on surface roughness at a cutting speed of 80m/min. as increased, the first depth of cut from 0.1mm to 0.15mm, then the surface roughness was decreased. Then the surface roughness was decreased as the first depth of cut decreased from 0.15mm to 0.25mm. The figure above it indicates that as the first depth of cut increases then the surface roughness was increase.

Effect of second depth of cut on surface roughness

Figure 4.14, 4.15, 4.16, and 4.17 shows the effect of the second depth of cut on surface roughness at a different cutting speed of 60m/min, 80m/min, 100 m/min, and 120 m/min respectively. The average surface roughness (y) and the feed rate (x) are represented by the polynomial curve fitted equation. R is called the confidence interval. When R-value is more than 0.95 the experiment and mathematical curve fitting values are well agreed. As the increasing second depth of cut from 0.1mm to 0.15mm, the surface roughness was increased. Then as the first depth of cut increases, the surface roughness also increases.

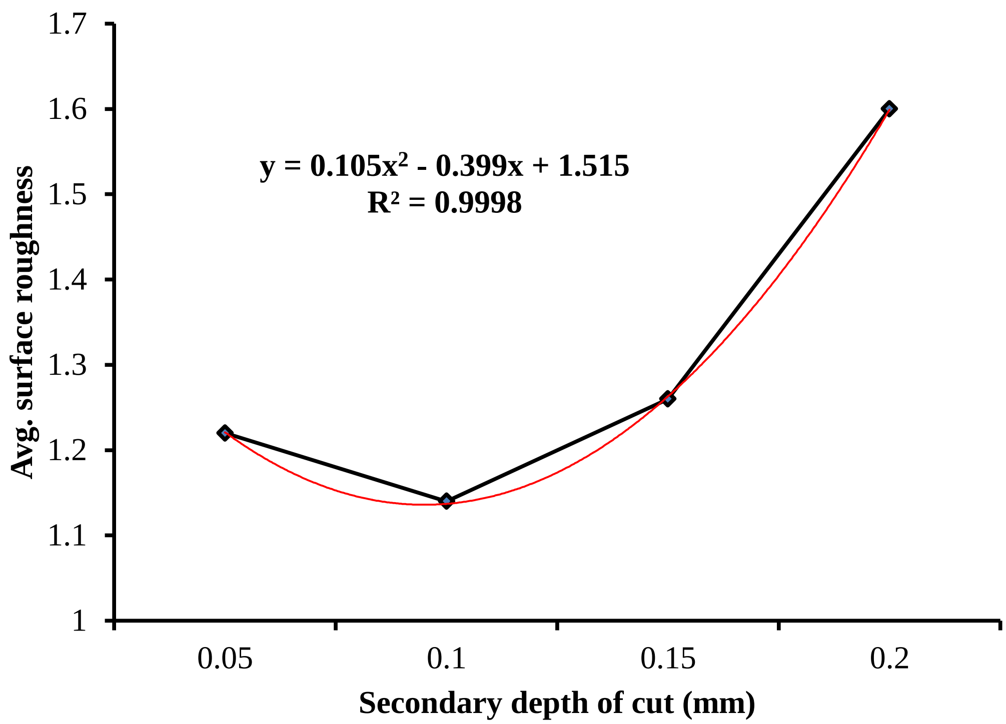

Figure 4.14 Effect of second depth of cut on surface roughness at v=60 m/min

Figure 4.13 shows the effect of the second depth of cut on surface roughness at a cutting speed of 60m/min. as increase second depth of cut from 0.05mm to 0.1mm, then the surface roughness was decreased. Then the surface roughness was decreased as the second depth of cut decreased from 0.1mm to 0.2mm. The figure above it indicates that as the second depth of cut increases then the surface roughness was increase.

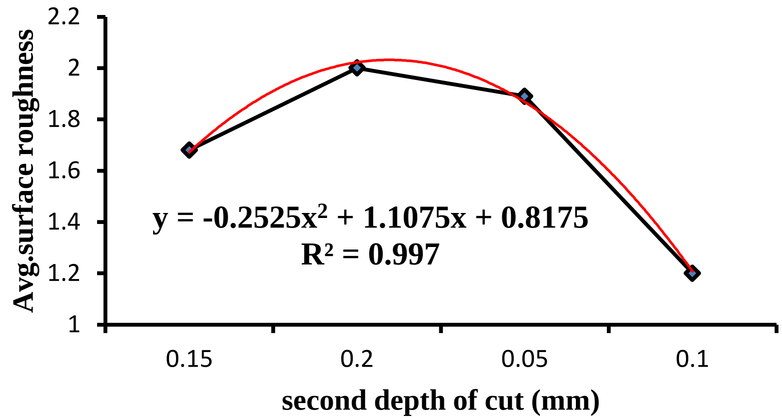

Figure 4. 15 Effect of Second Depth of Cut on Surface Roughness at v= 80 m/min

Figure 4.15 shows the effect of the second depth of cut on surface roughness at a cutting speed of 80m/min. as increase the second depth of cut from 0.05mm to 0.1mm, then the surface roughness was increased. Then the surface roughness was decreased as the second depth of cut decreased from 0.1mm to 0.2mm. The figure above it indicates that as the second depth of cut increases then the surface roughness was decrease.

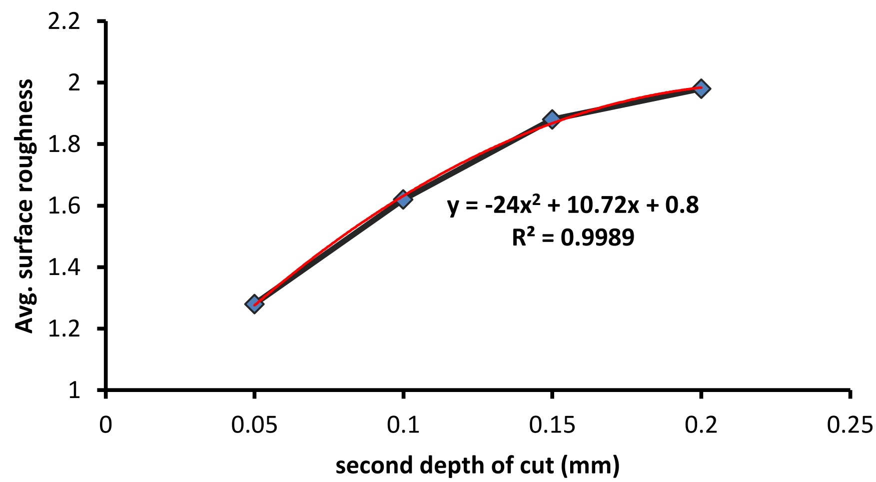

Figure 4.16 Effect of Second Depth of Cut on Surface Roughness at v= 100 m/min

Figure 4.13 shows the effect of the second depth of cut on surface roughness at a cutting speed of 100m/min. as increase the second depth of cut from 0.05mm to 0.20mm, then the surface roughness increases. The figure above it indicates that as the second depth of cut increases then the surface roughness was increase.

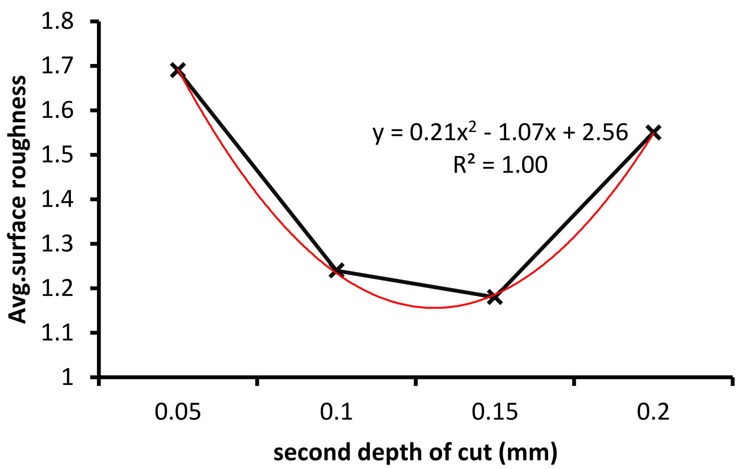

Figure 4. 17 Effect of Second Depth of Cut on Surface Roughness at v = 120 m/min

Figure 4.13 shows the effect of the second depth of cut on surface roughness at a cutting speed of 120m/min. as increase the second depth of cut from 0.05mm to 0.15mm, then the surface roughness was decreased. Then the surface roughness was increased as the second depth of cut decreased from 0.15mm to 0.20mm. The figure above it indicates that as the second depth of cut increases then the surface roughness was increase. As the depth of cut increases at constant spindle speed, the surface roughness becomes increased. Because at higher depths of cut, higher cutting forces are demanded to remove the bigger amount of the material. Increasing cutting forces leads to the appearance of the machine tool vibration which affects negatively the surface roughness.

4.3.4 Predict the Performance of Optimum Level

To predict the optimal response, four factors of parameters are selected by a small mean; v4f3d12d21 is the optimal level of the parameter mean for the surface roughness value. To find the predicted value of the responses (surface roughness value), the following linear regression equation is used.

$$y_{opt} = \mathrm{m} + (\mathrm{m}v_4 - \mathrm{m}) + (\mathrm{m}f_3 - \mathrm{m}) + (\mathrm{m}d1_2 - \mathrm{m}) + (\mathrm{m}d2_1 - \mathrm{m}) \quad (4.3)$$

Where m is the average performance means value for surface roughness, $m\mathrm{v}_4$ is the optimum level value for parameter v, mf_3 is the optimum level value for parameter f, $m\mathrm{d}1_2$ is the optimum level value for parameter d1, and $\mathrm{md}2_1$ is optimum level value for parameter d2.

The average value of surface roughness $(m = \frac{R_a}{16}) = 1.55$

$m\text{v}_4$ = 1.475 is optimum level value for factor v,

$m\text{f}_3$= 1.480 is optimum level value for factor f,

$m\text{d1}_2$= 1.400 is optimum level value for factor d1.

$m\text{d2}_1$= 1.365 is optimum level value for factor d2

y_{opt} = 1.55+ (1.475 – 1.55) + (1.480 -1.55) + (1.400 -1.55) + (1.365 -1.55)

y_{opt} = **1.07** (predict mean value for surface roughness)

4.3.5 Analysis of S/N Ratio for Surface Roughness

The Taguchi method uses the S/N ratio to measure the variations of the surface roughness value in the experimental design. The equations used for calculating the signal-to-noise ratios are based on the characteristics of the response variables being reported. In this experimental work, the response variables are smaller-the-better. Table 4.4 presents the calculations of S/N Ratios for surface roughness values results using the design of experiments. Table 4.3 presents the response table for a signal-to-noise ratio for smaller is the better for this study. Example of calculation for response Table for a signal-to-noise ratio for factor v (cutting speed) is as follows:

S/N ratio at level 1(v_1) = $\frac{(-1.72720-4.29688-5.00840-4.08240)}{4}$ = -3.77872

S/N ratio at level 2(v_2) = $\frac{(-3.86249-3.97314-3.04577-3.63687)}{4}$ = -3.62956

S/N ratio at level 3(v_3) = $\frac{(-4.50619-6.10703-4.08240-2.1445)}{4}$ = -4.21003

S/N ratio at level 4(v_4) = $\frac{(-4.55773-3.75041-0.98436-3.80663)}{4}$ = -3.2747

In a similar manner calculated the S/N ratio for factors f, d1, and d2 in each level. After calculating the average S/N ratio for each factor, the delta value is calculated. Delta value was calculated by subtracting the minimum value from the maximum value for each cutting parameter.

Delta = maximum value – minimum value = -3.2747825+ 4.21003= 0.935

Table 4. 4 Response Table for S/N Ratio Effect (For Small is Better)

Levels	Cutting speed	Feed rate	First depth of cut	Second depth of cut
	V	F	d1	d2
1	-3.779	-3.663	-3.397	**-2.667**
2	-3.630	-4.532	**-2.822**	-4.143
3	-4.210	**-3.280**	-4.225	-4.686
4	**-3.275**	-3.418	-4.8648	-2.87
Delta	0.935	1.252	1.626	2.029
Rank	4	3	2	1

The factor with the greatest effect on the S/N ratio from Table 4.4 is the second depth of cut (Delta = 2.029, Rank = 1). The factor with the least effect on the S/N ratio is a cutting speed (Delta = 0.935, Rank = 4). Since the main effect plots for the S/N ratio helps adjust the S/N to a better value. Those parameter levels with better surface finish value of specimens that means **v4f3d12d21** will be taken as a possible parameter combination for better values. The significant factors in the order increasing by affecting surface roughness are second depth of cut, first depth of cut, feed rate, and cutting speed as it's seen in Table 4.17.

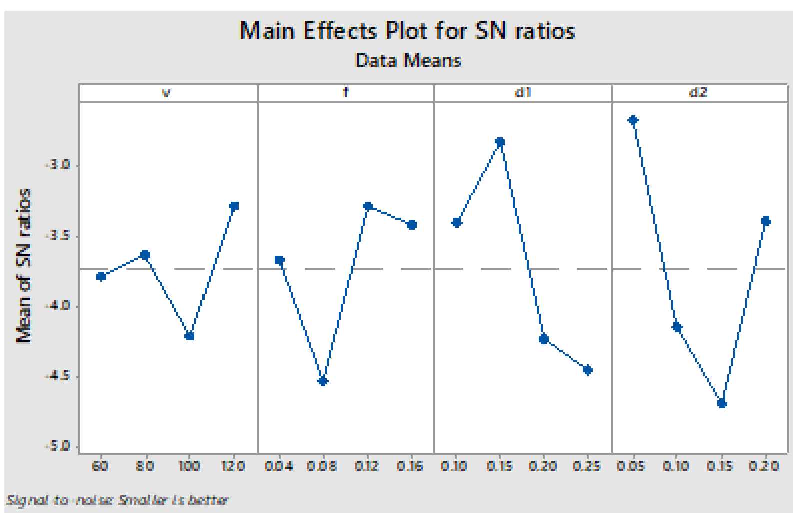

Figure 4. 18 Main Effects Plot for S/N Ratios

The numerical value of the peak point in each graph shows the best value of that particular parameter at that level. They also indicate the optimum conditions in the range of the experimental conditions. The most effective parameter to enhance the surface roughness is the second depth of cut weight percentage when compared with other cutting factors and cutting speed has the least effect on the surface roughness. Since the S/N ratio used for this study is smaller the better and smallest S/N ratio was selected as shown in Figure 4.18. That is cutting speed at level 4, feed rate at level 3, first depth of cut, and second depth of cut at level 2 and level 1 respectively **(v4f3d12d21**) were selected.

4.3.6 Predict the Performance of Optimum Level

For predicting the optimum response, four factors of parameters were selected by a large S/N ratio, $\mathbf{v_4f_3d1_2d2_1}$ is the optimum level of parameters S/N ratio for surface roughness value. To find out the predicted value of the responses (surface roughness value) the following linear regression equation is used.

$$y_{opt} = \text{m} + (\text{m}v_4 - \text{m}) + (\text{m}f_3 - \text{m}) + (\text{m}d1_2 - \text{m}) + (\text{m}d2_1 - \text{m}) \quad (4.4)$$

Where, m is the average performance S/N ratio for surface roughness, $m\text{v}_4$ is the optimum level value for parameter v, $m\text{f}_3$ is the optimum level value for parameter f, $m\text{d}1_2$ is the optimum level value for parameter d1, and $\text{md}2_1$ is optimum level value for parameter d2.

The average value of the S/N ratio $(m = \frac{S/N}{16}) = -3.723$

$y_{opt} = -3.723 + (-3.275+3.723) + (-3.280+3.723) + (-2.822+3.723) + (-2.667+3.723)$

y_{opt} = -0.874125 (predict value for S/N ratio).

4.3.7 ANOVA for Surface Roughness

The purpose of the analysis of variance (ANOVA) was to find which parameters significantly affect the quality characteristic. ANOVA is the statistical technique used to find the influence of all control parameters. In the analysis of variance, the percentage contributions of each control factor were used to measure the corresponding effects on the performance characteristics.

Table 4. 5 Analysis of Variance for Surface Roughness Value

Source	DOF	SS	MSS	F-value	P-value	%C	Significance
V	3	0.06260	0.02087	1.82	0.317	5.83%	less significant
F	3	0.11995	0.0399’8	3.49	0.166	8.92%	Significant
d1	3	0.20145	0.06715	5.86	0.090	15.41%	Significant
d2	3	0.29065	0.9688	8.46	0.042	64.99%	Highly significant
Error	3	0.03435	0.01145			4.84%	
Total	15	0.70900				100%	

Where DOF = degree of freedom, SS = sum of squares, MSS = mean sum of squares, %C = percentage of contribution, F= F-values, and P = P- value generated from Minitab 17 statistical software.

From Table 4.5, it was observed that the cutting speed weight percentage (5.83%), feed rate (8.92%), first depth of cut (15.41%), and second depth of cut (64.99%) have significant influences on the surface roughness of AISI 1050 steel material. Therefore, the second depth of cut was a highly significant effect parameter on the surface roughness of AISI 1050 steel during double tool turning.

4.3.8 Regression Model for Surface Roughness

Utilizing the experimental data, the mathematical model for surface roughness has been developed using multiple linear regression (MLR) analysis. The dependent variable surface roughness can be conceived as a linear combination of the independent variables, namely cutting speed, feed rate, first depth of cut, and second depth of cut (Sahoo. et.al, 2012). The data was analyzed by Minitab 17 software.

Table 4. 6 ANOVA for Surface Roughness Model

Source	DF	Adjss	Adjms	f-value	p-value	Remarks
Regression	4	0.213875	0.053469	1.19	0.00369	Significant
Speed	1	0.003380	0.003380	0.08	0.00789	
Feed	1	0.026645	0.026645	0.59	0.004580	
Depth1	1	0.132845	0.132845	2.95	0.00114	
Depth2	1	0.051005	0.051005	1.13	0.00213	
Error	11	0.495125	0.045011			
Total	15	0.709000				

When regression analysis was employed by applying the least-squares method to the experimental data to obtain the coefficient of this equation, the following equation was attained for Ra.

$$Ra = 1.288- 0.00065v - 0.91 f + 1.630 d1 + 1.010 d2$$

$$R^2 = 96.52\%$$

Models are developed using uncoded units. ANOVA was useful for identifying the level of significance of the model developed. The F test was used to determine the significance test. If the calculated value of the F ratio is higher than the tabulated value of the F ratio then the model is significant at the desired α level. Depending on F- the value P- the value (probability of significance) was then calculated. If the p-value for a term appears less than 0.05 (for a 95% confidence level) then it can be concluded that the model is also significant in the selected response. The result of the ANOVA of the surface roughness model is shown in Table 4.6. This analysis is carried out for a level of confidence of 95% (Sahoo. et.al, 2012.).

The examination of residuals has investigated the adequacy of the modal. The residuals, which are the differences between the respective observed response and the predicted response, were examined using normal probability plots of the residuals and the plots of the residuals versus the predicted response.

The normal probability plot shown in Figure 4.19 shows the normal distribution and the histogram of residual values well agreed the same trends were obtained from the S/N plot shown in Figure 4.20

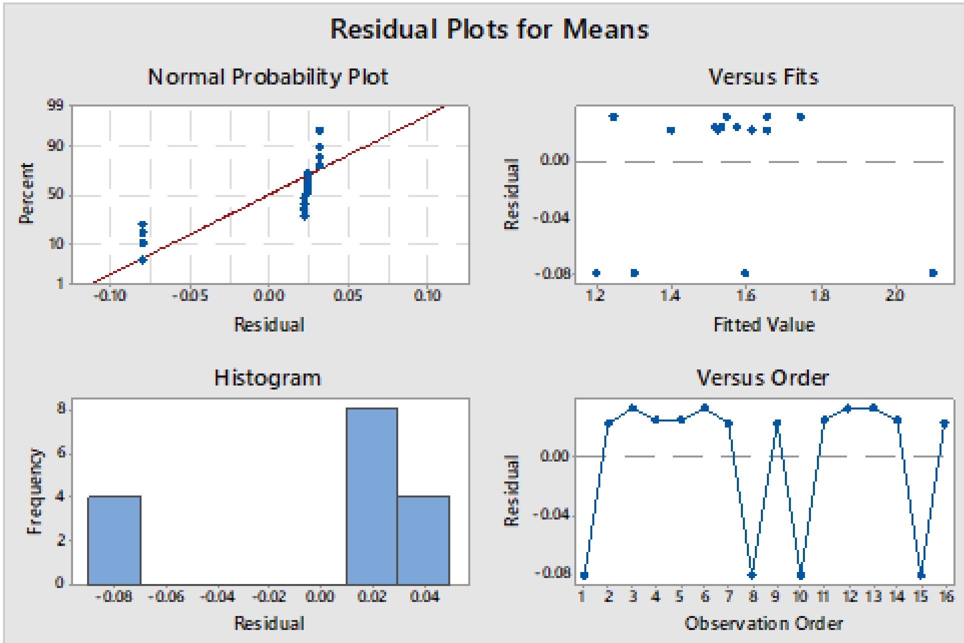

Figure 4. 19 Residual Plots for Means of Surface Roughness

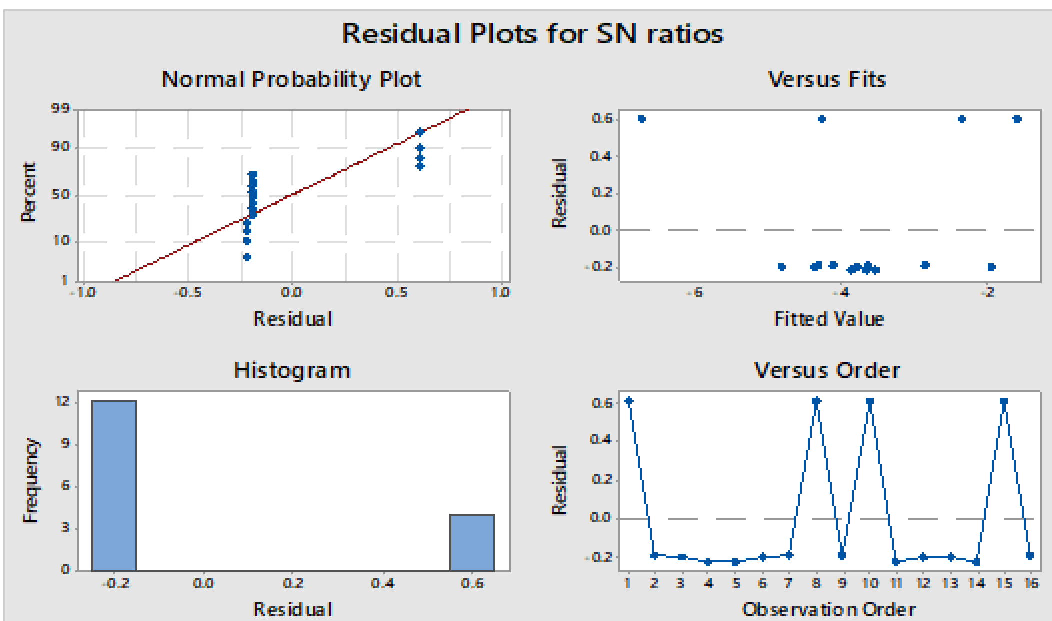

Figure 4. 20 Residual plot for S/N rations

4.3.9 Determining the Optimum Condition

From the Table 4.3, and Table 4.4, it was observed that cutting speed weight percentage optimum level value 120m/min, feed optimum level value 0.12mm/rev, first depth of cut optimum level value 0.15mm, and second depth of cut optimum level value 0.05mm makes the response S/N ratio values large. Therefore, the optimum processing parameters signal to noise (S/N) ratio was selected.

Table 4.7 presents the optimum parameters setting selected for surface roughness obtained from the design of the experiment and experimental results. The selected optimum parameters in this study were at higher cutting speed, at a medium first depth of cut, medium feed rate, and at the minimum second depth of cut which**,** is at **v4f3d12d21.**

Table 4. 7 optimum parameters setting levels and their values

Controllable factors	Level selected	Value of levels	Ranks of affecting the response
Speed	4	120	4
Feed	3	0.12	3
Depth1	2	0.15	2
Depth2	*1*	0.05	1

4.3.10 Confirmation Test for surface roughness

The obtained optimal combination of process parameters was verified with the predicted result. The optimum combination of parameters obtained from Table 4.8 was (**v4f3d12d21**) at 120 m/min cutting speed, 0.12 mm/rev feed rate, and 0.15 mm first depth of cut and 0.05mm second depth of cut.

Table 4. 8 Optimum and Predicted values of cutting parameters

Response	Optimal parameter	Predicted values		Experimental value	
Ra (m)	**V4f3d12d21**	mean	S/N ratio	Mean	S/N ratio
		1.07	-0.874125	1.12	-0.984536

From Table 4.8 and figure 4.20, it was indicated that the result between the experimental result and the predicted one is very small. The values predicted by using the Taguchi method are approximately near to the value which was experimentally obtained. This verifies that the experimental results of surface roughness are strongly correlated with the predicted results.

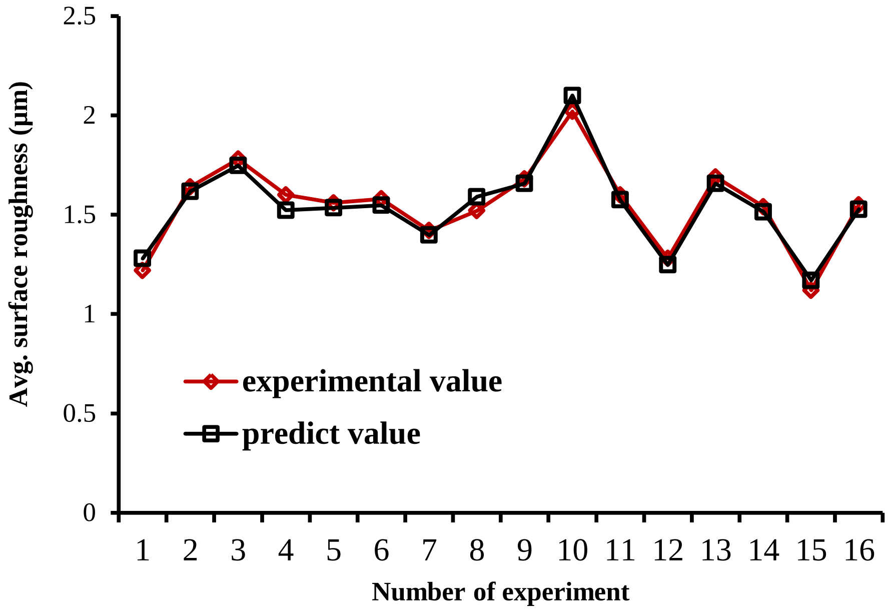

Figure 4. 21 Plot of Predict Value using Taguchi Method and Actual Experimental Value

As observed from Table 4.9 and figure 4.22, it clearly shows that the comparison between the experimental value and predicted value was very acceptable at each turned specimen. The variation between the experimental value and predicted value using the Taguchi method was very small.

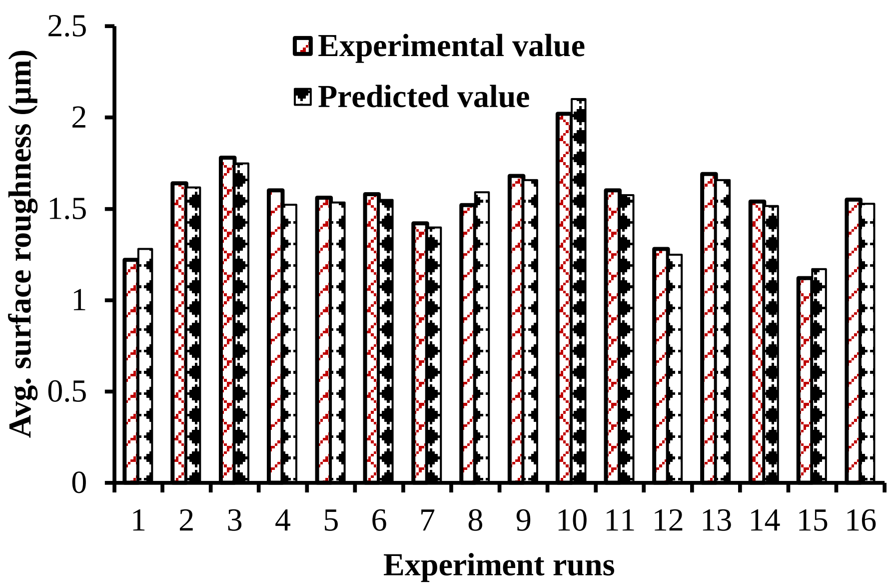

Figure 4. 22 comparisons between the experimental value and predicted value of surface roughness

Table 4. 9 Comparison between Experimental and Predicted Surface Roughness Values

No. exp.	Experimental value	Predict value	Variation	%Variation
1	1.22	1.28	-0.06	4.91
2	1.64	1.6175	0.0225	1.37
3	1.78	1.7475	0.0325	1.83
4	1.60	1.5225	0.0775	4.84
5	1.56	1.535	0.025	1.60
6	1.58	1.5475	0.0325	2.057
7	1.42	1.3975	0.0225	1.55
8	1.52	1.59	-0.07	4.61
9	1.68	1.6575	0.0225	1.34
10	2.02	2.1	-0.08	3.96
11	1.60	1.575	0.025	1.5625
12	1.28	1.2475	0.0325	2.54
13	1.69	1.6575	0.0325	1.92
14	1.54	1.515	0.025	1.6233
15	1.12	1.17	-0.05	4.46
16	1.55	1.5275	0.0225	1.45

4.4 Analysis of Material Removal Rate (MRR)

Material Removal Rate (MRR) is the amount of material removed per unit time. MRR in metal cutting is a volume of chips removed in one minute and is measured in a three-dimensional quantity. MRR is also a measure of metal cutting productivity. This volume is based on the area of a circular ring of a cylinder and its sectional length. The number of materials removed during the dual tool turning process of AISI 1050 steel for each experiment is calculated using Equation 3.11 and reported in Table 4.10.

As can be seen from Table 4.11 and Figure 4.10, in experiment number sixteen (V = 120 m/min, f = 0.16 mm/rev, d1 = 0.10 mm and d2 = 0.15 mm) the material removal rate was maximum and the minimum material removal rate was reached in experiment number one (V = 60 m/min, f = 0.04 mm/rev, d1 = 0.10 mm and d2 = 0.05 mm).

Material removal rate (MRR) is important to increase the productivity of machining operations by increasing the number of chips removed from the workpiece or product being machined.

Table 4. 10 Material Removal Rate Results

Exp. No	Cutting parameters				MRR (mm^3/sec)	S/N Ratio
	Speed (mm/sec)	Feed (mm/rev)	Depth-1 (mm)	Depth-2 (mm)		
1	1,000	0.04	0.10	0.05	6.000	15.5630
2	1,000	0.08	0.15	0.10	20.000	26.0206
3	1,000	0.12	0.20	0.15	42.000	32.4650
4	1,000	0.16	0.25	0.20	72.000	37.1466
5	1,333.33	0.04	0.15	0.15	18.667	25.4213
6	1,333.33	0.08	0.10	0.20	48.000	33.6248
7	1,333.33	0.12	0.25	0.05	24.000	27.6042
8	1,333.33	0.16	0.20	0.10	53.333	34.5400
9	1,666.67	0.04	0.20	0.20	30.000	29.5425
10	1666.67	0.08	0.25	0.15	46.667	33.3802
11	1,666.67	0.12	0.10	0.10	50.000	33.9794
12	1,666.67	0.16	0.15	0.05	40.000	32.0412
13	2,000	0.04	0.25	0.10	20.000	26.0206
14	2,000	0.08	0.20	0.05	24.000	27.6042
15	2,000	0.12	0.15	0.20	108.000	40.6685
16	2,000	0.16	0.10	0.15	112.000	40.9844

Machining parameter optimization is highly necessary for surface finish. Based on experimental outcomes, the material removal rate was obtained at the optimum cutting parameters which as 112mm^3/sec. Since the optimum cutting speed at which the best surface finish was obtained at the highest level values at this level

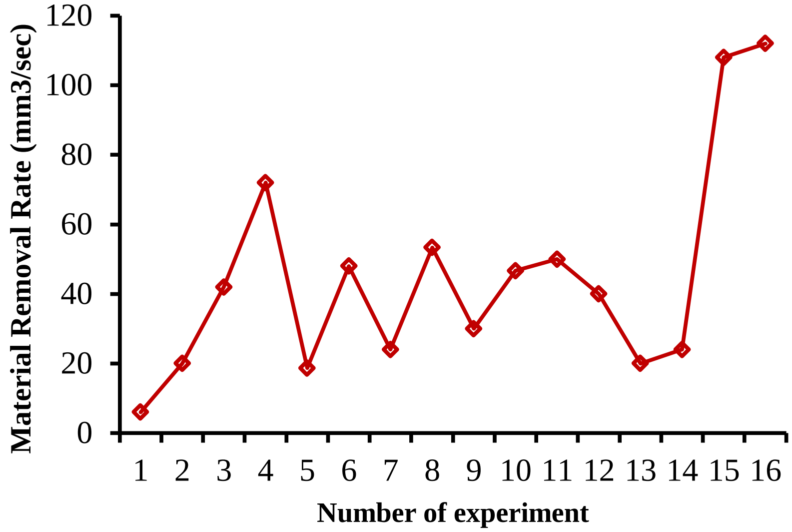

Figure 4. 23 Variation of MRR during Experiment

4.4.1 Parametric Optimization of Material Removal Rate (MRR)

A Response table for each response features such as the mean and signal-to-noise ratio of MRR was calculated. The answer table shows which factors have the greatest influence on the response and which level of the factor is associated with higher or lower answer parameters. Steps to generate the response table.

1. Calculates the selected response characteristics for cutting speed, feed rate, first depth of cut, and second depth of cut at each level.

The response for each factor is calculated as example shown for factor v.

For factor v, the mean

$$\text{At level 1}(v_1) = \frac{(6+20+42+72)}{4} = 35$$

$$\text{At level 2}(v_2) = \frac{(18.667+48+24+53.333)}{4} = 36$$

$$\text{At level 3}(v_3) = \frac{(30+46.667+50+40)}{4} = 41.667$$

$$\text{At level 4}(v_4) = \frac{(20+24+108+112)}{4} = 66$$

In a similar manner calculated the mean for factors f, d1, and d2 in each level.

2. After this delta values are calculated, which is the difference between the highest average response characteristic value and the lowest average response characteristic values for levels of that factor.
3. By considering the delta values ranks are allotted from high to low. The factor with the highest delta value is ranked one.

Table 4. 11 Response Table for Mean Effects Plot for larger is the better

Levels	Cutting parameters			
	Speed(v)	Feed(f)	First depth (d1)	Second depth (d2)
1	35	18.67	**54**	23.50
2	36	34.67	46.67	35.83
3	41.67	56	37.33	54.83
4	**66**	**69.33**	40.67	**64.50**
Delta	31	50.67	16.67	41
Rank	3	1	4	2

From Table 4.11 Response Table for the mean material removal rate analysis observed that the amount of material removed during machining operations is primarily affected by the feed rate compared to other cutting parameters. At experiment number four (0.16 mm/rev), eleven (0.12 mm/rev), twelve (0.12 mm/rev), and sixteen (0.16 mm/rev) the maximum material removal rate was reached, at this point the feed rate value is maximum and the minimum material removal rate was in the experiment obtained number one (0.04 mm/rev), five (0.04 mm/rev), nine (0.04 mm/rev) and thirty (0.05 mm/rev) With this number of experiments, the value of the feed rate is minimal. From this, it was concluded that the feed rate was of great importance for the material removal rate.

The most significant factor that affects the MRR value for turning of AISI 1050 during the double tool turning process was feed rate; feed rate affects highly level of material removal rate followed by the second depth of cut. While the cutting speed was the third influential factor and the first depth of cut was the least significant factor that affects material removal rate.

4.4.2 Main Effects of MRR

As observed from Figure 4.23 Material Removal Rate was affected by the feed rate, while the feed rate increased, the material removal rate was increased and also the material removal rates increased with an increase in cutting speed. Generally, the higher feed rate was achieved higher material removal rate. This feed rate was the main significant factor in improving the rate of productivity during the double tool turning of AISI 1050 steel.

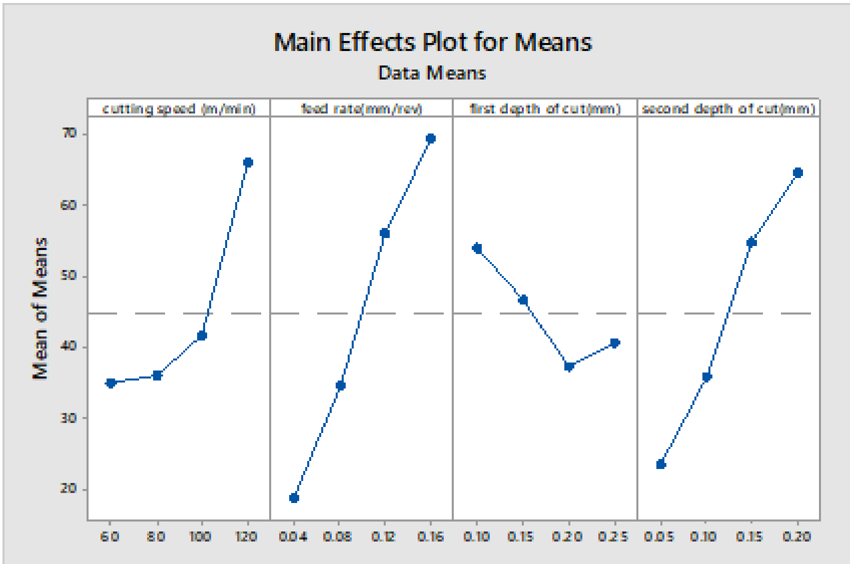

Figure 4. 24 Main Effect of MRR

4.4.3 Predict the Performance of Optimum Level

For predicting the optimum response, four factors of parameters were selected by large mean values at v4f4d11d24 are the optimum levels of parameters for MRR value. For optimum response, the predicting value is approximate. To find out the predicted value of the responses (MRR value) the following linear regression equation is used.

$$y_{opt} = \mathrm{m} + (\mathrm{m}v_4 - \mathrm{m}) + (\mathrm{m}f_4 - \mathrm{m}) + (\mathrm{m}d1_1 - \mathrm{m}) + (\mathrm{m}d2_4 - \mathrm{m}) \quad (4.5)$$

Where, m is the average performance mean value ratio for MRR, $m\mathrm{v}_4$ is the optimum level value for parameter v, $m\mathrm{f}_2$ is the optimum level value for parameter f, $m\mathrm{d}1_1$ is the optimum level value for parameter d1, and $\mathrm{md}2_4$ is optimum level value for parameter d2.

The average value of the mean $(m = \frac{MRR}{16}) = 44.67$

y_{opt} = 44.67+ (66- 44.67) + (69.33- 44.67) + (54- 44.67) + (64.50- 44.67)

y_{opt} = 110.67 (predict value for S/N ratio).

4.4.4 Interaction Effects of Cutting Parameter on MRR

The interaction effect clearly shows a variety of material removal rates at different cutting parameters.

Effects of Feed Rate on MRR

Figure 4.25 shows the effect of feed rate on material removal rate at constant cutting speed. As increasing feed rate from 0.04 mm/rev to 0.16 mm/rev, the material removal rate was increased at a constant cutting speed of 60m/min. But at 80m/min of cutting speed, the material removal rate was increased initially with an increasing feed rate from 0.04mm/rev to 0.08mm/rev m/min and then decreased when the feed rate was increased to 0.12mm/rev and then increased when the cutting speed was increased to 0.16mm/rev. As increasing feed rate from 0.04 mm/rev to 0.08 mm/rev and 0.08m/rev to 0.16 mm/rev the material removal rate was increased and decreased respectively at a constant cutting speed of 100m/min. Finally, at 120m/min of cutting speed, the material removal rate was increased initially by increasing cutting speed from0.04mm/rev to 0.16mm/rev. from this; it was concluded as the feed rate increased, the material removal rate was increased.

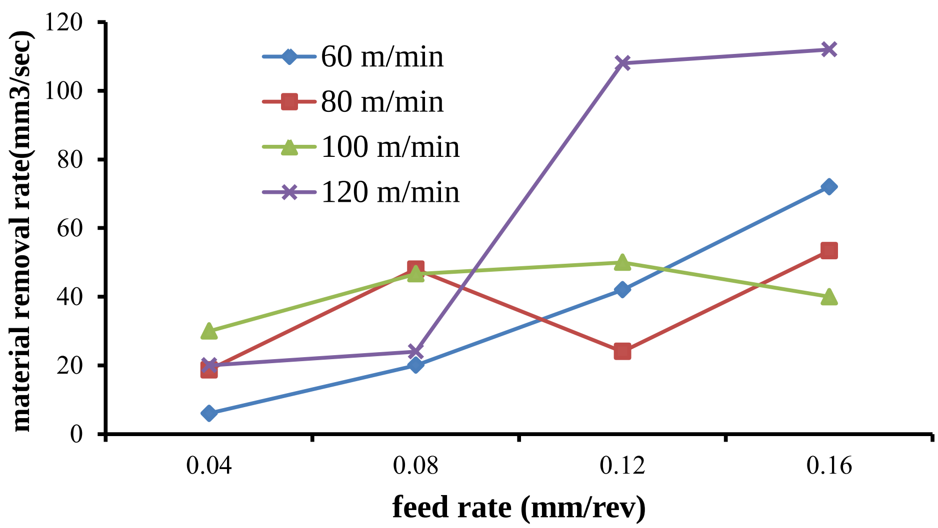

Figure 4. 25 Effect of Feed Rate on MRR at constant cutting speed

Effect of first depth of cut on MRR

As observed Figure 4.26 shows the effect of the first depth of cut on the material removal rate at constant cutting speed. As the increasing first depth of cut from 0.1 mm to 0.25 mm, then the material removal rate was increased at a constant cutting speed of 60 m/min. But at 80 m/min of the first depth of cut the material removal rate was increased initially with the increasing first depth of cut from 0.1 mm to 0.150 mm and then decreased when the first depth of cut was increased from 0.15 mm to 0.20 mm. as increasing first depth of cut from 0.1 mm to 0.20mm, the material removal rate was increased and as the increasing first depth of cut from 0.2 mm to 0.25mm, material removal rate was increased at constant cutting speed 100 m/min. as the increasing first depth of cut from 0.1 mm to 0.25mm the material removal rate was increased at a cutting speed of 120m/min. As increase depth of cut, the material removal rate was increased.

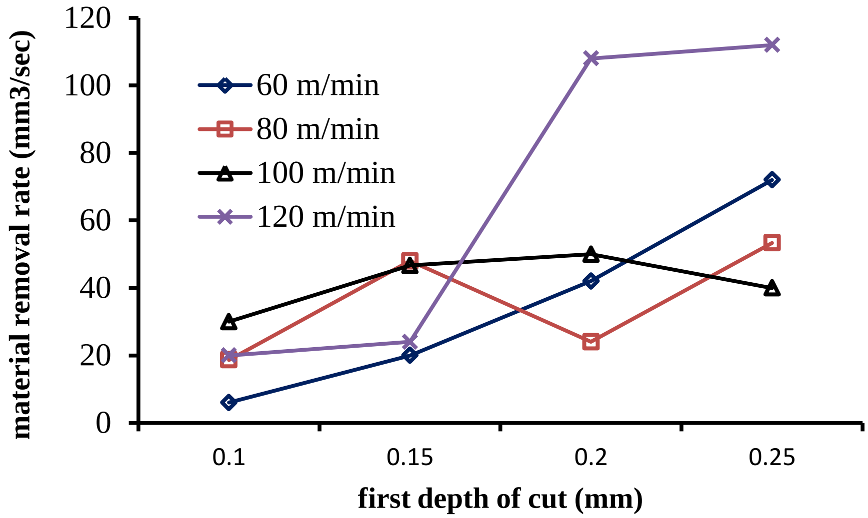

Figure 4. 26 effects of first depth of cut on MRR

Effect of Cutting Speed and Second Depth of Cut on MRR

As observed in Figure 4.27 Show the effect of the second depth of cut on Material Removal Rate at a constant cutting speed of 60m/min, 80m/min, 100m/min, and 120m/min. As the increasing second depth of cut from 0.05mm to 0.20, then increase material removal rate at a constant cutting speed of 60 m/min. But at 80m/min of the cutting speed, the material removal rate was increased initially by increasing the second depth of cut from 0.10 mm to 0.08 mm and then decreased when the second depth of cut was increased to 0.2mm. As the increasing second depth of cut from 0.05mm to 0.15mm and 0.15mm to 0.20mm, then the material removal rate was increased and the material removal rate was decreased respectively at a constant cutting speed of 100m/min. As the increasing second depth of cut from 0.5mm to 0.20 mm, the material removal rate was increased at a constant cutting speed of 120 m/min.

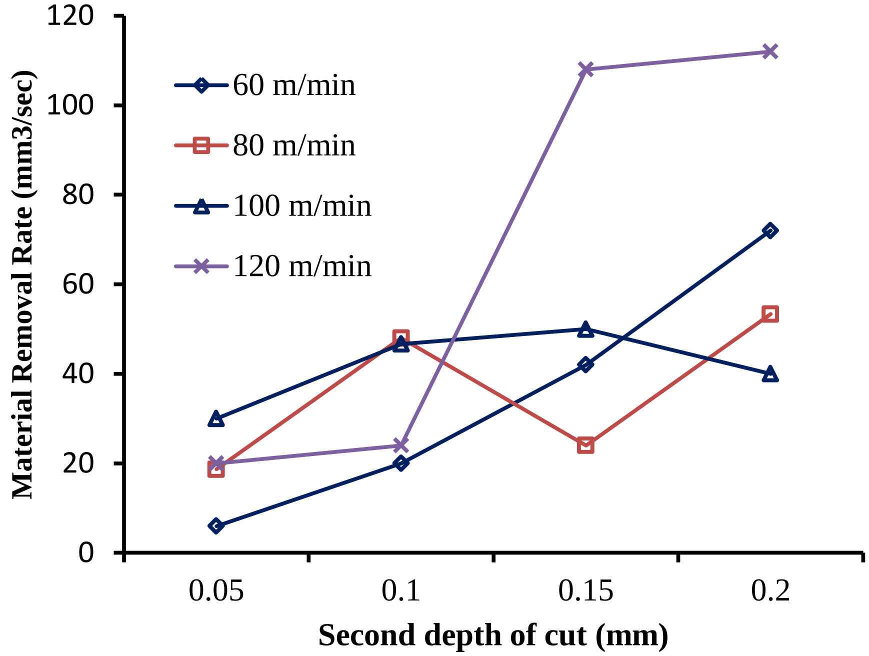

Figure 4. 27 Effect of Second of Depth of Cut on MRR

Effect of Feed Rate and First Depth of Cut on MRR

As can be seen, Figure 4.28 shows the effect of the first depth of cut on material removal rate at constant feed rate of 0.04mm/rev, 0.08mm/rev, 0.012mm/rev, and 0.16mm/rev respectively. As the increasing first depth of cut from 0.1mm to 0.20mm, and from 0.20mm to 0.25mm the material removal rate was increased and material removal rate was decreased at a constant feed rate of 0.04mm/rev. But at 0.08mm/rev of the feed rate, the material removal rate was increased initially with an increasing first depth of cut from 0.10 mm to 0.15 mm and then decrease when the first depth of cut was increased to 0.25mm. The material removal rate was decreased as increasing first depth of cut from 0.10 mm to 0.15 mm and then increased when the first depth of cut was increased to 0.25mm at a constant feed rate of 0.12mm/rev. Generally, the material removal rate increases within an increase in the first depth of cut. But due to the increase, the continuous in-depth cut has an impact on surface roughness, tool wear, and tooltip temperature it was limited.

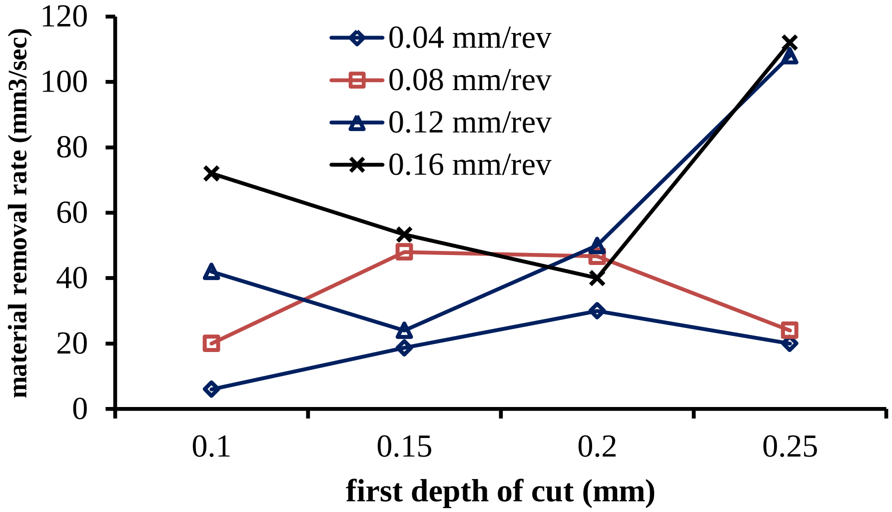

Figure 4. 28 Effects of First Depth of Cut and Feed Rate on MRR

Effect of Feed Rate vs. Second Depth of Cut on MRR

Figure 4.29 shows that suggest the effect of the second depth of cut on material removal rate at constant feed rate of 0.04mm/rev, 0.08mm/rev, 0.012mm/rev, and 0.16mm/rev respectively. As the second depth of cut increased from 0.05mm to 0.20mm, and 0.20mm to 0.25mm the material removal rate was increased and material removal rate was increased respectively at a constant feed rate of 0.04mm/rev. But at 0.08mm/rev of the feed rate, the material removal rate was initially increased with the increase of the second depth of cut from 0.05mm to 0.10mm and then decreased when the second depth of cut was increased to 0.0.2mm. Hence, the material removal rate increase, as increasing the cutting speed, feed rate, and depth of cut.

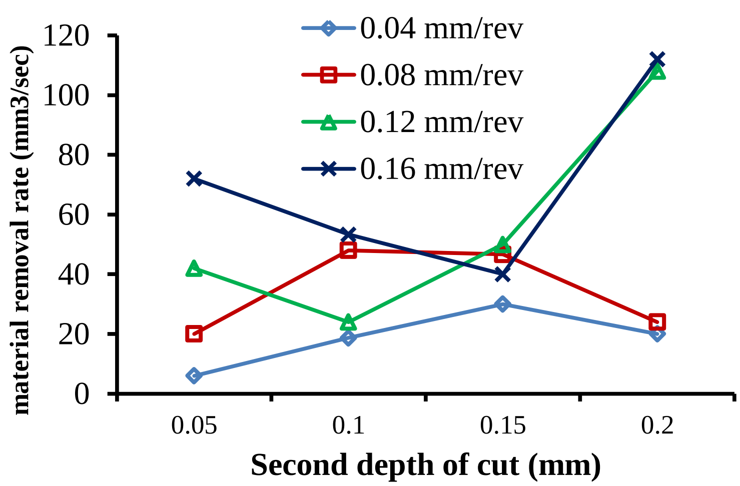

Figure 4. 29 effect of the second depth of cut on MRR varies of feed rate.

4.4.5 Response Tables and Analysis of Material Removal Rate for S/N Ratio Results

Table 4. 12 Response Table for S/N Ratio

Levels	Cutting parameters			
	Speed(v)	Feed(f)	First depth (d1)	Second depth (d2)
1	27.80	24.14	31.04	25.70
2	30.30	30.16	31.04	30.14
3	32.24	33.68	31.04	33.06
4	**33.82**	**36.18**	31.04	**35.25**
Delta	6.02	12.04	0.00	9.54
Rank	3	1	4	2

By looking at the MRR in Table 4.12 and the main effect plot for the S/N ratios, the feed rate weight percentage has the greatest effect (Delta = 12.04, Rank = 1), and the factor with the second effect on the S/N ratio is the second depth of cut (Delta = 9.54, Rank = 2), third is the cutting speed (Delta = 6.02, Rank = 3) and the least effect on the (S/N) ratio was the first depth of cut (Delta = 0.00, Rank = 4). The optimal parameter combination is **v4f4d11d24**, for increasing the material removal rate of AISI 1050 steel.

4.4.6 Main Effects of S/N Ratio

The numerical value of the peak in each graph shows the best value of that particular parameter at that level. The most effective parameter to maximize the MRR is the feed rate compared to other cutting factors, and the first depth of cut has the least impact on the MRR value. Since the S/N ratio was selected, the cutting speed was set at level four (120 m/min), the feed at level four (0.16 mm/rev), the first depth of cut at level one (0.10mm), and the second depth of cut at level four (0.05mm) was selected.

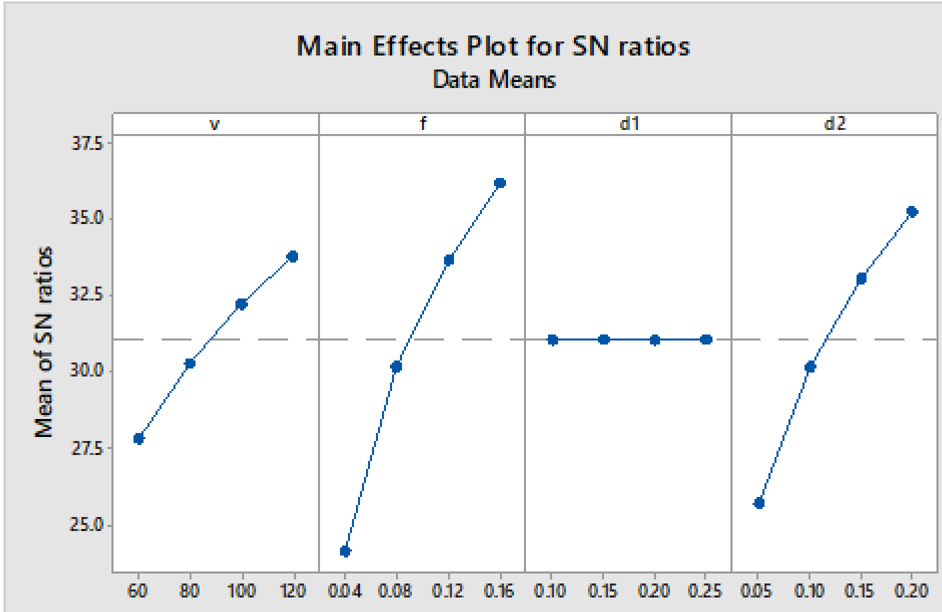

Figure 4. 30 Main Effects of S/N ratios on MRR

4.4.7 Predict the Performance of Optimum Level

For predicting the optimum response, four factors of parameters are selected by large mean values at v4f4d1d24 are the optimum levels of parameters for MRR value. To find out the predicted value of the responses (MRR value) the following linear regression equation is used.

$$y_{opt} = \mathrm{m} + (\mathrm{m}v_4 - \mathrm{m}) + (\mathrm{m}f_4 - \mathrm{m}) + (\mathrm{m}d1_1 - \mathrm{m}) + (\mathrm{m}d2_4 - \mathrm{m}) \qquad (4.6)$$

Where, m is the average performance S/N ratio for MRR, $m\mathrm{v}_4$ is the optimum level value for parameter v, $m\mathrm{f}_4$ is the optimum level value for parameter f, $m\mathrm{d}1_1$ is the optimum level value for parameter d1, and $\mathrm{md}2_4$ is optimum level value for parameter d2.

The average value of the S/N ratio ($m = \frac{S/N}{16}$) = 29.163

y_{opt} = 29.163 + (33.82 -29.163) + (36.18 - 29.163) + (31.04-29.163) + (35.25-29.163)

y_{opt} = 43.1673 (predict value for S/N ratio)

4.4.8 ANOVA (Analysis of Variance) for MRR

Analysis of Variance (ANOVA) is performed to find out the influence and performance of each process Parameter in machining.

Table 4. 13 Analysis of Variance for MRR

Source	DOF	SS	MSS	F-value	P-value	%C	Significance
V	3	2530.7	843.6	4.46	0.129	18.21 %	Significant
F	3	6051.6	2017.2	10.43	0.043	43.55 %	High significant
d1	3	643.6	214.5	1.11	0.467	4.63 %	Less significant
d2	3	4091.1	1363.7	7.05	0.071	29.44 %	Medium significant
Error	3	580	193.3			4.17 %	
Total	15	13896.9					

4.4.9 Regression Model for MRR

Utilizing the above data, the mathematical model for MRR has been developed using multiple linear regression (MLR) analysis. The dependent variable material removal rate can be conceived as a linear combination of the independent variables, namely cutting speed, feed rate, and first depth of cut and second depth of cut. The data was analyzed by Minitab 17 software.

Table 4.14 ANOVA for MRR Model

Source	DF	Adjss	Adjmss	f-value	p-value	Remarks
Regression	4	12475.5	3118.9	24.14	0.000	Significant
Speed	1	1947.0	1947.0	15.07	0.003	
Feed	1	6008.9	6008.9	46.50	0.000	
Depth1	1	486.8	486.8	3.77	0.078	
Depth2	1	4032.8	4032.8	31.21	0.000	
Error	11	1421.4	129.2			
Total	15	13896.9				

When regression analysis is employed by applying the least-squares method to the experimental data to obtain the coefficient of this equation, the following equation is attained for MRR.

MRR = -68.4+0.493v+433.3f-98.7d1+142d2

$$R^2 = 97.67\%,\ R^2(Adj) = 91.35\%$$

From the linear model Table 4.15; regression is significant as the p-value is less than 0.05. The Regression Model presented a high determination coefficient (R^2=0.9767) which indicates the goodness of fit for the model and the high significance of the model.

4.4.10 Determining the Optimum Condition

From the Table 4.12 and Table 4.13, it's observed that cutting speed weight percentage optimum level value 120 m/min, feed optimum level value 0.16mm/rev, first depth of cut optimum level value 0.25mm and second depth of cut optimum level value 0.15mm makes the response S/N ratio values large. Therefore, the optimum processing parameters signal to noise (S/N) ratio was selected.

Table 4.15 presents the optimum parameters setting selected for MRR obtained from the design of the experiment and experimental results. The selected optimum parameters in this study were at minimum cutting speed, at higher feed, at a minimum first depth of cut, and medium second depth of cut which**,** is at **v4f4d11d24.**

Table 4.15 Optimum Parameters setting levels and their values

Controllable factors	Level selected	Value of levels	Ranks of affecting the response
Speed	4	120	3
Feed	4	0.16	1
Depth1	1	0.10	4
Depth2	4	0.15	2

4.4.11 Confirmation Test of MRR

The obtained optimal combination of process parameters was verified with the predicted result. The optimum combination of parameters obtained from Table 4.16 was (v4f4d11d24) at 120m/min cutting speed, 0.16 mm/rev feed, and 0.10 mm first depth of cut and 0.15mm second depth of cut.

Table 4. 16 Optimum and predicted values of cutting parameters

Response	Optimal parameter	Predicted values		Experimental value	
MRR (mm3/sec)	V4f4d11d24	mean	S/N ratio	Mean	S/N ratio
		110.67	43.1673	112	40.9844

Experimental Value Versus Predict Value on Material Removal Rate (MRR)

The comparison between the Experimental value and Predicted value of Material Removal Rate is very near this indicating acceptable. The variation between the experimental value and predicted value using the Taguchi method was very small.

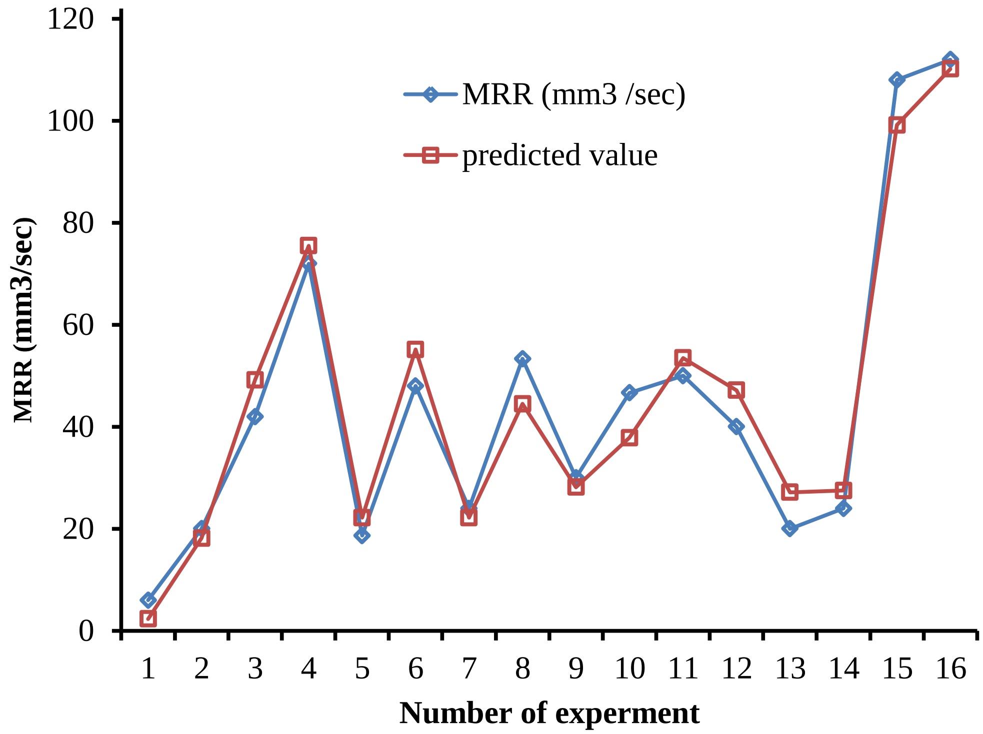

Figure 4. 31 Plot of predicted using Taguchi method and actual experimental of MRR

4.5 Analysis of Grey Relational Analysis of Surface Roughness and Material Removal Rate

The consequences obtained from various researches are considered in detail and are discussed in the following sub-division. The investigation analysis data such as surface roughness, material removal rate, and cutting tooltip temperature are transformed into an S/N ratio. Subsequently, the response parameter of surface roughness and material removal rate is converted into an S/N ratio using Taguchi analysis. The normalizing sequence for both parameters is calculated from the S/N ratio. By using the normalizing sequence value deviation sequence is calculated. The Grey relational coefficient for both parameters is calculated by using the deviation sequence values. Finally, GRG is developed from the GRC.

Table 4. 17 shows the GRG of surface roughness (Ra) and material removal rate MRR of AISI 1050 steel material.

No. exp.	Response parameter		S/N ratio		Normalizing sequence		Deviation of sequence		Grey relational Coefficient		
	Ra(m)	MRR(mm ^{3}/sec)	Ra	MRR	Ra	MRR	Ra	MRR	Ra	MRR	GRG
1	1.22	6.000	-1.72720	15.5630	0.663	0	0.34	1	0.6	0.3	0.75
2	1.64	20.000	-2.54210	26.0206	0.407	0.411	0.59	0.59	0.46	0.5	0.71
3	1.78	42.000	-2.27887	32.4650	0.423	0.665	0.58	0.34	0.46	0.6	0.63
4	1.60	72.000	-4.08240	37.1466	0.217	0.849	0.78	0.15	0.39	0.8	0.59
5	1.56	18.667	-3.86249	25.4213	0.243	0.388	0.76	0.61	0.4	0.5	0.45
6	1.58	48.000	-3.28706	33.6248	0.308	0.710	0.69	0.29	0.42	0.6	0.51
7	1.42	24.000	-1.86843	27.6042	0.643	0.474	0.36	0.53	0.58	0.4	0.49
8	1.52	53.333	-3.63687	34.5400	0.243	0.746	0.76	0.25	0.39	0.6	0.48
9	1.68	30.000	-4.13652	29.5425	0.211	0.550	0.79	0.45	0.38	0.5	0.44
10	2.02	46.667	-5.93330	33.3802	0	0.701	1	0.30	0.3	0.6	0.46
11	1.60	50.000	-5.84512	33.9794	0.722	0.724	0.28	0.72	0.64	0.4	0.52
12	1.28	40.000	-1.58362	32.0412	0.588	0.648	0.41	0.35	0.55	0.5	0.57
13	1.69	20.000	-1.79810	26.0206	0.477	0.411	0.52	0.59	0.49	0.4	0.47
14	1.54	24.000	-3.75041	27.6042	0.255	0.744	0.75	0.26	0.4	0.6	0.53
15	1.12	108.000	-0.98436	40.6685	1	0.988	0	0.01	1	0.9	0.99
16	1.55	112.000	-4.34968	40.9844	0.187	1	0.81	0	0.38	1	0.69

4.5.1 Mean Effect Plot of Grey Relational Analysis (GRA) of Surface Roughness and MRR

As observed from Table 4.18 the main effects plots for means show that the optimum condition for GRG of the Surface Roughness and Material Removal Rate is at cutting speed (120 m/min), feed rate (0.12 mm/rev), first depth of cut (0.15mm), second of the depth of cut (0.20mm).

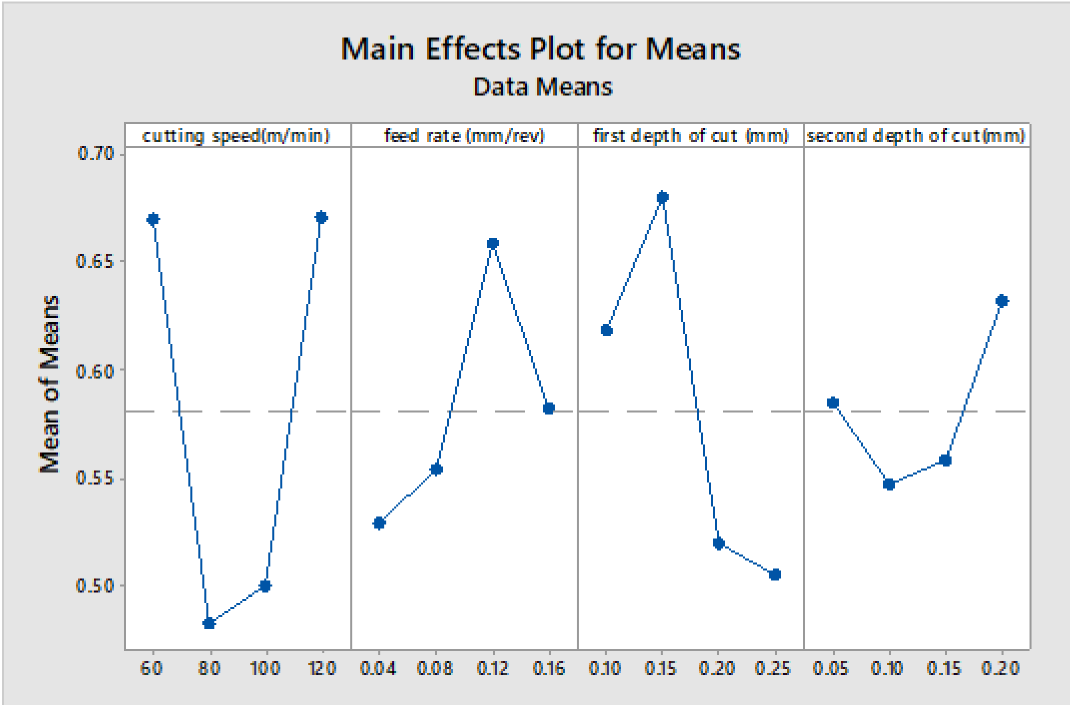

Figure 4. 32 main effect plots for means of GRG

4.5.2 Response Table for Means of GRA of Surface Roughness and MRR

The Response Table of the GRG of Surface Roughness and Material Removal Rate shows that cutting speed has the highest contribution in increasing the grey relational grade of the machining of AISI 1050 steel material with a delta number of 0.1887. While the first depth of cut is the second contributing factor in increasing the grey relational grade of the machining of AISI 1050 steel material with a delta number of 0.1750. The third ranker contributing factor is feed rate with a delta number of 0.13000. Likely the second depth of cut takes the fourth with a delta number of 0.0850.

Table 4. 18 Response table for means of GRG

Level	Cutting speed	Feed rate	First depth of cut	Second depth of cut
1	0.6700	0.5287	0.6188	0.5850
2	0.4825	0.5537	0.6800	0.5475
3	0.5000	0.6587	0.5200	0.5588
4	0.6712	0.5825	0.5050	0.6325
Delta	0.1887	0.1300	0.1750	0.0850
Rank	1	3	2	4

4.5.3 ANOVA of Grey Relational Analysis (GRA)

The last column of the ANOVA table shown in Table 4.19 indicates the percentage of contribution (Pc) in which cutting speed has the highest level of contribution (40.67%) followed by the first depth of cut (26.07%). While the feed rate and second depths of cut are the least contributors (11.98% and 5.39%) respectively.

Table 4. 19 ANOVA for Gray Relational Grade

Source	DOF	SS	MSS	F-value	P-value	%C	Significance
V	3	0.12932	0.043106	2.56	0.230	40.67%	High significant
F	3	0.03808	0.012693	0.75	0.589	11.98%	Significant
d1	3	0.08289	0.027631	1.64	0.347	26.07%	Significant
d2	3	0.01714	0.005714	0.34	0.801	5.39%	Less significant
Error	3	0.05053	0.016843			15.89%	
Total	15	0.31796				100%	

4.5.4 Confirmation Test for the grey relational grade (GRG)

Once the combination of process parameters and their level was obtained, the final step is to verify the predicted results against the experiment results.

Table 4. 20 Optimum and Predicted values of cutting parameters

Response	Optimal Parameter	Predicted Values	Experimental Value
GRG	V4f3d12d24	mean	Mean
		0.899	0.99

4.6 Analysis of cutting tooltip temperature

4.6.1 The experimental value of tooltip temperature

During the external turning process, the heat was generated due to friction created between the cutting tool and workpiece. The quality of heat produced during the machining process varies with the types of workpiece material being machined, cutting parameters used, and machining conditions. The turning of AISI 1050 steel material using a ceramics tool was characterized by the moderate temperature at the tooltip. Table 4.21 presents the obtained temperature for various cutting parameters at the tooltip during dry turning.

Table 4. 21 Experimental Results of Cutting Tooltip Temperature

Exp. No	Cutting parameters				Avg. Temp. (c^0)		S/N Ratio	
	Speed (m/min)	Feed (mm/rev)	Depth-1 (mm)	Dept-2 (mm)	Tool1	Tool2	Tool1	Tool2
1	60	0.04	0.10	0.05	41.5	40.2	-32.3610	-32.0845
2	60	0.08	0.15	0.10	44.6	41.8	-32.9867	-32.4235
3	60	0.12	0.20	0.15	47.8	43.6	-33.5886	-32.7897
4	60	0.16	0.25	0.20	50.5	48.6	-34.0658	-33.7327
5	80	0.04	0.15	0.15	56.8	50.4	-35.0870	-34.0486
6	80	0.08	0.10	0.20	52.4	52.6	-34.3866	-34.4197
7	80	0.12	0.25	0.05	59.2	49.2	-35.4464	-33.8393
8	80	0.16	0.20	0.10	55.4	50.1	-34.8702	-33.9968
9	100	0.04	0.20	0.20	62.5	64.6	-35.9176	-36.2047
10	100	0.08	0.25	0.15	68.6	60.8	-36.7265	-35.6781
11	100	0.12	0.10	0.10	60.4	60.2	-35.6207	-35.5919
12	100	0.16	0.15	0.05	61.9	56.8	-35.8338	-35.0870
13	120	0.04	0.25	0.10	82.5	58.9	-38.3291	-35.4023
14	120	0.08	0.20	0.05	78.5	54.9	-37.8974	-34.7914
15	120	0.12	0.15	0.20	72.6	70.2	-37.2187	-36.9267
16	120	0.16	0.10	0.15	68.7	67.8	-36.7391	-36.6246

Table 4.21 and Figure 4.33 shows that the tooltip temperature reading was taken from the average reading. The maximum average temperature of 82.5^0c for the first cutting tool and 70.2 for the second cutting tool was founded in experiments number thirteen and fifteen on machining parameters were 120m/min cutting speed, 0.04mm/min feed rate, 0.25mm first depth of cut and 0.10mm second depth of cut and 120m/min cutting speed, 0.12mm/rev feed rate, 0.15mm first depth of cut and 0.20mm second depth of cut respectively. The minimum temperature was obtained at experiment number one 41.5 and 40.2 for the first and second

cutting tools respectively on the cutting speed(60m/min) feed rate (0.04mm/rev), first depth of cut (0.10mm), and second depth of cut (0.05mm) machining parameters. Therefore, the increase in cutting speed leads to an increase in tooltip temperature generated.

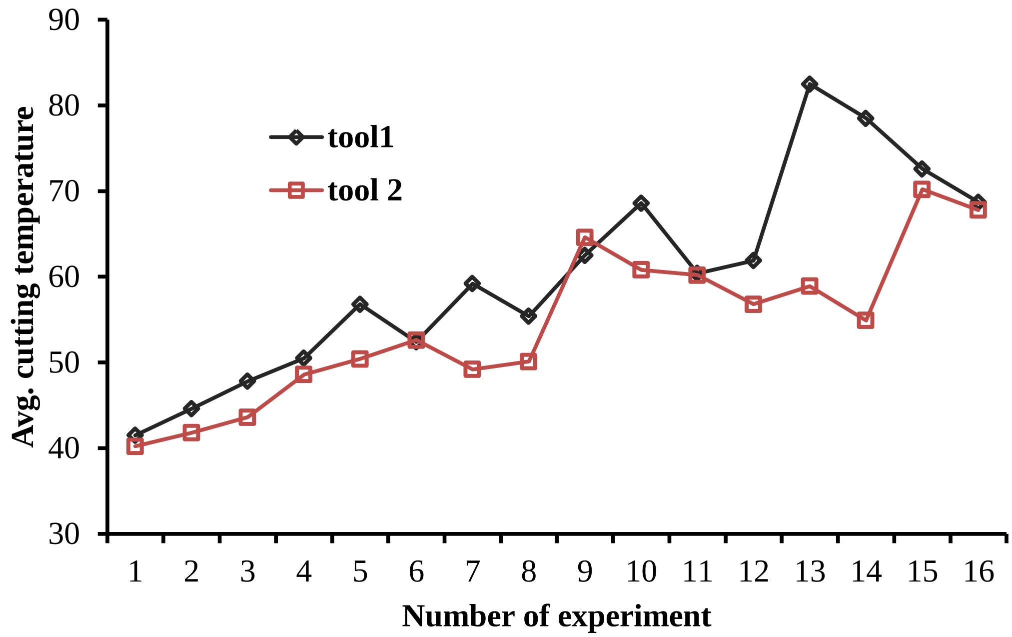

Figure 4. 33 variations of the experimental value of cutting tooltip temperature

4.6.2 Parametric Optimization of Cutting Tooltip Temperature

A response table for each response features such as the mean and signal-to-noise ratio of cutting tool tip temperature for each response is calculated. The answer table shows which factors have the greatest influence on the response, and which level of the factors have associated with higher or lower answer parameters. Steps to generate the response table

1 Calculates the selected response characteristics for cutting speed, feed, first depth of cut, and second depth of cut at each level.

The response for each factor is calculated as example shown for factor v.

For factor v, the mean

$$\text{At level } 1(v_1) = \frac{(41.5+44.6+47.8+50.5)}{4} = 416.1$$

$$\text{At level } 2(v_2) = \frac{(56.8+52.4+59.2+55.4)}{4} = 55.95$$

$$\text{At level } 3(v_3) = \frac{(62.5+68.6+60.4+61.9)}{4} = 63.95$$

$$\text{At level } 4(v_4) = \frac{(82.5+78.5+72.6+68.7)}{4} = 75.575$$

In a similar manner calculated mean for factors f, d1, and d2 in each level and also the response table for each response feature such as mean and signal-to-noise ratio is also calculated similar manner for cutting tooltip 2 temperatures.

2 After this delta values are calculated, which is the difference between the highest average response characteristic value and the lowest average response characteristic values for levels of that factor.

3 By considering the delta values ranks are allotted from high to low. The factor with the highest delta value is ranked one.

Table 4. 22 Response Table for Mean Effects Plot for Cutting Tooltip1 Temperature (smaller is better)

Levels	Cutting parameters			
	Speed(v)	Feed(f)	First depth (d1)	Second depth (d2)
1	**46.1**	**60.83**	**55.75**	**60.27**
2	55.95	61.02	58.98	60.73
3	63.35	60.00	61.05	60.47
4	75.575	59.13	65.20	59.50
Delta	29.48	1.90	9.45	1.23
Rank	1	3	2	4

Table 4.22 and Table 4.23 shows that Response Table for the mean cutting tooltip 1 temperature analysis observed that the amount of heat generated during machining operations is primarily affected by cutting speed compared to other cutting parameters.

Table 4. 23 Response Table for Mean Effects Plot for Cutting Tooltip 2 Temperature

Levels	Cutting parameters			
	Speed(v)	Feed(f)	First depth (d1)	Second depth (d2)
1	**43.55**	**53.52**	**51.20**	**50.27**
2	50.57	52.52	54.80	52.75
3	60.60	55.80	53.30	55.65
4	62.95	55.83	54.38	59.00
Delta	19.40	3.30	1.90	8.73
Rank	1	3	4	2

4.6.3 Main Effects of Cutting Tooltip Temperature

4.6.3.1 Main Effects of Cutting Tooltip1 Temperature

As observed from Figure 4.33 implies the effect of cutting tooltip1 temperature on individual cutting parameters. The change in the first depth of cut and cutting speed has a very high effect on cutting temperature while the second depth of cut and feed rate has a moderate effect on cutting temperature. For the given range of cutting parameters, cutting speed has been found as the most significant parameter.

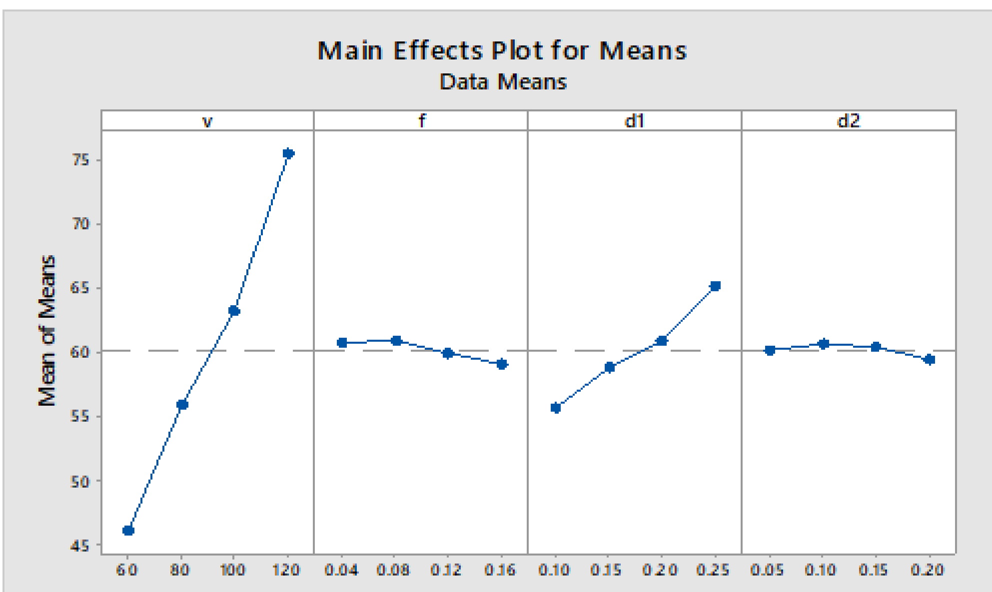

Figure 4. 34 main effects of cutting tooltip 1 temperature

4.6.3.2 Main Effects of Cutting Tooltip 2 Temperature

Figure 4.34 shows that indicate the effect of cutting tooltip 2 temperatures on individual cutting parameters. The change in the second depth of cut and cutting speed has a very high effect on cutting tooltip2 temperature while the first depth of cut and feed rate have a moderate effect on cutting temperature. For the given range of cutting parameters, cutting speed has been found as the most significant parameter.

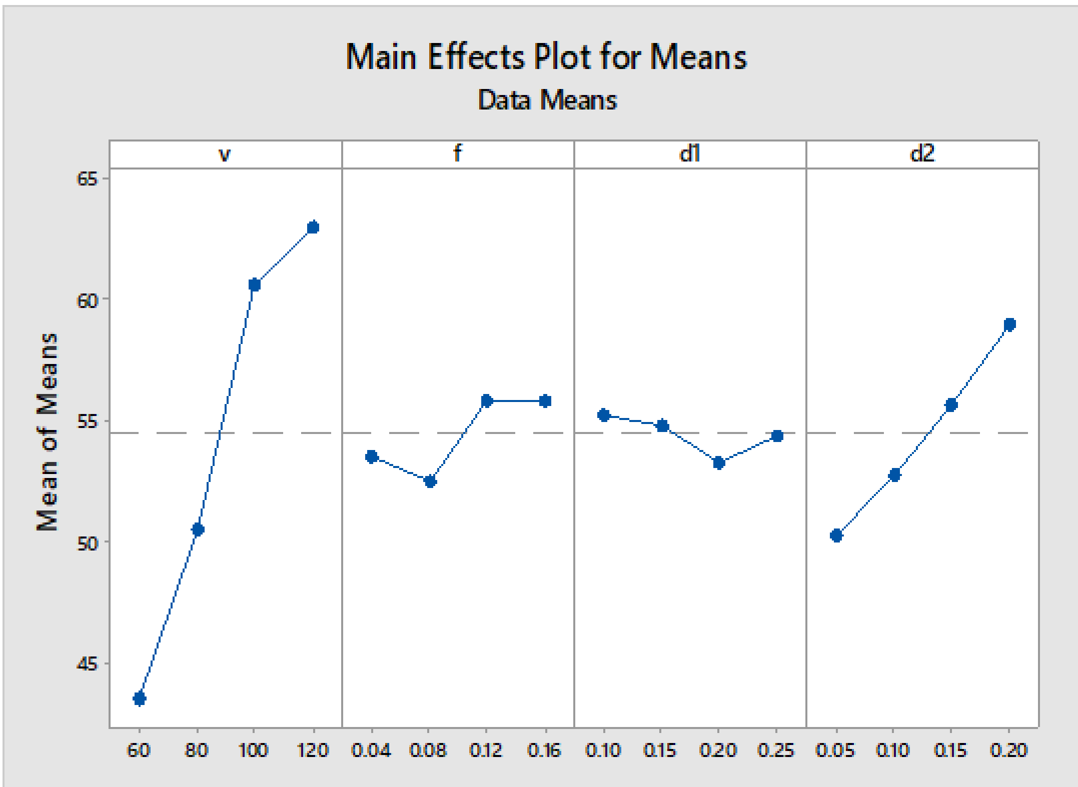

Figure 4. 35 Main Effects of Cutting Tooltip2 Temperature

4.6.4 Response Tables and Analysis of S/N ratio for Cutting Tooltip1 Temperature

By looking at the cutting tooltip1 temperature in Table 4.35 and the main effect plot for the S/N ratios, the cutting speed weight percentage has the greatest effect (Delta = 4.30, Rank = 1), and the factor with the second effect on the S/N ratio is the second depth of cut (Delta = 1.37, Rank = 2), third is the first depth of cut (Delta = 0.15, Rank = 3) and the least effect on the (S/N) ratio was the feed rate (Delta = 0.12, Rank = 4). The optimal parameter combination is **v1f1d11d21**, for decreasing the cutting tooltip 1 temperature of AISI 1050 steel.

Table 4. 24 Response table for S/N for Cutting Tooltip 1 Temperature (smaller is better)

	Cutting parameters			
	Speed(v)	Feed(f)	First depth (d1)	Second depth (d2)
1	**-33.25**	**-35.32**	**-34.78**	**-35.38**
2	-34.95	-35.50	-35.28	-35.45
3	-36.02	-35.47	-35.38	-35.54
4	-37.55	-35.38	-36.14	-35.40
Delta	4.30	0.12	1.37	0.15
Rank	1	4	2	3

4.6.5 Main Effects of S/N Ratio for cutting tooltip 1 temperature

The numerical value of the maximum in each graph shows the best value of that particular parameter at that level. The most effective parameter to minimize the cutting tooltip 1 temperature is the second depth of cut compared to other cutting factors, and the feed rate has the least impact on the cutting tool tip temperature value. Since the S/N ratio was selected, the cutting speed was set at level one (60 m/min), the feed at level one (0.04 mm/rev), the first depth of cut at level one (0.10mm), and the second depth of cut at level one (0.05mm) was selected.

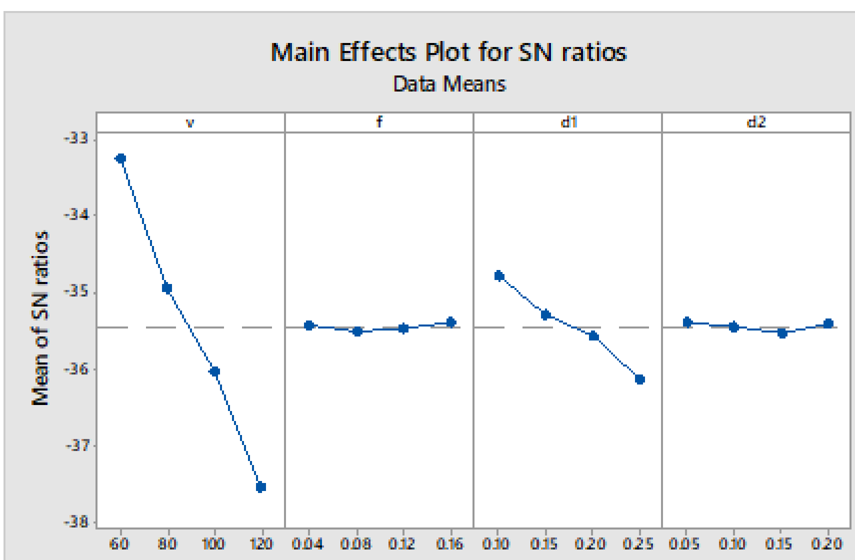

Figure 4. 36 main effects for S/N ratios on cutting tooltip 1 temperature

4.6.6 Predict the Performance of Optimum Level for cutting tooltip 1 temperature

For predicting the optimum response, four factors of parameters are selected by large mean values at v1f1d11d21 are the optimum levels of parameters for cutting tool tip1 temperature value. To find out the predicted value of the responses (Cutting Tooltip1 Temperature Value) the following linear regression equation is used.

$$y_{opt} = \text{m} + (\text{m}v_1 - \text{m}) + (\text{m}f_1 - \text{m}) + (\text{m}d1_1 - \text{m}) + (\text{m}d2_1 - \text{m}) \quad (4.7)$$

Where m is the average performance S/N ratio for cutting tooltip temperature, $m\text{v}_1$ is the optimum level value for parameter v, $m\text{f}_1$ is the optimum level value for parameter f, $m\text{d1}_1$ is the optimum level value for parameter d1, and md2_1 is optimum level value for parameter d2.

$$\text{The average value of the S/N ratio } (m = \frac{S/N}{16}) = -35.4422$$

y_{opt} = -35.4422+ (-33.25+35.4422) + (-35.42+35.4422) + (-34.78+35.4422) + (-35.38+35.4422)

y_{opt} = -32.5091 (predict value for S/N ratio)

4.6.6 Response Tables and Analysis of S/N Ratio for Cutting Tooltip 2 Temperature

By looking at the cutting tooltip2 temperature in Table 4.36 and the main effect plot for the S/N ratios, the cutting speed weight percentage has the greatest effect (Delta = 3.18, Rank = 1), and the factor with the second effect on the S/N ratio is the second depth of cut (Delta = 1.37, Rank = 2), third is the feed rate (Delta = 0.53, Rank = 3) and the least effect on the (S/N) ratio was the first depth of cut (Delta = 0.23, Rank = 4). The optimal parameter combination is **v1f1d11d21**, for decreasing the cutting tooltip2 temperature of AISI 1050 steel.

Table 4. 25 Response table for S/N for cutting tooltip 2 temperature

Levels	Cutting parameters			
	Speed(v)	Feed(f)	First depth (d1)	Second depth (d2)
1	**-32.76**	**-34.44**	**-34.68**	**-33.95**
2	-34.08	-34.33	-34.62	-34.35
3	-35.64	-34.79	-34.45	-34.79
4	-35.94	-34.86	-34.66	-35.32
Delta	3.18	0.53	0.23	1.37
Rank	1	3	4	2

4.6.7 Main effects of S/N ratio for Cutting Tooltip2 Temperature

The numerical value of the peak in each graph shows the best value of that particular parameter at that level. The most effective parameter to minimize the Cutting Tooltip2 Temperature is the cutting speed compared to other cutting factors, and the feed rate has the least impact on the cutting tooltip2 temperature value. Since the S/N ratio was selected, the cutting speed was set at level one (60 m/min), the feed at level one (0.04 mm/rev), the first depth of cut at level one (0.10mm), and the second depth of cut at level one (0.05mm) was selected.

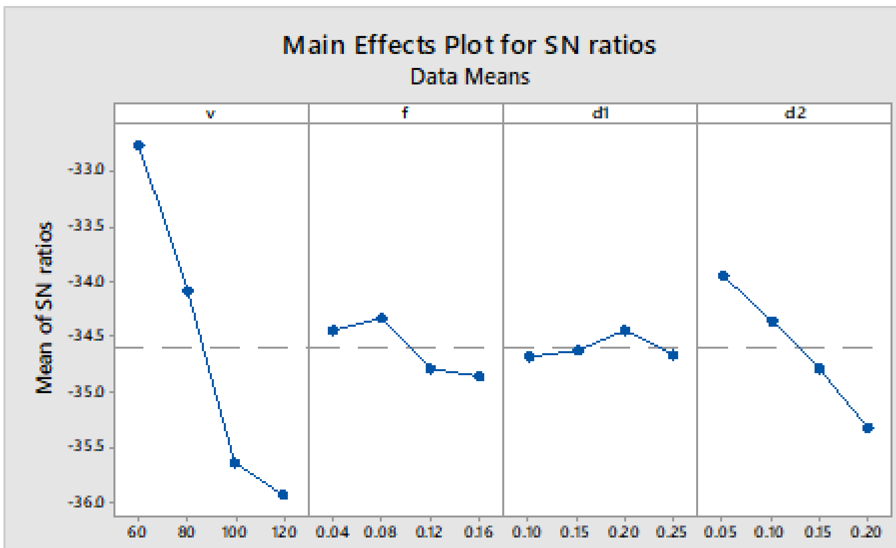

Figure 4. 37 Main Effects for S/N ratios of Cutting Tooltip2 Temperature

4.6.8 Predict the Performance of Optimum Level for cutting tooltip2 temperature

For predicting the optimum response, four factors of parameters are selected by large mean values at v1f1d11d21 are the optimum levels of parameters for cutting tooltip2 temperature value. To find out the predicted value of the responses (cutting tooltip2 temperature value) the following linear regression equation is used.

$$y_{opt} = \mathrm{m} + (\mathrm{m}v_1 - \mathrm{m}) + (\mathrm{m}f_1 - \mathrm{m}) + (\mathrm{m}d1_1 - \mathrm{m}) + (\mathrm{m}d2_1 - \mathrm{m}) \quad (4.8)$$

Where m is the average performance S/N ratio for cutting tooltip, $m\mathrm{v}_1$ is the optimum level value for parameter v, $m\mathrm{f}_1$ is the optimum level value for parameter f, $m\mathrm{d1}_1$ is the optimum level value for parameter d1, and $\mathrm{md2}_1$ is optimum level value for parameter d2.

The average value of the S/N ratio $(m = \frac{S/N}{16}) = -34.60259375$

$$y_{opt} = -34.60259375 + (-32.76+34.60259375) + (-34.44+34.60259375 + (-34.68+34.60259375) + (-33.95+34.60259375)$$

y_{opt} = -32.0156 (predict value for S/N ratio)

4.6.9 Interaction Effects of cutting parameter on cutting tooltip temperature

The cutting temperature in the cutting tooltip depends to a great extent on the friction between tool-workpiece materials and causes the undesirable temperature in the cutting tool which leads to rapid wear of cutting material by softening of the tooltip. The plot of the cutting parameter versus an average temperature is shown in figures 4.37 -4.41.

Effects of feed rate and cutting speed on both cutting tooltip temperature

Figure 4.38(a, b) observed the variation of cutting tooltip temperature during machining of AISI 1050 steel with machining parameters for both cutting tools. Figure 4.38 (a) shows that the maximum temperature was obtained at a cutting speed of 120m/min and 0.04mm/rev feed rate, and the minimum temperature was obtained at a cutting speed of 60m/min and 0.04mm/rev for cutting tooltip 1 temperature. Figure 4.38 (b) shows that the maximum temperature was obtained at a cutting speed of 120m/min and 0.12mm feed rate, and the minimum temperature was obtained at a cutting speed of 60m/min and 0.04mm/rev feed rate for cutting tooltip 2 temperature. At 60 m/min cutting speed for both the cutting, tooltip temperature was increased within increased feed rate. It is observed that the cutting temperature increases as the cutting speed increases with the corresponding feed rate due to high friction at the tool-work interface.

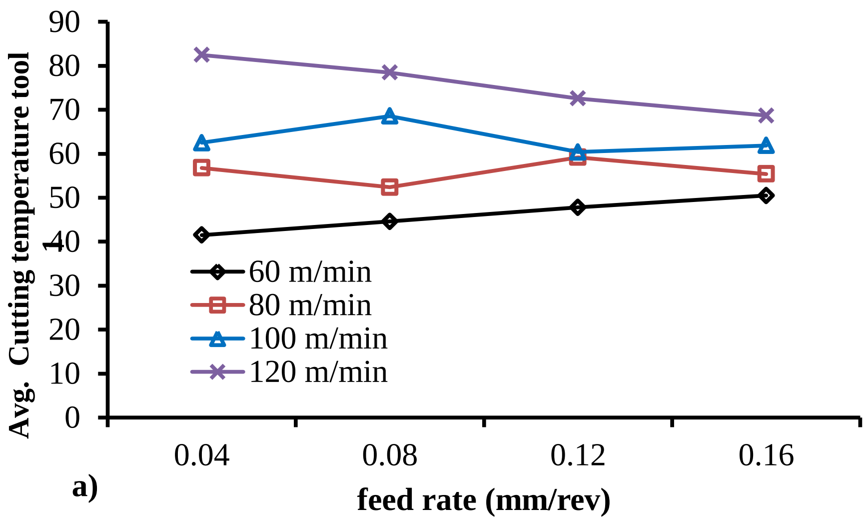

a)

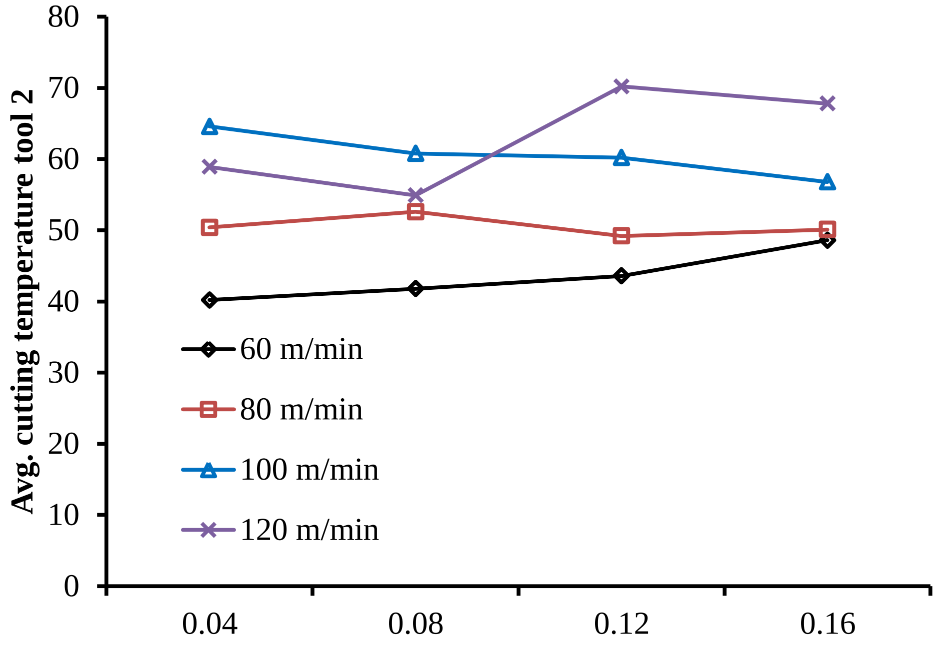

b)

Figure 4. 38 (a, b) Plot of the effect of feed rate on cutting tooltip temperature

Effect of first depth of cut and cutting speed on cutting tooltip temperature

Figure 4.39 (a, b) shows the effect first depth of cut on the tooltip temperature. It is observed that the variation of tooltip temperature during machining with cutting parameter for both cutting tooltip. The maximum temperature was obtained at a cutting speed of 120m/min and 0.1mm first depth of cut, the minimum temperature was obtained at a cutting speed of 60m/min and 0.1mm for cutting tooltip 1 temperature. Then the maximum temperature was obtained at a cutting speed of 120m/min and 0.2mm first depth of cut, and the minimum temperature was obtained at a cutting speed of 60m/min and 0.1mm at the first depth of cut for cutting tooltip 2 temperatures. At 60 m/min cutting speed for both the cutting, tooltip temperature was increasing within increase first depth of cut.

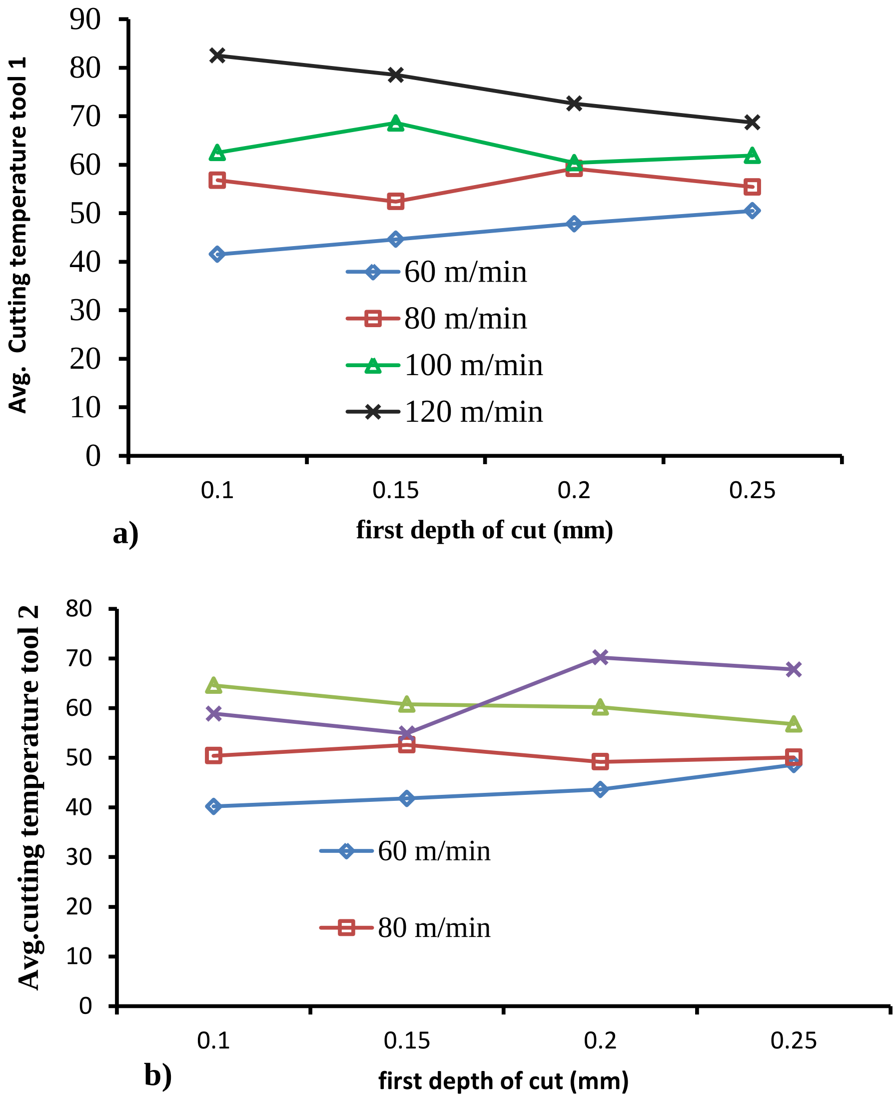

Figure 4. 39(a, b) Plot of the effect of first depth of cut on cutting tooltip temperature

Effect of second depth of cut and cutting speed on tooltip temperature

As observed from Figure 4.40 (a, b) shows the effect first depth of cut on the tooltip temperature. It is observed that the variation of tooltip temperature during machining with cutting parameter for both cutting tooltip. The maximum temperature was obtained at a cutting speed of 120m/min and 0.0.05mm second depth of cut, and minimum temperature was obtained at a cutting speed of 60m/min and 0.05mm for cutting tooltip 1 temperature. Then the maximum temperature was obtained at a cutting speed of 120m/min and 0.15mm first depth of cut, and minimum temperature was obtained at a cutting speed of 60m/min and 0.1mm second depth of cut for cutting tooltip 2 temperatures. At 60 m/min cutting speed for both the cutting, tooltip temperature was increased within increase the second depth of cut.

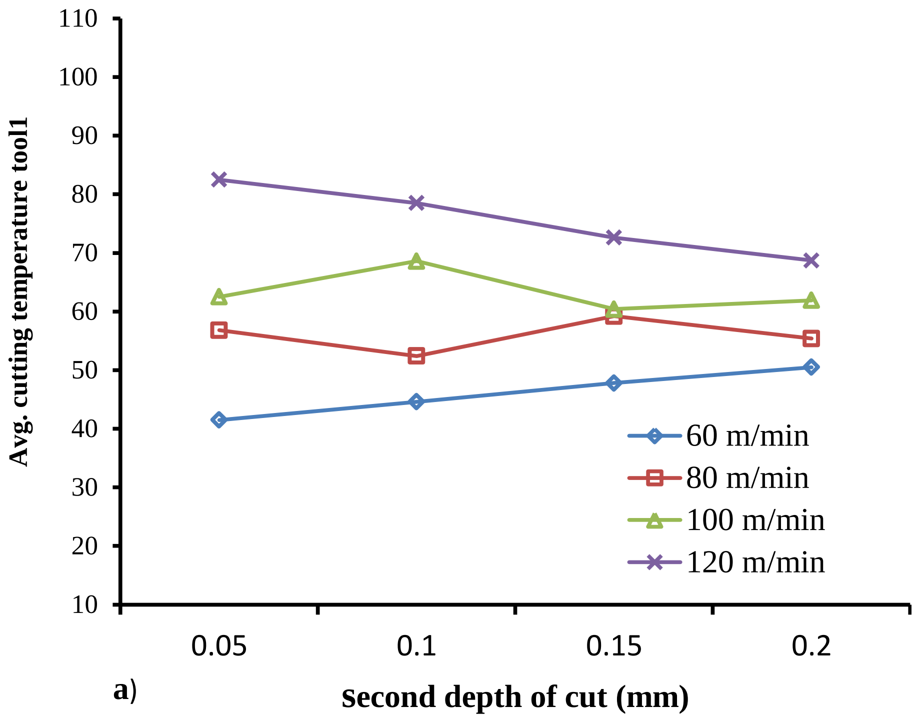

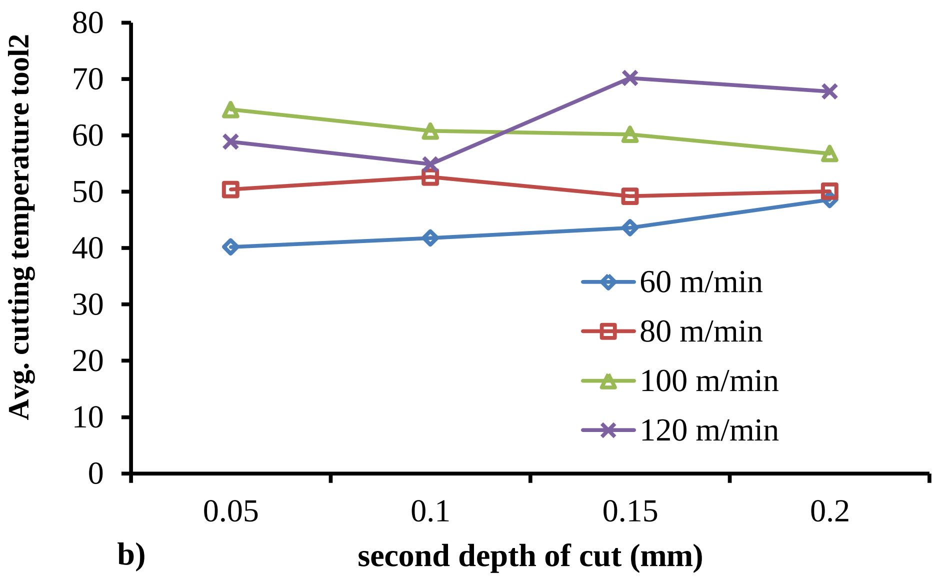

Figure 4. 40 (a, b) Plot of Effect Second Depth of Cut and Cutting Speed on Cutting Tooltip Temperature

Effects of the first depth of cut and feed rate on cutting tooltip temperature

Figure 4.41 (a, b) shows the effects of the first depth of cut with tooltip temperature during the machining of the material. As increase the second depth of cut from 0.1mm to 0.25mm, the cutting tool tip temperature was an increase for both cutting tools. The friction produced between the cutting tooltip and workpiece during the machining process influenced on cutting temperature in the cutting tooltip. The undesirable temperature produced in the cutting tool leads to rapid wear of cutting tool materials by softening of the tooltip.

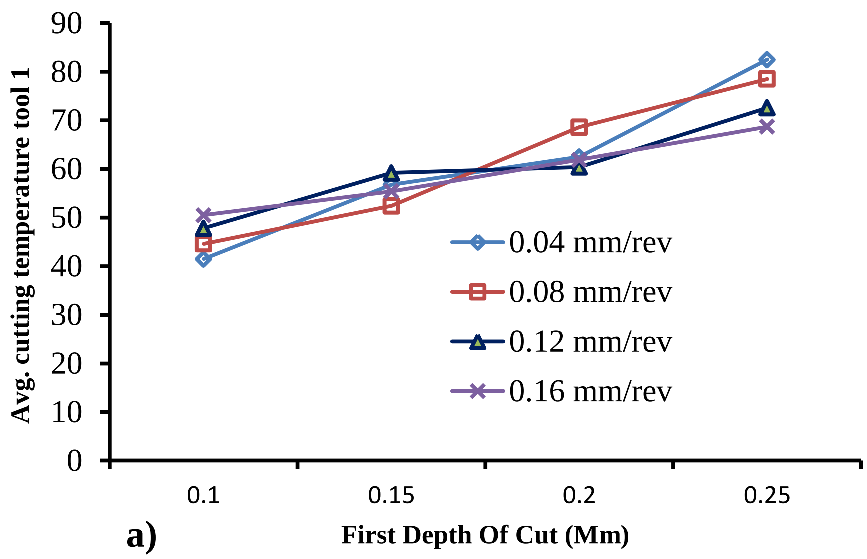

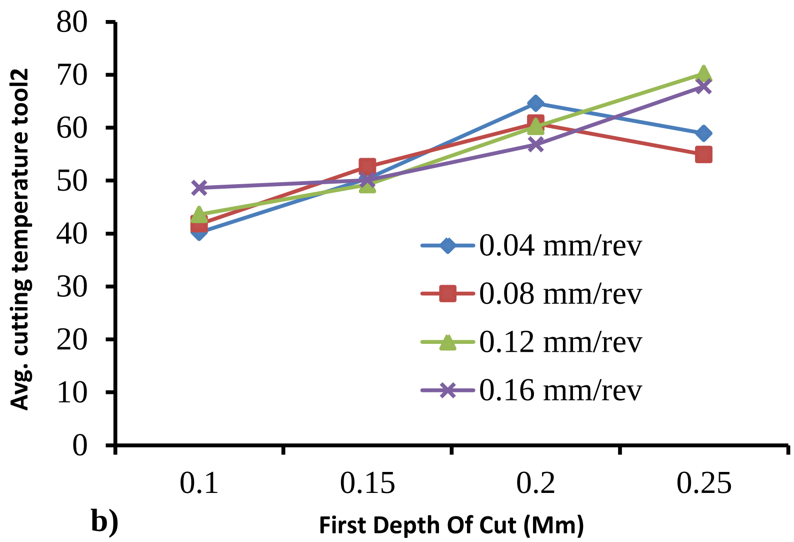

Figure 4. 41(a, b) Effect of Feed Rate and First Depth of Cut on Cutting Tooltip Temperature

Effects of the first depth of cut and feed rate on cutting tooltip temperature

Figure 4.42 (a, b) shows the effects of the first depth of cut with tooltip temperature during the machining of the material at a constant feed rate. As increase the second depth of cut from 0.05mm to 0.20mm, the cutting tool tip temperature was an increase for both cutting tools. An increase in the second depth of cut leads to cutting temperature increment. But at the obtained optimum cutting parameter of the second depth of cut of 0.05mm the minimum cutting temperature of 40.2^{0}C was achieved. Generally, the four machining parameters are found to be a dominant effect on tooltip temperature and the result of experimental outcomes gives a good due about the values of tooltip temperature achieved, as well as the effect of some cutting parameters.

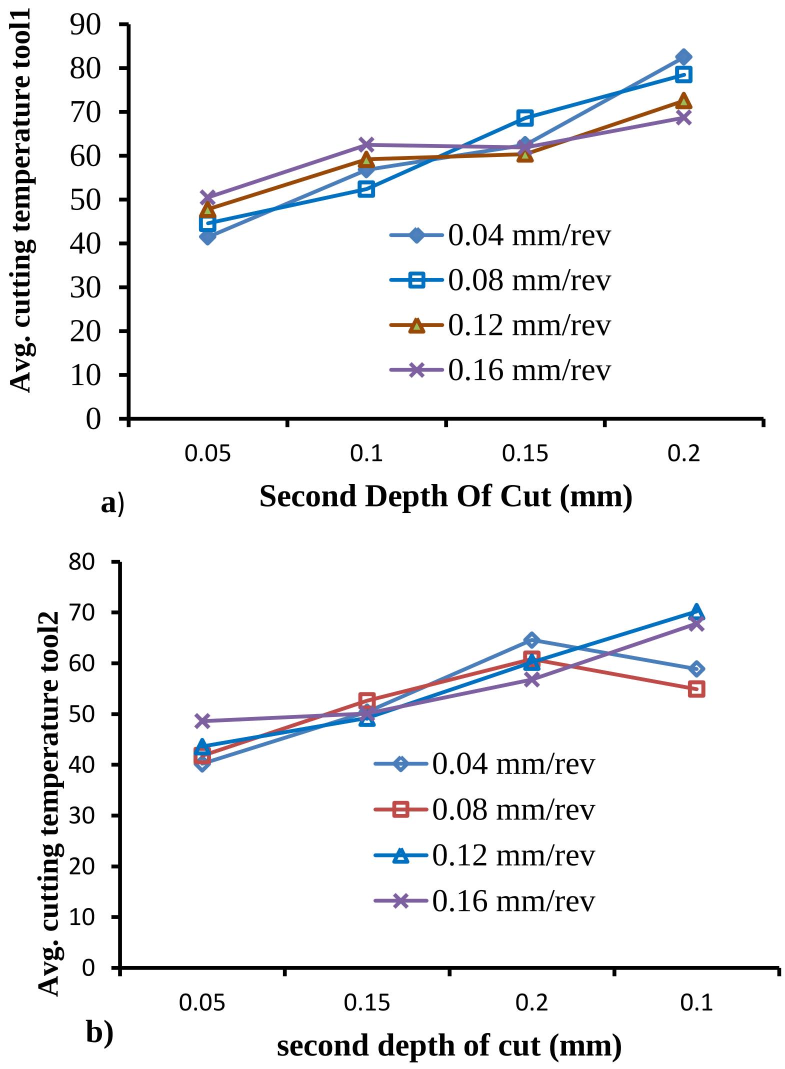

Figure 4. 42(a, b) Effect of Second Depth of Cut on Cutting Tooltip Temperature

Also, optimum cutting parameters (cutting speed 60m/min, feed rate 0.04mm/rev, first depth of cut 0.10 mm, and second depth of cut 0.05mm) were resulted in the optimum machining condition by giving acceptable cutting temperature readings and are relatively minimal as compared to remaining parameters.

During the cutting of metal, the temperature of the interaction area of the cutting tool and workpiece becomes high. The temperature affects not only the rate of wear of the cutting tool but also the integrity of the workpiece surface such as residual stress, hardness, and expansion-contraction during and after machining. Surface damage by oxidation, rapid corrosion, and burning.

4.6.10 ANOVA for Cutting Tooltip Temperature

4.6.10.1 ANOVA for Cutting Tooltip1 Temperature

The last column of the ANOVA table shown in table 4.26 indicates the percentage of contribution (Pc) in which cutting speed has the highest level of contribution (89.32%) followed by the first depth of cut (9.07%). While the second depth of cut and feed rate are the least contributors (0.61%and 0.44%) respectively.

Table 4. 26 ANOVA for Cutting Tool Tip1 Temperature Value

Source	DOF	SS	MSS	F-value	P-value	%C	Significance
V	3	1852.71	617.571	87.80	0.002	89.32%	High Significant
F	3	9.04	3.012	0.43	0.748	0.44%	least significant
d1	3	188.07	62.691	8.91	0.053	9.07%	Significant
d2	3	3.36	1.119	0.16	0.917	0.61%	less significant
Error	3	21.10	7.034			1.02%	
Total	15	2074.28					

4.6.10.2 ANOVA for Cutting Tooltip 2 Temperature

In the last column of the ANOVA as indicated in Table 4.27, the percentage of contribution (Pc) in which cutting speed has the highest level of contribution (80.37%) followed by the second depth of cut (14.04%). While the feed rate and the first depth of cut are the least contributors (2.74%and 0.66%) respectively.

Table 4. 27 ANOVA for Cutting Tooltip2 Temperature Value

Source	DOF	SS	MSS	F-value	P-value	%C	Significance
V	3	975.58	325.192	42.39	0.006	80.66%	Highly Significant
F	3	33.08	11.027	1.44	0.386	2.74%	less significant
d1	3	8.04	2.679	0.35	0.786	0.66%	Least Significant
d2	3	169.84	56.12	7.38	0.067	14.04%	medium significant
Error	3	23.01	7.671			1.90%	
Total	15	1209.54					

4.6.11 Regression Model for Cutting Tooltip temperature

A Regression model provides a function that describes the relationship between one more independent variable and response, dependent, or target variables. Using the experimental data, the mathematical model for cutting tooltip temperature has been developed using multiple linear regression analysis. The dependent variable cutting tooltip temperature can be independent variables.

Table 4. 28 ANOVA of Regression Model of Cutting Tooltip1 Temperature

Source	DF	C (%)	Adj SS	Adj MS	F-Value	P-Value
Regression	4	97.89%	2030.45	507.61	127.40	0.000
v	1	88.54%	1836.49	1836.49	460.92	0.000
f	1	0.36%	7.50	7.50	1.88	0.197
d1	1	8.93%	185.14	185.14	46.47	0.000
d2	1	0.06%	1.33	1.33	0.33	0.576
Error	11	2.11%	43.83	3.98		
Total	15	100.00%				

Table 4. 29 ANOVA of the Regression model of cutting tooltip2 temperature

Source	DF	C	Adj SS	Adj MS	F-Value	P-Value
Regression	4	92.92%	1123.87	280.967	36.07	0.000
v	1	76.97%	930.93	930.930	119.52	0.000
f	1	1.71%	20.71	20.706	2.66	0.131
d1	1	0.26%	3.16	3.160	0.41	0.537
d2	1	13.98%	169.07	169.071	21.71	0.001
Error	11	7.08%	85.68	7.789		
Total	15	100.00%				

Regression Equation

Tool 1 = 8.65 + 0.4791 v - 15.3 f + 60.85 d1 - 5.15 d2

Model Summary

S = 1.99608   R-sq.=97.89%   R-sq. (Adj)=97.97.12

Regression Equation

Tool 2 = 15.30 + 0.3411 v + 25.4 f - 8.0 d1 + 58.1 d2

Model Summary

S= 2.79084   R-sq. = 92.92%   R-sq. (Adj) = 92.87

4.6.12 Confirmation Test of Cutting Tooltip Temperature

The obtained optimal combination of process parameters was verified with the predicted result. The optimum combinations of parameters obtained from Table 4.30 were (v1f1d11d21) and (v1f1d11d21) at 60m/min cutting speed, 0.04 mm/rev feed, 0.10 mm first depth of cut, and 0.05mm second depth of cut and for cutting tooltip1 temperature and cutting tooltip2 temperature respectively.

Table 4. 30 Optimum and Predicted values of cutting parameters

Response	Optimal parameter	Predicted values		Experimental value	
Cutting tool 1	V1f1d11d21	Mean	S/N ratio	Mean	S/N ratio
		42.2187	-32.5091	41.5	-32.3610
Cutting tool 2	V1f1d11d21	Mean	S/N ratio	mean	S/N ratio
		39.2937	-32.0156	40.2	-32.0845

4.6.13 Experimental and Predicted Values of Cutting Tooltip Temperature

As observed from Table 4.31 show that the Experiment and predicted value of cutting tooltip temperature were very close for both cutting tool temperatures. It can be seen that the difference between the experimental result and the predicted results is very small for both. The values predicted by using the Taguchi approach are approximately near to the value which is experimentally obtained. This verifies that the experimental results of cutting tool tip temperature are strongly correlated with the predicted results. The percentage error is calculated by subtracting the predicted value from the experimental value and dividing the result for the experiment value multiple by 100%. For each experiment, the variation of experiment value and predicted value are calculated. The calculated value is very similar all variation calculated value is less than 5% this indicates that the variation value of cutting tooltip temperature is strongly correlated with each other.

Table 4. 31 Comparison between Predicted Value and Actual Experimental Value of Cutting Tooltip Temperature

Exp. No	Experimental value		Predicted value		Variation		% variation	
	Tool 1	Tool2	Tool 1	Tool2	Tool1	Tool 2	Tool1	Tool2
1	41.5	40.2	42.2187	39.2937	-0.72	0.9063	1.73	2.25
2	44.6	41.8	46.0938	40.3687	-1.49	1.43	3.35	3.42
3	47.8	43.6	46.8937	45.0438	0.9063	-1.444	1.9	3.31
4	50.5	48.6	49.1937	49.4937	1.3	-0.893	2.6	1.84
5	56.8	50.4	55.4937	51.2938	1.31	-0.894	2.3	1.77
6	52.4	52.6	51.4937	54.0438	0.9063	-1.444	1.73	2.77
7	59.2	49.2	60.6937	47.7688	-1.49	1.43	2.52	2.9
8	55.4	50.1	56.1187	49.1938	-0.7187	0.906	1.29	1.81
9	62.5	64.6	63.9937	63.1687	-1.4937	1.43	2.38	2.21
10	68.6	60.8	69.3187	59.8937	-0.7187	0.906	1.05	1.49
11	60.4	60.2	59.0938	61.0938	1.31	-0.894	2.16	1.48
12	61.9	56.8	60.9938	58.2438	0.9062	-1.444	1.5	2.54
13	82.5	58.9	81.5937	60.3438	0.9063	-1.443	1.09	2.45
14	78.5	54.9	77.1938	55.7938	1.3062	-0.893	1.7	1.62
15	72.6	70.2	73.3187	69.2938	-0.7187	0.9062	0.98	1.29
16	68.7	67.8	70.1938	66.3688	-1.4938	1.4312	2.17	2.11

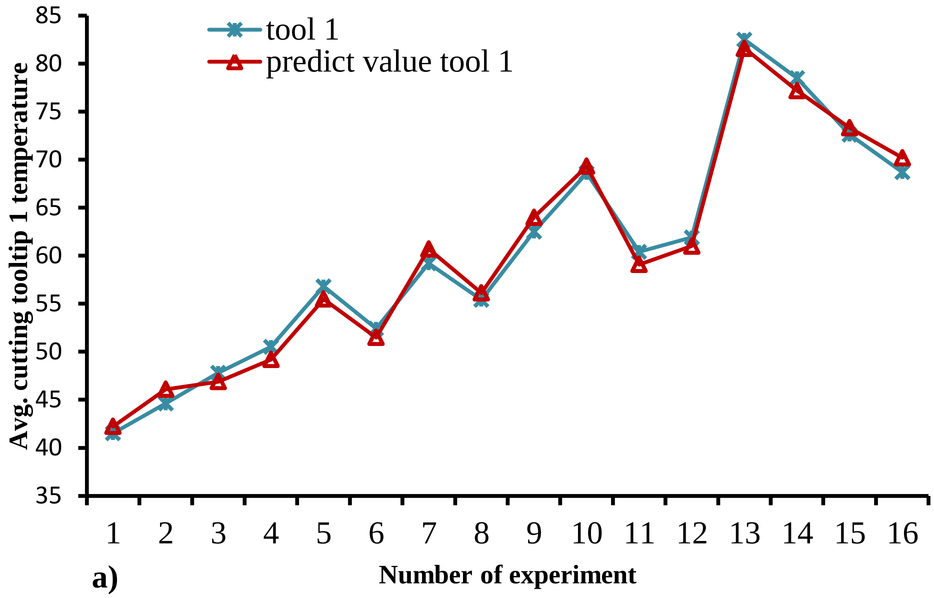

a)

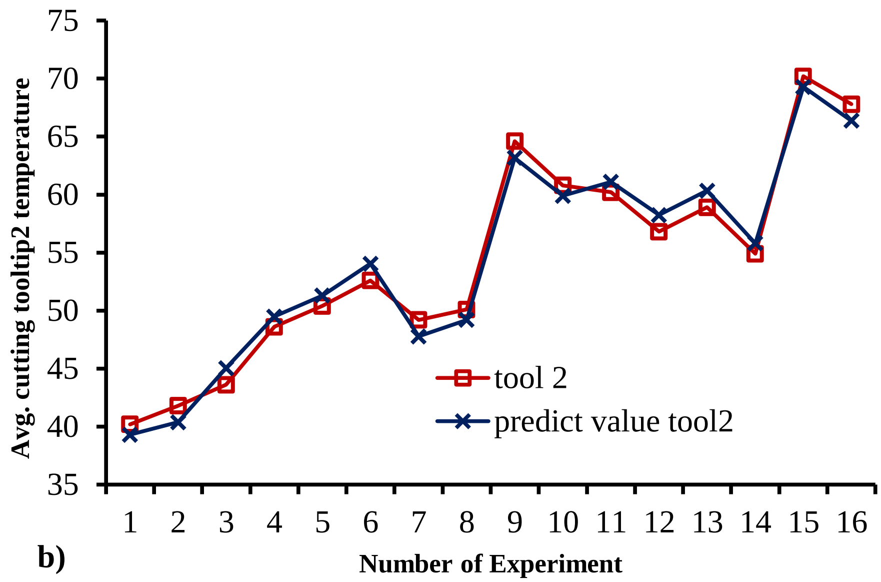

b)

Figure 4. 43(a, b) Plot of Predicted Value using Taguchi Method and Actual Experimental Value of Cutting Tooltip Temperature

Figure 4.31(a, b) shows that the Experiment and predicted value of cutting tooltip temperature were very close for both cutting tool temperatures. It can be seen that the difference between the experimental result and the predicted results is very small for both. The values predicted by using the Taguchi approach are approximately near to the value which is experimentally obtained. This verifies that the experimental results of cutting tool tip temperature are strongly correlated with the predicted results.

4.7 Analysis of Grey Relational Analysis of Cutting Tooltip1 and 2 Temperatures

The results obtained from various experimentations are analyzed in detail and are discussed in the following subsections. The experimental investigation data from cutting parameters such as cutting speed, feed rate, first depth of cut, and second depth of cut are transformed into Signal-to-Noise (S/N) ratio. After the Response Parameters of the cutting tool tip temperature are converted into an S/N ratio using Taguchi analysis. The normalizing sequence for both parameters is calculated from the S/N ratio. By using the normalizing sequence value deviation sequence is calculated. The Gray relational coefficient for both parameters is calculated using the deviation sequence values. Finally, the GRG is developed from the GRC.

Table 4. 32 Show that the GRG Development for the Cutting Tooltip 1 and 2 Temperature

Exp. Run	Response parameter		S/N ratios		Normalizing sequence		Deviation sequence		Grey relational coefficient		Grey relational analysis
	Tool 1	Tool 2	Tool 1	Tool 2	Tool 1	Tool 2	Tool1	Tool2	Tool 1	Tool2	GRD
1	41.5	40.2	-32.3610	-32.0845	0.45	0.08	0.55	0.92	0.48	0.35	0.42
2	44.6	41.8	-32.9867	-32.4235	0.74	0.55	0.26	0.45	0.66	0.53	0.60
3	47.8	43.6	-33.5886	-32.7897	0	0	1	1	0.33	0.33	0.33
4	50.5	48.6	-34.0658	-33.7327	0.91	0.85	0.09	0.15	0.85	0.77	0.81
5	56.8	50.4	-35.0870	-34.0486	0.19	0.23	0.81	0.77	0.38	0.64	0.51
6	52.4	52.6	-34.3866	-34.4197	0.87	0.42	0.13	0.58	0.79	0.46	0.63
7	59.2	49.2	-35.4464	-33.8393	0.12	0.27	0.88	0.73	0.36	0.41	0.39
8	55.4	50.1	-34.8702	-33.9968	0.22	0.44	0.78	0. 56	0.39	0.47	0.43
9	62.5	64.6	-35.9176	-36.2047	0.53	0.54	0.47	0.46	0.52	0.52	0.52
10	68.6	60.8	-36.7265	-35.6781	0.26	0.73	0.74	0.27	0.40	0.65	0.53
11	60.4	60.2	-35.6207	-35.5919	0.61	0.7	0.39	0.3	0.64	0.83	0.74
12	61.9	56.8	-35.8338	-35.0870	0.46	0.43	0.54	0.57	0.48	0.47	0.48
13	82.5	58.9	-38.3291	-35.4023	0.91	0.93	0.09	0.07	0.85	0.88	0.87
14	78.5	54.9	-37.8974	-34.7914	0.51	0.73	0.44	0.27	0.53	0.65	0.59
15	72.6	70.2	-37.2187	-36.9267	1	1	0	0	1	1	1
16	68.7	67.8	-36.7391	-36.6246	0.25	0.53	0.75	0.47	0.4	0.52	0.46

4.7.1 Analysis of Main Effects of GRG on Cutting Tooltips 1 and 2 Temperature

Show the main effects plots for means show that the optimum condition for GRG of the tooltip temperature is at cutting speed (120 m/min), feed rate (0.12mm/rev), first depth of cut (0.15mm), second of the depth of cut (0.20mm).

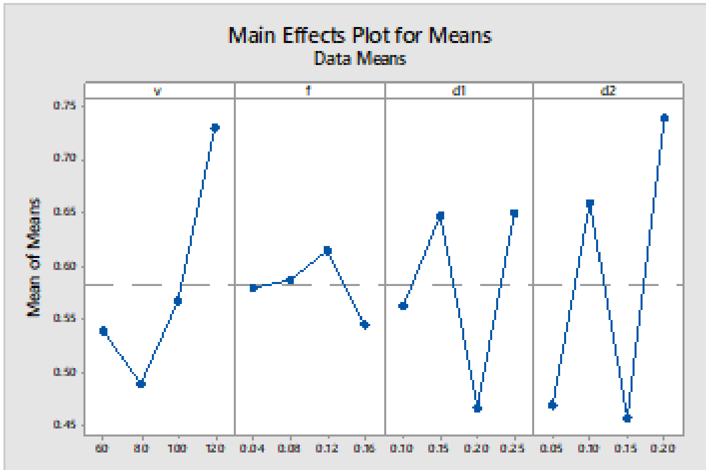

Figure 4. 44 Plots of Main Effects of Means of GRG of Cutting Tooltip1 and 2 Temperatures

4.7.2 Response Table for Means of GRG of Cutting Tooltip Temperature

The Response Table of the cutting tool tip temperature shows that the second depth of cut has the highest contribution in decreasing the cutting tool tip temperature of the machining with a delta number of 0.2825. While cutting speed is the second contributing factor in increasing, the cutting tool tip temperature of the machining within a delta number of 0.2400. The third ranker contributing factor is the first depth of cut with a delta number of 0.1825 likely the feed rate takes the fourth delta number of 0.0700.

Table 4. 33 Response table for means of GRG of cutting tooltip temperature

Level	Cutting speed(m/min)	feed rate (mm/rev)	First depth of cut (mm)	Second depth of cut (mm)
1	0.5400	0.5800	0.5625	0.4700
2	0.4900	0.5875	0.6475	0.6600
3	0.5675	0.6150	0.4675	0.4575
4	0.7300	0.5450	0.6500	0.7400
Delta	0.2400	0.0700	0.1825	0.2825
Rank	2	4	3	1

4.7.3 Analysis of variance of GRG of cutting tooltip temperature

The ANOVA table shown in Table 4.34 indicates the percentage of contribution (Pc) in which the second depth of cut has the highest level of contribution (45.10%) followed by cutting speed (24.69%), first depth of cut (17.10%) and feed rate (1.90%) respectively.

Table 4. 34 ANOVA of GRG of the Cutting Tooltip temperature

Source	DF	Contribution	Adj SS	Adj MS	F-Value	P-Value
cutting speed (m/min)	3	24.69%	0.129369	0.043123	2.20	0.267
feed rate (mm/rev)	3	1.90%	0.009969	0.003323	0.17	0.910
first depth of cut (mm)	3	17.10%	0.089619	0.029873	1.53	0.368
second depth of cut (mm)	3	45.10%	0.236369	0.078790	4.03	0.141
Error	3	11.20%	0.058719	0.019573		
Total	15	100.00%				

4.7.3 Confirmation test of grey relation grade of cutting tooltip temperature

Table 4. 35 Optimum and Predicted values of cutting parameters

Response	Optimal Parameter	Predicted Values	Experimental Value
GRG.	V4f3d12d24	mean	mean
		0.98	1

4.8 Analysis Observation of Chip Morphology

The chips from the machining test were collected, mounted, and measured. The type of chip is imperative in metal cutting operation because it influences product accuracy, tool life, surface finish, and operator safety. In general, chip control is greatly affected by cutting conditions used during the machining operation. Figure 4.45 shows the photographic chip images obtained in the machining operation. In general, when the feed rate increases, then the chip thickness increases.

This impact is because of the viable infiltration of dry machining at the cutting zone, creating a significant decrease in cutting temperatures, reducing the friction between the contact surfaces, and decreasing the bond between the chip and cutting tool coming in the reduction in chip size (Sivaiah & Chakradhar, 2016). At the point, when the feed rate was increased from 0.04 mm/rev to 0.16 mm/rev and also the depth of cut increased, the chips are thicker.

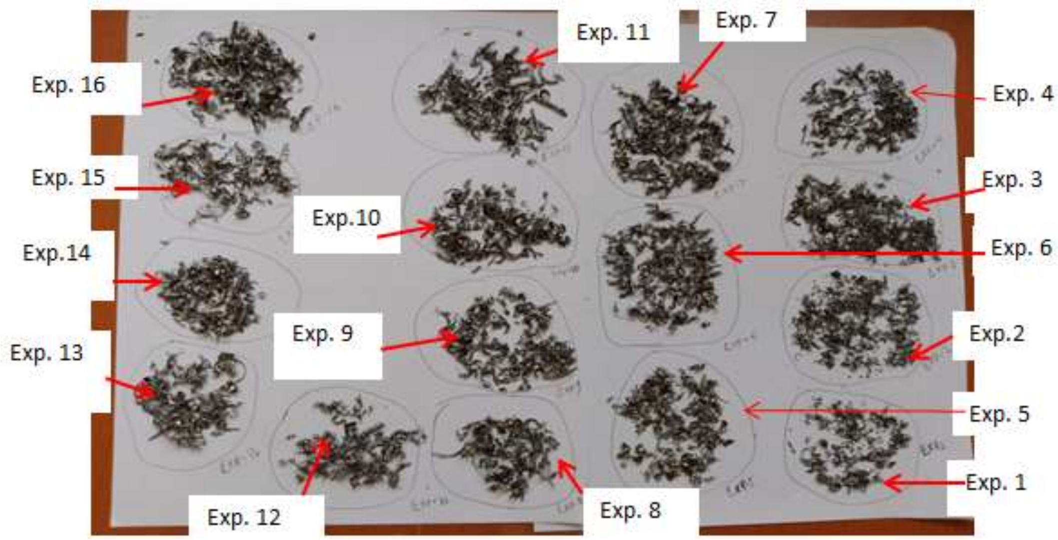

Figure 4. 45 Chip Morphology Generated from Machined workpiece

In analyzing the chip morphology, Table 4.36 confirmed that as the feed reduced and the cutting speed increased, a reduction of chip thickness has occurred this is due to a substantial contact area on the rake face and a small shear plane area at the low cutting speed which results in thinner chips formation. In contrast, with an increase in chip thickness due to increased feed because of severe compressive stresses generated ahead of the tool rake, thereby a large volume of material becomes plastic deformation which resulted in a thick chip. The highest chip thickness which is 0.58 mm was achieved at the maximum feed rate value, 0.16 mm/rev, and the lowest chip thickness 0.1 mm was achieved at a lower feed rate value of 0.04 mm/rev. Also, the maximum and minimum lengths of chips were identified as the longest is 12.6 mm and the smallest is 5.2 mm respectively. For every sixteen experimental studies measure the maximum, minimum thickness, and length of chips generated from the double tool turning operations of AISI 1050 steel materials in dry machining conditions.

Table 4. 36 Observed the Length (mm) and Thickness of the Chip (mm) from Chip Morphology.

Exp. No	Cutting parameters				Length of chip	Thickness of chip
	Speed	Feed	Depth-1	Dept-2		
1	60	0.04	0.10	0.05	5.2	0.1
2	60	0.08	0.15	0.10	6.0	0.18
3	60	0.12	0.20	0.15	6.6	0.38
4	60	0.16	0.25	0.20	7.2	0.44
5	80	0.04	0.15	0.15	6.9	0.17
6	80	0.08	0.10	0.20	7.5	0.22
7	80	0.12	0.25	0.05	8.2	0.39
8	80	0.16	0.20	0.10	8.6	0.54
9	100	0.04	0.20	0.20	7.3	0.28
10	100	0.08	0.25	0.15	7.8	0.32
11	100	0.12	0.10	0.10	9.2	0.37
12	100	0.16	0.15	0.05	10.6	0.56
13	120	0.04	0.25	0.10	9.8	0.24
14	120	0.08	0.20	0.05	9.6	0.33
15	120	0.12	0.15	0.20	10.8	0.40
16	120	0.16	0.10	0.15	12.6	0.58

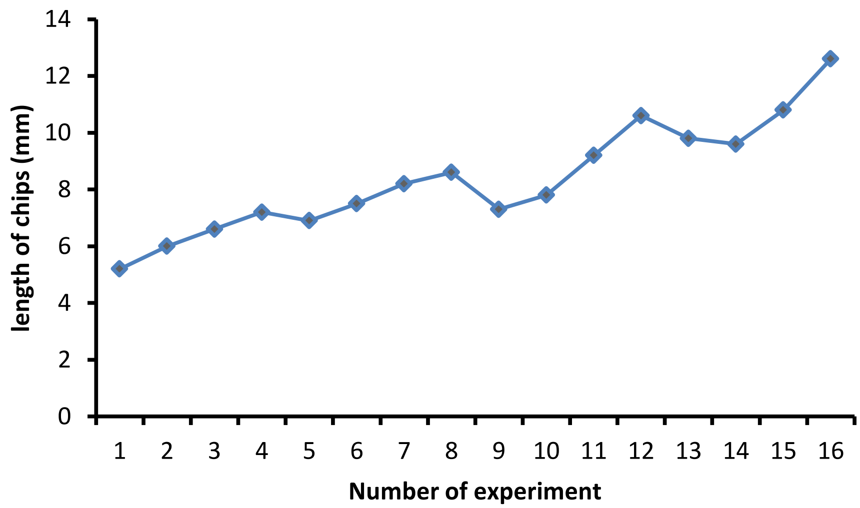

Figure 4. 46 Generated Length of Chips during the Experiments

As shown in figure 4.46 as increasing cutting parameters during the machining process, the generated chips length was increased. Also, the maximum and minimum lengths of chips were identified as the longest is 12.6 mm and the smallest is 5.2 mm respectively.

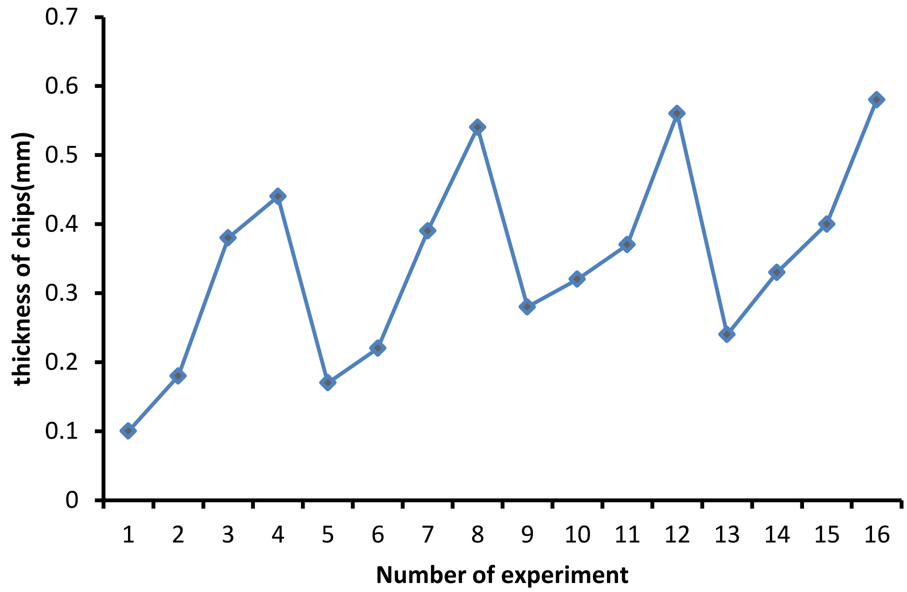

Figure 4. 47 Generated Thickness of Chips during the Experiments

Figure 4.47 shows the variation in chip thickness generated during the experimental study in dry conditions. The highest chip thickness which is 0.58 mm was achieved at the maximum feed rate value, 0.16 mm/rev, and the lowest chip thickness 0.1 mm was achieved at a lower feed rate value of 0.04 mm/rev. As observed maximum chip thickness was obtained at the maximum value of feed rate. As the feed rate increased the thickness of the chip generated was thicker.

CHAPTER FIVE

5 CONCLUSION AND RECOMMENDATIONS

5.1 Conclusion

The current study was focused on the investigation and parametric optimization of machining carried out on the double cutting tool turning on AISI 1050 steel material during dry condition with ceramics inserted cutting tools. The main cutting parameters in this study were the first depth of cut, second depth of cut, feed rate, and spindle speed. The effects of these cutting parameters on surface roughness, material removal rate, cutting tooltip temperature, the combination of surface roughness and material removal rate, and both cutting tooltip temperature were studied using Taguchi L16 orthogonal array and signal-to-noise method, Regression Analysis, and Grey Relational Analysis Method for the combination of response and also consideration was given chip morphology or chip mechanism study. Selection of cutting parameters was done based on knowledge found in the literature, recommendations of tool manufacturers' current industrial practice, and experience. The role of each factor was identified by the analysis of variance (ANOVA) for each response. Therefore, based on the experimental results the following conclusions were drawn.

- ✓ The experiment works with the Taguchi method based on the orthogonal array was an effective and efficient way of reducing the number of experiments; accordingly, the resources can be saved in turning of AISI 1050 steel workpiece material.
- ✓ In the turning of AISI 1050 steel for least surface roughness (high surface quality), the cutting speed of 120 m/min, feed rate of 0.16mm/rev, medium first depth of cut of 0.15mm and second depth of cut of 0.05mm was selected that is v4f4d12d21 and optimized cutting parameters to get low surface roughness which was the high surface finish of the machined part.
- ✓ Analysis of variance (ANOVA) shows that the second depth of cut was the most significant parameter for surface roughness followed by the first depth of cut, feed rate, and cutting speed, affected by 64.99%, 15.41%, 8.92 %, and 5.83 % respectively.

- ✓ The analytical results with ANOVA analysis showed that the feed rate (the most significant factor) contributed 43.55 %, whereas the second depth of cut, cutting speed and first depth of cut contribution was 29.44 %, 18.21 %, and 4.63 % for MRR.
- ✓ The experimental results with ANOVA analysis showed that the cutting speed (the most significant factor) contributed 89.32 %, whereas the first depth of cut, second depth of cut, and feed rate contribution were 9.07 %, 0.61%, and 0.44 % for cutting tooltip1 temperature and the cutting speed (the most significant factor) contributed 80.66 %, whereas the second depth of cut, feed rate, first depth of cut contribution were 14.04 %,2.27 %, and 0.66 % for- cutting tooltip 2 temperature
- ✓ The predicted values of R^2 are 0.9652 for surface roughness and 0.9767 for MRR are reasonably well. Its value is greater than 95% and the closest to one is the best value to fit the model.
- ✓ The variation between experimental and predicted values at the optimal combination of parameter settings for Ra, MRR, and both cutting tooltip temperatures lie within 4.46 %, 1.09 %, 1.73 % for tool 1, and 2.25 %for tool 2 respectively. This confirms the excellent reproducibility of the experimental conclusions.
- ✓ Results of the analysis of variance indicate that cutting speed was the most significant factor for considering surface roughness and material removal rate together as the P-value is less than 0.05. Feed and depth of cut are insignificant from the ANOVA study.
- ✓ From the study, the usefulness and potential of ceramic insert cutting tool for turning process under dry condition possess good surface finish which benefits to substitute the traditional grinding operation.

5.2 Recommendations

Based on the conclusions of this study, the researcher forwards the following recommendations.

- ✓ In this study double tool turning of AISI 1050 steel material has been used this can be further extended to other materials types to study the effects of cutting parameters on the surface under different machining environments of double tool turning operations.
- ✓ The metal fabrication, automotive, and spare part manufacturing industries can use the optimized turning parameter for dry turning of AISI 1050 steel to achieve the product with minimum surface roughness.

5.3 Scope of future work

As a future research work, the following will be carried out by any interested person:-

- ✓ Analyses the effect of cutting forces exerted and tool wear rate during the double cutting tool turning operation.
- ✓ Study effect of response variables with different cutting tools.
- ✓ Study the other output factors like power consumption, and tool life.
- ✓ Mathematical modeling and numerical analysis of cutting force, cutting temperature
- ✓ Study the effect of different cutting tools with similar cutting parameters.
- ✓ Study the effect of tool geometry like nose radius and rake angle on the surface roughness, cutting temperature, tool life, and machining cost.
- ✓ Study effects of the cutting parameter of stress, strain, and tooltip deformation may be conducted using numerical simulation and modeling. Because those parameters are difficult to investigate by experimenting with double cutting tool turning operation.

REFERENCES

A. (1994). *Fundamentals of Machining and Machine Tools: 3rd (Third) edition* (10800th ed.). CRC Press.

Abas, M., Sayd, L., Akhtar, R., Khalid, Q. S., Khan, A. M., & Pruncu, C. I. (2020), 'Optimization of machining parameters of aluminum alloy 6026-T9 under MQL-assisted turning process'. *Journal of Materials Research and Technology*, *9*(5): pp. 10916–10940.

An, Q., Wang, C., Xu, J., Liu, P., & Chen, M. (2014), 'Experimental investigation on hard milling of high-strength steel using PVD-AlTiN coated cemented carbide tool,' *International Journal of Refractory Metals and Hard Materials*, *43*: pp. 94–101.

Ay, M. (2019), 'Effect of cutting parameters on surface roughness, tool temperature, and vibration in turning of AISI 316 Ti stainless steel,' *Materials Testing*, *61*(1): pp. 71–79.

Budak, E., & Ozlu, E. (2007), 'Analytical Modeling of Chatter Stability in Turning and Boring Operations: A Multi-Dimensional Approach,' *CIRP Annals*, *56*(1): pp. 401–404.

Basmaci, G. (2018), 'Optimization of Machining Parameters for the Turning Process of AISI 316 L Stainless Steel and Taguchi Design,' *Acta Physica Polonica A*, *134*(1): pp. 260

Chan, Y. L., & Xu, X. (2015), 'Evaluation and comparison of lubrication methods in finish machining of hardened steel mold inserts,' *Proceedings of the Institution of Mechanical Engineers, Part B: Journal of Engineering Manufacture*, *231*(14): pp. 2458–2467.

Chandra, P., Rao, C. P., Kiran, R., & Kumar, V. R. (2018), 'Influence Of Machining Parameter On Cutting Force And Surface Roughness While Turning Alloy Steel,' *Materials Today: Proceedings*, *5*(5): pp. 11794–11801.

Chandrasheker, J., Manda, M., & Kumar, D. (2017), 'Optimization of Cutting Parameters for Turning AISI 316 Stainless Steel Based on Taguchi Method,' *IOSR Journal of Mechanical and Civil Engineering*, *14*(01): pp. 01–09.

Chen, W. (2000), 'Cutting forces and surface finish when machining medium hardness steel using CBN tools,' *International Journal of Machine Tools and Manufacture*, *40*(3): pp. 455–466.

Chinchanikar, S., & Choudhury, S. (2014), 'Evaluation of Chip-tool Interface Temperature: Effect of Tool Coating and Cutting Parameters during Turning Hardened AISI 4340 Steel,' *Procedia Materials Science*, *6*: pp. 996–1005.

Das, R., & Hazarika, M. (2019), 'A study on the effect of process parameters on the vibration of the cutting tool in turning operation,' *Journal of Physics: Conference Series*, *1240*(1): pp. 012086.

Das, S., Das, S., Gautam, S., & Gautam, C. (2020), 'Optimization of wear coefficient and coefficient of friction of borosilicate glass ceramics using Taguchi coupled grey fuzzy logic technique,' *Materials Today: Proceedings*, *27*: pp. 1579–1589.

Davis, B., Dabrow, D., Ju, L., Li, A., Xu, C., & Huang, Y. (2017), 'Study of Chip Morphology and Chip Formation Mechanism During Machining of Magnesium-Based Metal Matrix Composites,' *Journal of Manufacturing Science and Engineering*, *139*(9): pp.

Deepak, D., & Rajendra, B. (2016), 'Optimization of Machining Parameters for Turning of Al6061 Using Robust Design Principle to Minimize the Surface Roughness,' *Procedia Technology*, *24*: pp. 372–378.

Dharmalingam, S., Subramanian, R., & Kök, M. (2013), 'Optimization of abrasive wear performance in aluminum hybrid metal matrix composites using Taguchi–grey relational analysis,’ *Proceedings of the Institution of Mechanical Engineers, Part J: Journal of Engineering Tribology*, *227*(7): pp. 749–760.

Dikshit, M. K., Puri, A. B., Maity, A., & Banerjee, A. J. (2014), ‘Analysis of Cutting Forces and Optimization of Cutting Parameters in High-Speed Ball-end Milling Using Response Surface Methodology and Genetic Algorithm,’ *Procedia Materials Science, 5*: pp. 1623–1632.

Diniz, A. E., & José De Oliveira, A. (2004), ‘Optimizing the use of dry cutting in rough turning steel operations,’ *International Journal of Machine Tools and Manufacture*, *44*(10): pp. 1061–1067.

Dogra, M., Sharma, V. S., & Dureja, J. (2011), ‘Effect of tool geometry variation on finish turning – A Review,’ *Journal of Engineering Science and Technology Review*, *4*(1): pp. 1–13.

Duc, P. M., Giang, L. H., Dai, M. D., & Sy, D. T. (2020), ‘An experimental study on the effect of tool geometry on tool wear and surface roughness in hard turning,’ *Advances in Mechanical Engineering*, *12*(9): pp. 168781402095988.

El-Wardany, T., Mohammed, E., & Elbestawi, M. (1996), ‘Cutting temperature of ceramic tools in high-speed machining of difficult-to-cut materials,’ *International Journal of Machine Tools and Manufacture*, *36*(5): pp. 611–634.

Fei, N. C., Mehat, N. M., & Kamaruddin, S. (2013), ‘Practical Applications of Taguchi Method for Optimization of Processing Parameters for Plastic Injection Moulding,’ A Retrospective Review. *ISRN Industrial Engineering*, *2013*: pp. 1–11.

Groover, M. P. (2022). *Fundamentals of Modern Manufacturing: Materials, Processes, and Systems* (7th ed.). Wiley.

Guo, Y., & Yen, D. W. (2004), ‘A FEM study on mechanisms of discontinuous chip formation in hard machining,’ *Journal of Materials Processing Technology*, *155–156*: pp. 1350–1356.

Gupta, S., Chandra, V., & Kumar, P. (2019), ‘Assessment Of Machining Parameters On En-24 Steel Under Dry, Wet, And Mql Conditions Using Multi-Coated Inserts,’ *Journal of Physics: Conference Series*, *1240*(1): pp. 012141.

Huang, H., Yin, S. C., & Nazar, L. F. (2001), ‘Approaching Theoretical Capacity of LiFePO[sub 4] at Room Temperature at High Rates,’ *Letters*, *4*(10): pp. 170.

Jouini, N., Gautier, A., Revel, P., Mazeran, P. E., & Bigerelle, M. (2009), ‘Multi-scale analysis of high precision surfaces by Stylus Profiler, Scanning White-Light Interferometry,’ and Atomic Force Microscopy. *International Journal of Surface Science and Engineering*, *3*(4): pp. 310.

Kaladhar, M. (2019), ‘Evaluation of hard coating materials performance on machinability issues and material removal rate during turning operations,’ *Measurement*, *135*: pp. 493–502.

Kalidasan, R., Senthilvelan, S., Dixit, U., & Vaibhav, J. (2016), ‘Double tool turning: machining accuracy, cutting tool wear, and chip-morphology’ *International Journal of Precision Technology*, *6*(2): pp. 142.

Kalidasan, R., Yatin, M., Sarma, D., Senthilvelan, S., & Dixit, U. (2016), ‘An experimental study of cutting forces and temperature in multi-tool turning of grey cast iron,’ *International Journal of Machining and Machinability of Materials*, *18*(5/6): pp. 540.

Kam, M., & Demirtaş, M. (2021), ‘Analysis of tool vibration and surface roughness during turning process of tempered steel samples using Taguchi method,’ *Proceedings of the Institution of Mechanical Engineers, Part E: Journal of Process Mechanical*

Karkalos, N., Galanis, N., & Markopoulos, A. (2016), 'Surface roughness prediction for the milling of Ti–6Al–4V ELI alloy with the use of statistical and soft computing techniques,' *Measurement*, *90*: pp. 25–35.

Karthik, M., Raju, V., Reddy, K. N., Balashanmugam, N., & Sankar, M. (2020), 'Cutting parameters optimization for surface roughness during dry hard turning of EN 31 bearing steel using CBN inserts,' *Materials Today: Proceedings*, *26*: pp. 1119–1125.

Keblouti, O., Boulanouar, L., Azizi, M. W., & Yallese, M. A. (2017), 'Effects of coating material and cutting parameters on the surface roughness and cutting forces in dry turning of AISI 52100 steel,' *Structural Engineering and Mechanics*, *61*(4): pp. 519–526.

Khare, S. K., & Agarwal, S. (2017), 'Optimization of Machining Parameters in Turning of AISI 4340 Steel under Cryogenic Condition using Taguchi Technique,' *Procedia CIRP*, *63*: pp. 610–614.

Kong, X., Li, B., Jin, Z., & Geng, W. (2011), 'Broaching Performance of Superalloy GH4169 Based on FEM,' *Journal of Materials Science & Technology*, *27*(12): pp. 1178–1184.

Martowibowo, S. Y., & Kemala Damanik, B. (2021), 'Optimization of Material Removal Rate and Surface Roughness of AISI 316L under Dry Turning Process using Genetic Algorithm,' *Manufacturing Technology*, *21*(3): pp. 373–380.

Mia, M., Dey, P. R., Hossain, M. S., Arafat, M. T., Asaduzzaman, M., Shoriat Ullah, M., & Tareq Zobaer, S. (2018), 'Taguchi S/N based optimization of machining parameters for surface roughness, tool wear, and material removal rate in hard turning under MQL cutting conditions,' *Measurement*, *122*: pp. 380–391.

Musavi, S. H., Sepehrikia, M., Davoodi, B., & Niknam, S. A. (2022), 'Performance analysis of developed micro-textured cutting tool in machining aluminum alloy 7075-T6:

assessment of tool wear and surface roughness,’ *The International Journal of Advanced Manufacturing Technology*.

OZel, T., Hsu, T. K., & Zeren, E. (2004), ‘Effects of cutting edge geometry, workpiece hardness, feed rate, and cutting speed on surface roughness and forces in finish turning of hardened AISI H13 steel,’ *The International Journal of Advanced Manufacturing Technology*, *25*(3–4): pp. 262–269.

Patel, V. D., & Gandhi, A. H. (2019), ‘Analysis and modeling of surface roughness based on cutting parameters and tool nose radius in turning of AISI D2 steel using CBN tool,’ *Measurement*, *138*: pp. 34–38.

Prasad, D., Krishna, P., & Rao, S. (2012), ‘Prediction of Surface Finish and Optimization of Machining Parameters in Turning,’ *Advanced Materials Research*, *463–464*: pp. 679–683.

Patokar, P., Trikal, S. P., & Patil, C. (2016), ‘Experimental Investigation of Machining Time in Turning Mild Steel Component using Multi-Tool Turning Method,’ *International Journal for Scientific Research & Development*|, *3*(11): pp. 492–496.

Qehaja, N., Jakupi, K., Bunjaku, A., Bruçi, M., & Osmani, H. (2015), ‘Effect of Machining Parameters and Machining Time on Surface Roughness in Dry Turning Process,’ *Procedia Engineering*, *100*: pp. 135–140.

Qureshi, M. R., Sharma, S., Singh, J., Khadar, S. A., & Baig, R. U. (2020), ‘Evaluation of surface roughness in the turning of mild steel under different cutting conditions using a backpropagation neural network,’ *Proceedings of the Estonian Academy of Sciences*, *69*(2): pp. 109.

R., S., & K.S., J. (2017), ‘Wear analysis on EN8, EN9, and EN24,’ *World Journal of Engineering*, *14*(3): pp. 188–192.

Ranjan Das, S., Panda, A., & Dhupal, D. (2018), 'Hard turning of AISI 4340 steel using coated carbide insert: Surface roughness, tool wear, chip morphology, and cost estimation,' *Materials Today: Proceedings*, *5*(2): pp. 6560–6569.

Ravi Kumar, S., & Kulkarni, S. K. (2017), 'Analysis of Hard Machining of Titanium Alloy by Taguchi Method,' *Materials Today: Proceedings*, *4*(10): pp. 10729–10738. \

Sahoo, A. K., Baral, A. N., Rout, A. K., & Routra, B. (2012), 'Multi-Objective Optimization and Predictive Modeling of Surface Roughness and Material Removal Rate in Turning Using Grey Relational and Regression Analysis,' *Procedia Engineering*, *38*: pp. 1606–1627.

Sahu, S., & Choudhury, B. (2015), 'Optimization of Surface Roughness Using Taguchi Methodology & Prediction of Tool Wear in Hard Turning Tools,' *Materials Today: Proceedings*, *2*(4–5): pp. 2615–2623.

Sarker, I., Nasher Khan Pathan, M. A., & Akter, M. (2018). *Parametric study of surface roughness in turning of AZ31B Mg alloy under different cooling conditions*.

Senthil Kumar, A., Raja Durai, A., & Sornakumar, T. (2003), 'Machinability of hardened steel using alumina-based ceramic cutting tools,' *International Journal of Refractory Metals and Hard Materials*, *21*(3–4): pp. 109–117.

Shahid, M. (2020), 'Optimization of Turning Process Parameters in Machining Heat Treated Steel,' *International Journal for Research in Applied Science and Engineering Technology*, *8*(9): pp. 121–125.

Sharma, V. S., Dhiman, S., Sehgal, R., & Sharma, S. K. (2008), 'Estimation of cutting forces and surface roughness for hard turning using neural networks,' *Journal of Intelligent Manufacturing*, *19*(4): pp. 473–483.

Singh, R., Shadab, M., & Rai, R. (2018), 'Optimization of machining process parameters in conventional turning operation of Al5083/B4C composite under dry conditions,' *Materials Today: Proceedings*, *5*(9): pp. 19000–19010.

Siva Surya, M. (2022), 'Optimization of turning parameters while turning Ti-6Al-4V titanium alloy for surface roughness and material removal rate using response surface methodology,' *Materials Today: Proceedings*.

Siva Surya, M., Shalini, M., & Sridhar, A. (2017), 'Multi-Response Optimization On En19 Steel Using Grey Relational Analysis Through Dry & Wet Machining,' *Materials Today: Proceedings*, *4*(2): pp. 2157–2166.

Sivaiah, P., & Chakradhar, D. (2016), 'Influence of cryogenic coolant on turning performance characteristics: A comparison with wet machining,' *Materials and Manufacturing Processes*, *32*(13): pp. 1475–1485.

Sun, L., Yang, S., Yang, L., Zhao, P., Wu, P., & Jiang, Z. (2015), 'A New Model of Grinding Forces Prediction for Machining Brittle and Hard Materials,' *Procedia CIRP*, *27*: pp. 192–197.

Syed Irfan, S., Vijay Kumar, M., & Rudresha, N. (2019), 'Optimization of Machining Parameters in CNC Turning of En45 By Taguchi's Orthogonal Array Experiments,' *Materials Today: Proceedings*, *18: pp.* 2952–2961.

Tang, L., Sun, Y., Li, B., Shen, J., & Meng, G. (2019), 'Wear performance and mechanisms of PCBN tool in dry hard turning of AISI D2 hardened steel,' *Tribology International*, *132*: pp. 228–236.

Thangarasu, S. K., Shankar, S., Tony Thomas, A., & Sridhar, G. (2018), 'Prediction of Cutting Force in Turning Process-an Experimental Approach,' *IOP Conference Series: Materials Science and Engineering*, *310*: pp. 012119.

Trikal, S. P., Patokar, P., & Patil, C. (2016). Evaluation of Surface Roughness of Mild Steel Component Turned using Multi-Tool Turning Method. *International Journal*

Umbrello, D., Hua, J., & Shivpuri, R. (2004), 'Hardness-based flow stress and fracture models for numerical simulation of hard machining AISI 52100 bearing steel,' *Materials Science and Engineering: A*, *374*(1–2): pp. 90–100.

V.V.D.Sahithi, T.Malayadrib, & Srilatha, N. (2019), 'Optimization Of Turning Parameters On Surface Roughness Based On Taguchi Technique,' *Materials Today: Proceedings*, *18*: pp. 3657–3666.

Venkata Vishnu, A., Venkata Ramana, M., & Tilak, K. (2018), 'Experimental Investigations of Process Parameters Influence on Surface Roughness in Turning of EN-353 Alloy Steel under Different Machining Environments,' *Materials Today: Proceedings*, *5*(2): pp. 4192

Yallese, M. A., Chaoui, K., Zeghib, N., Boulanouar, L., & Rigal, J. F. (2009), 'Hard machining of hardened bearing steel using cubic boron nitride tool,' *Journal of Materials Processing Technology*, *209*(2): pp. 1092–1104.

Zhang, X., Wu, S., Wang, H., & Liu, C. R. (2011), 'Predicting the Effects of Cutting Parameters and Tool Geometry on Hard Turning Process Using Finite Element Method,' *Journal of Manufacturing Science and Engineering*, *133*(4): pp.

Zhang, Z., Yao, P., Wang, J., Huang, C., Cai, R., & Zhu, H. (2019), 'Analytical modeling of surface roughness in precision grinding of particle reinforced metal matrix composites considering the nanomechanical response of the material,' *International Journal of Mechanical Sciences*, *157–158*: pp. 243–253.

Zhenchao, Y., Yang, X., Yan, L., Jin, X., & Quandai, W. (2018), 'The effect of milling parameters on surface integrity in high-speed milling of ultrahigh strength steel,' *Procedia CIRP*, *71*: pp. 83–88.

APPENDIXES

Journal of Materials Research and Technology

Experimental Investigation and Parametric Optimization of Double Cutting Tool Turning During Dry Condition for AISI 1050 Steel

--Manuscript Draft--

Manuscript Number:	
Article Type:	Original article
Keywords:	AISI 1050 steel; cutting parameter; surface roughness; material removal rate; Taguchi method
Corresponding Author:	Moera Gutu, Ph.D Adama Science and Technology University Adama, ETHIOPIA
First Author:	Moera Gutu, Ph.D
Order of Authors:	Moera Gutu, Ph.D
	Kasahun Nuguse Alemu
	Hirpa G. Lemu
Abstract:	Optimizing the machining parameters during machining process is important to achieve certain desired machined surface quality. Optimizing cutting parameters to get a high surface finish that reduces mechanical failures caused by wear and corrosion in the same way to increases the productivity of mechanical parts. In this research double tool turning on AISI 1050 steel material was conducted using ceramic inserted cutting tool. Taguchi L16 orthogonal array has been selected for the design of the experiments, signal-to-noise, Regression analysis for each response, and grey relational analysis-based optimization was used. Analysis of variance (ANOVA) was used to determine influences of cutting parameters and mathematical model was done using regression analysis on surface roughness. The results of variance presented influence of cutting speed, feed rate, first depth of cut, and second depth of cut were 8.83%, 16.92%,28.41%, and 40.99% respectively on surface roughness. The minimum surface roughness attained for the optimum cutting parameter was 1.12µm. the results revealed that the developed predictive models provide a close relationship between the predicted values and experimental values for all response values. The moderate tooltip temperatures of 72.60C and 70.2 0C were measured for both single and double tool turning respectively. Material removal rate was high due to double tool turning used and maximum of 112 mm3/sec.
Suggested Reviewers:	Dr.Guteta kabeta Kabeta, PhD Assistant professor, Adama Science and Technology University uni100@yahoo.com related area of research
	Mesay Alemu Tolcha, Ph.D Associate professor, Jimma University alemu170@yahoo.com his research work is same
	Hirpa G. Lemu, Ph.D professor, University of Stavanger hirpa.g.lemu@uis.no He is working in similar research area
Opposed Reviewers:	

To,
The Editor in Chief

Date: 26.5.2022

Materials Research and Technology

Subject: Submission of an article, "Experimental Investigation and Parametric Optimization of Double Cutting Tool Turning During Dry Condition for AISI 1050 Steel

Kasahun Nuguse Alemu[a], Moera Gutu Jiru[b] and *[C]Hirpa G. Lemu

[a,b] Department of Mechanical Engineering
Adama Science and Technology University
[C]Faculty of Science and Technology, University of Stavanger, Norway

Emails: [a]kasahunuguse1234@gmail.com
[b]moera.guta@astu.edu.et
[C]*Hirpa.g.lemu@uis.no

Sir,

Enclosed here with an article file name "Experimental Investigation and Parametric Optimization of Double Cutting Tool Turning During Dry Condition for AISI 1050 Steel" for your kind consideration for publication in your esteemed journal " Materials Research and Technology. **I certify that above mentioned article has not been published/submitted elsewhere.**

Yours faithfully

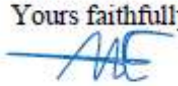

(Dr. Moera Gutu)
Associate,
Dept. of Manufacturing Engineering,
School of Mechanical Chemical Materials Engineering,
Adama Science and Technology University.
Mobile: +251-994923477

Mechanical and Physical Properties of AISI 1050 steel material

Table 1.1 Mechanical properties of AISI 1050 steel material is as follows

Mechanical properties	Metric	Empirical
Hardness, Brielle	187	187
Hardness, Knoop	209	209
Hardness, Vickers	196	196
Hardness, Rockwell	58	58
Tensile strength, yield	515 Mpa	74700psi
Tensile strength, ultimate	655Mpa	95000psi
Elongation at break	15% in 50 mm	15% in 50 mm
Modulus of elasticity	205 Gpa	29700ksi
Poisson’s ratio	0.290	0.290
Shear modulus	80.0 Gpa	11600 ksi

Table 1.2 Physical properties of AISI 1050 steel material is as follows

Physical properties	Metric	Empirical
Density	$7.85\, gm/cm^3$	$0.284\, lb/in^3$

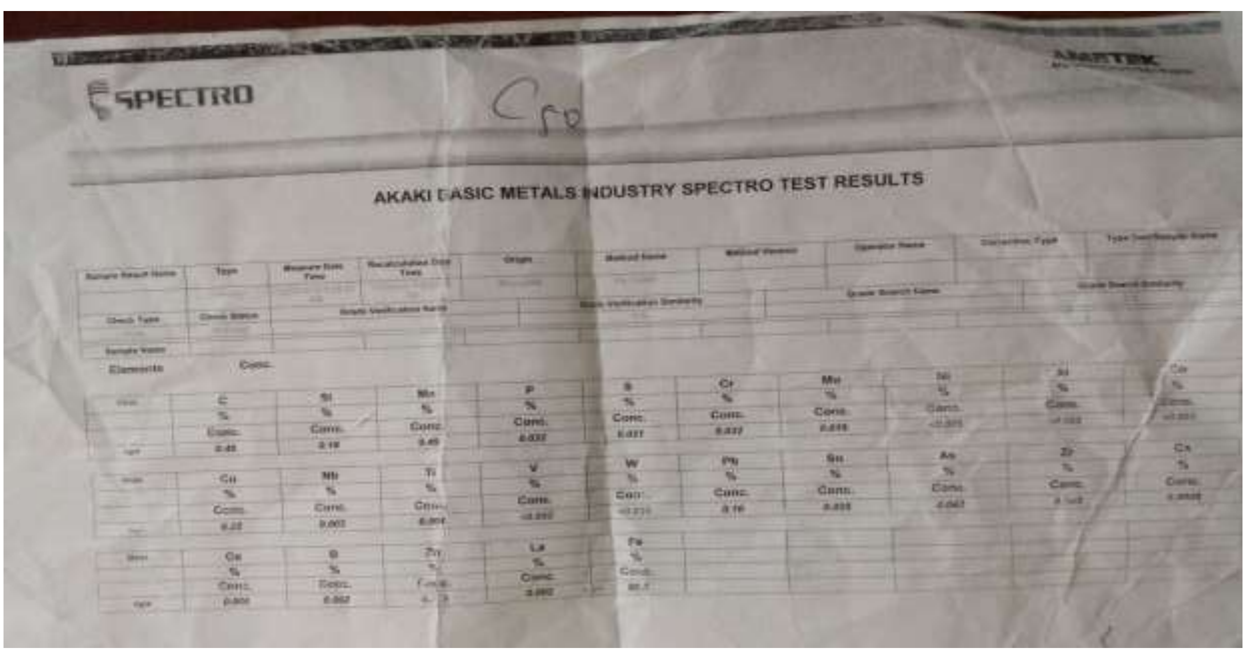
SPECTRO

AKAKI BASIC METALS INDUSTRY SPECTRO TEST RESULTS

C % Conc.	Si % Conc.	Mn % Conc.	P % Conc.	S % Conc.	Cr % Conc.	Mo % Conc.	Ni % Conc.	Al % Conc.	Co % Conc.
[illegible]	[illegible]	[illegible]	[illegible]	[illegible]	[illegible]	[illegible]	[illegible]	[illegible]	[illegible]

Cu % Conc.	Nb % Conc.	Ti % Conc.	V % Conc.	W % Conc.	Pb % Conc.	Sn % Conc.	As % Conc.	Zr % Conc.	Ce % Conc.
[illegible]	[illegible]	[illegible]	[illegible]	[illegible]	[illegible]	[illegible]	[illegible]	[illegible]	[illegible]

Ca % Conc.	B % Conc.	Zn % Conc.	La % Conc.	Fe % Conc.
[illegible]	[illegible]	[illegible]	[illegible]	[illegible]

Minilab software and design of L16 orthogonal array